# Quantifying the effects of transmitter-receiver geometry variations on the capabilities of airborne electromagnetic survey systems to detect targets of high conductance

By

Shane W. Hefford

A thesis submitted to the

Faculty of Graduate Studies and Research

In partial fulfillment of the requirements for the degree of

Master of Science, Department of Earth Sciences

Carleton University

Ottawa, Ontario

April 2006

*Your file Votre référence*
*ISBN: 978-0-494-16496-9*
*Our file Notre référence*
*ISBN: 978-0-494-16496-9*

**Abstract**

Exploration using time-domain electromagnetic (EM) systems is very successful when detecting conductive targets in the subsurface. These systems are most sensitive to highly conductive targets during the transmitter on-time. Data collected during the on-time is highly influenced by the geometric relationship between the transmitter and the receiver. Some systems do not have a fixed transmitter-receiver geometry, making the detection of highly conductive targets a challenge. Unless the geometry can be constrained, or corrections can be applied for these geometric variations, the ability to correctly detect and identify highly conductive targets cannot be fully realized.

The objectives of this thesis are to determine how the transmitter and the receiver move with respect to one another for various fixed-wing airborne EM systems; demonstrate why movement between the transmitter and the receiver compromises a system's ability to detect highly conductive targets; and estimate how accurately the transmitter-receiver geometry must be measured in order to detect a vertical target of high conductance for four configurations of airborne electromagnetic systems (GEOTEM, GEOTEM+, HeliGEOTEM and a Generic Concentric configuration). These objectives are achieved by analyzing the effect of the individual $x$, $y$, and $z$ transmitter and receiver offsets, the transmitter attitude (roll, pitch, and yaw), and transmitter loop deformation.

The level of accuracy required for each geometric variation between the transmitter and the receiver is dependent on: the type, shape, orientation and depth of the target, as well as the configuration of the exploration system. For this analysis, the GEOTEM system is

most sensitive to variations in the loop deformation followed by pitch, $x$-distance, $z$-distance, roll and $y$-distance. GEOTEM+ is similar to the GEOTEM system but is more sensitive to variations in pitch than loop deformation. The HeliGEOTEM system is most sensitive to variations in the pitch followed by loop deformation and $z$-distance then $x$-distance, roll and $y$-distance. The Generic Concentric system is most sensitive to loop deformation, $z$-distance, $x$- and $y$-distance, and roll and pitch. Of all the systems analyzed, the GEOTEM+ system has the lowest accuracy requirement followed by GEOTEM, HeliGEOTEM and the Generic Concentric. The Generic Concentric system requires an extremely high degree of accuracy for each variable.

**Acknowledgements**

I foremost like to thank my supervisors Dr. Claire Samson of Carleton University and Dr. Richard Smith of Fugro Airborne Surveys for their guidance during this project. Their openness and availability made this research project a very worthwhile and pleasurable experience. The project could not have been a success without their encouragement, enthusiasm, and support.

The GEOIDE Networks for Centres of Excellence through financial contributions and their Summer School training sessions generously supported this research project. I also thank Fugro for continued access to software and hardware throughout the duration of this project. I especially would like to thank the processing department at Fugro for their continued support and interest. Without their practice sessions I would not have had the confidence to present my work. I appreciate them allowing me to print my poster presentations for the GEOIDE Conferences.

Appendix I of this project could not have been achieved without significant support from Fugro Airborne Surveys. Moreover, much appreciation is extended to Bruce Magnus for his technical assistance with the Leica EDM and Laser tracking System. Thanks are also extended to Slava Gorokhovski, for assistance with operating the Leica system.

Appendix II of this project could not have been completed without the help of Chad English from Neptec who did a great job at explaining the SVS system and the general

theory behind it. This helped me understand how visual systems worked and how they were inappropriate as a solution to the problem outlined in this thesis.

Finally, I like to express my utmost gratitude to my wife Ashley, my friends and family who have supported me during this research project with their interest over the past two years.

**Table of Contents**

**List of Figures**

Figure 4.5: Maximum tolerable transmitter attitude angle variations permitted to successfully detect and identify a vertical plate with a conductance of 10000 Siemens as a function of the depth to the target for the GEOTEM system. Yaw has a negligible effect and is therefore omitted. For a target depth of 100 metres, roll requires an accuracy of ~6.3°; pitch requires variation less than ~0.13°. These angles are equivalent to movements of ~1 metre at the wingtips and ~2 centimetres at the nose of the aircraft respectively.

Figure 4.6: Top view of the aircraft and the transmitter loop. The loop is attached at the wing tips and at a long extension at the tail and at two smaller extensions at the front. The four marked points along the loop are those that are varied in the directions shown for the GEOTEM and GEOTEM+ analysis.

Figure 4.7: Deviation of the primary field from its nominal value as a function of displacement of the four mobile points midway between the attachment points along the transmitter loop shown in the previous figure for the GEOTEM configuration.

Figure 4.8: Maximum tolerable variations in order to successfully detect and identify a vertical plate with a conductance of 10000 Siemens as a function target depth, for each statistical parameter derived in the loop deformation analysis for the GEOTEM configuration. For a target depth of 100 metres, the mean acceptable movement requires 3.5 centimetres accuracy. For the case representing larger deviation from the nominal response (mean plus one standard deviation), the accuracy requirement is more stringent and equal to 2 centimetres at a target depth of 100 metres.

Figure 4.9: Comparison of all the variables for the GEOTEM configuration. Units for the pitch and roll have been converted to a distance measurement at the nose and the wing tip respectively.

Figure 4.10: Schematic diagram of the GEOTEM+ configuration. The mean altitude for the aircraft and transmitter is 120 metres. The receiver is located 250 metres behind and 70 metres below the centre of the transmitter loop.

Figure 4.11: Deviation of the primary field from its nominal value as a function of variations in receiver positions for the GEOTEM+ configuration.

Figure 4.12: Maximum tolerable receiver offsets permitted to successfully detect and identify a vertical plate with a conductance of 10000 Siemens as a function of target depth for the GEOTEM+ configuration. For a target depth of 100 metres, the required accuracy in the $z$-direction is ~11.9 metres, the required accuracy in the $y$-direction is ~5132 metres, and the required accuracy in the $x$-direction is ~1.3 metres.

Figure 4.13: Deviation of the primary field from its nominal value as a function of variations in transmitter attitude for the GEOTEM+ configuration. Note: The roll and yaw have such a minimal influence that they overlap close to zero.

Figure 4.23: Maximum tolerable transmitter attitude angle variations permitted to successfully detect and identify a vertical plate with a conductance of 10000 Siemens plotted as a function of the depth to the target depth for the HeliGEOTEM system. Yaw has a negligible effect and is therefore omitted. For a target depth of 100 metres, roll requires an accuracy of ~0.65°; pitch requires variation less than ~0.0064°. These angles are equivalent to movements of ~6.2 centimetres at the front or back edge of the loop, and ~0.062 centimetres at the side edge of the loop.

Figure 4.24: Top view of the HeliGEOTEM transmitter loop. The loop is a rigid construction and attached to the aircraft by a tow cable. The marked points along the loop are those that are varied in the directions shown for the HeliGEOTEM analysis.

Figure 4.25: Deviation of the primary field from its nominal value as a function of displacement of the four mobile points midway between the attachment points along the transmitter loop shown in the previous figure for the HeliGEOTEM configuration.

Figure 4.26: Maximum tolerable variations in order to successfully detect and identify a vertical plate with a conductance of 10000 Siemens as a function of target depth, for each statistical parameter derived in the loop deformation analysis for the HeliGEOTEM configuration. For example, for a target depth of 100 metres, the mean acceptable movement requires 0.15 centimetres accuracy. For the case representing larger loop deformation (mean plus one standard deviation), the accuracy requirement is more stringent and equal to 0.04 centimetres at a target depth of 100 metres.

Figure 4.27: Comparison of all the variables for the HeliGEOTEM configuration. Units for the pitch and roll have been converted to a distance measurement at the nose and the wing tip respectively. The HeliGEOTEM is most sensitive to pitch followed by *z*-distance and loop deformation. When plotted, the curves for z-distance and the loop deformation overlap exactly and are very close to the pitch and the *x*-distance.

Figure 4.28: Schematic diagram of the Generic Concentric configuration. The mean transmitter loop altitude is 35 metres. The receiver and the transmitter are on the same plane.

Figure 4.29: Underside view of the Generic Concentric configuration. The transmitter and the receiver are towed behind and below the aircraft. The transmitter is the larger outer loop (or series of outer loops) and the receiver is the inner loop (or series of inner loops).

Figure 4.30: Deviation of the primary field from its nominal value as a function of variations in receiver positions for the Generic Concentric configuration.

Figure 4.31: Maximum tolerable receiver offsets permitted to successfully detect and identify a vertical plate with a conductance of 10000 Siemens as a function of target depth for the Generic Concentric configuration. For example, for a target depth of 100

**List of Tables**

**List of Appendices**

**List of Acronyms**

AMT - Audio MagnetoTellurics

ATR - Automatic Target Recognition

CCD - Charged Coupled Device

CSAMT - Controlled Source AudioMagnetoTellurics

DC - Direct Current

EDM - Electronic Distance Measurement

EM - ElectroMagnetics

IP - Induced Potential

IR - Infrared

LiDaR - Light Detection and Ranging

PS - Power Search

PPM - Parts Per Million

RaDaR - Radio detection and Ranging

SQUID - Superconducing QUantum Interface Device

SVS - Space Vision System

TDEM - Time Domain ElectroMagnetic

VLF - Very Low Frequency

# 1. Introduction

## *1.1 Geophysics History*

Geophysics is a relatively young science dedicated to study of the physical properties of the earth, the atmosphere, and space. Geophysics initially arose as a means to explain such natural phenomena as earthquakes, volcanoes, auroras, etc., which had perplexed humankind since the beginning of history. Although Newton's Law of Universal Gravitation is credited as being the starting point for geophysics, the search for various natural resources started much earlier in ancient times.

Modern exploration geophysics arguably started with the recognition of a connection between magnetic properties and mineral deposits. A partial account began with the publication of *De re metallica* by Georgius Agricola as early as 1556 (Telford et al., 1990). A more substantial link between magnetic properties and mineral deposits was made in 1843 by Von Wrede (Telford et al., 1990). However, the first publication dedicated to geophysical exploration was not until 1879 with a book by Robert Thalén entitled *Untersuchung von Eisenerzfeldern durch Magnetische Messungen* (On the Examination of Iron Ore Deposits by Magnetic Methods) (Telford et al., 1990; Morrison, 2005). Although this publication contains general descriptions, it contains no survey data. The first published survey data was not until 1898 with a short paper entitled *Magnetische Untersuchungen im Harz* by Max Eschenhagen. This publication was an analysis of measurements the author had obtained from the Harz Mountains between 1888 and 1890. Similarly, Hermann Fritsche published a paper entitled *Die magnetischen Lokalabweichungen bei Moskau und ihre Beziehungen zur dortigen*

*Lokalattraction* in 1896 on magnetic measurements that he had made in 1893 near Moscow. In the 19th century, the science of geophysics finally evolved into a distinct scientific discipline that was an amalgamation of the older, more established sciences such as physical geography, geology, astronomy, meteorology, and physics (Telford et al., 1990; Morrison, 2005).

Currently, geophysics has progressed far beyond its humble beginning and includes such topics as: rheology, inverse theory, computer modeling, seismology, hydrothermal studies, volcanology, potential field methods (gravity and magnetics), electromagnetic surveying, space sciences, and geomorphology. Each topic can be subdivided into two main categories, theoretical and applied. Theoretical geophysics is typically more abstract and concentrates on the fundamental theories of the research topic or explaining natural phenomena. Applied geophysics is primarily focused on topics that have an industrial application. Such applications include groundwater, mineral and hydrocarbon exploration. Earth monitoring such as environmental assessments, earthquake analysis and mitigation might also be considered to fall into this category.

### *1.2 Society Demands Resources*

As society develops and the world population increases, the need for new and larger quantities of natural resources (renewable and non-renewable) intensifies. Societal demands for a large quantity of petroleum and metallic minerals is steadily increasing, despite efforts to reduce, reuse and recycle. Superimposed on this trend is the constantly changing demand for specific resources. For example, certain technological advances

have increased the demand for various minerals used in the fabrication of computer chips that previously were considered useless. Conversely, following the imposition of restrictions on "leaded" gasoline have been imposed in the mid-1980s, the use of lead has dramatically decreased (Kitman, 2000). To meet the increasing energy and material requirements, it is essential that science and technology evolve with societal needs. Prior to the twentieth century, exploration for petroleum and minerals was confined to observable deposits at the surface. As demand quickly increased during WWI and WWII in the mid-twentieth century and while conventional methods of finding new deposits were falling short of demand, more advanced methods of studying the subsurface were required (Telford et al., 1990). The demand for detecting mines, aircraft, gun fortifications and submarines during the world wars facilitated improved exploration instrumentation as well. For example, aircraft fitted with magnetometers were often used to locate submarines and ships in the ocean and handheld metal detectors were originally designed to locate land mines (Lawyer et al., 2001). Naturally, after the wars, these instruments found other practical uses in commercial exploration.

### *1.3 Geophysical Electromagnetic Methods*

Geophysical techniques are employed to acquire information about the subsurface that is otherwise unobtainable from the surface. Each technique responds to contrasts in specific physical properties that help differentiate one zone from another. From this observed inhomogeneity, Geophysicists can make inferences as to what may be cause of the variation. In some instances, however, a target may have the same physical property as the medium in which it is contained. The inability to perceive various homogeneities

is a limitation common to all geophysical techniques. Geophysics can only distinguish that which has some variation in time and/or space (Telford et al., 1990). Luckily, there are many different exploration techniques that reveal different physical properties and every target has some physical property that is not homogeneous with the medium in which it is hosted. It is up to the Geoscientist to determine which exploration technique will yield sufficient contrasts between the target and its host. Geophysical exploration methods are subdivided into five main categories: potential fields, seismic, radiometric, electric, and electromagnetic.

Exploration using electromagnetic (EM) methods has historically been used to locate and/or identify conductive targets at various scales. EM methods range from the most basic handheld metal detectors to find land mines in war zones and keys or coins at the beach, to large-scale surface loop transmitters and multiple component receivers used in many mineral exploration programs (Telford et al., 1990). Most mineral deposits have much greater conductivity than the rocks that host them and therein offers the means to differentiate areas of high mineral potential from those of low mineral potential (Telford et al., 1990).

Classification of the various electromagnetic systems is usually based on the combination of the transmitter type, receiver type and their configuration as shown in Table 1.1 (Swift, 1988). Electromagnetic sources are most often active and controlled and usually consist of a time-varying electrical and magnetic field. Based on the principles of electromagnetic induction, a transmitted primary field induces eddy currents in the

| Transmitter/Source | | | Receiver | | | |
|---|---|---|---|---|---|---|
| | | | Grounded wire | Wire and small coil | Small coil (ground) | Small coil (air) |
| Active | Grounded Wire | Inductive | Eltran | Controlled source AMT (CSAMT) | Some TDEM systems | |
| | Small Loop | | | | Slingram | Airborne EM |
| | | | | | Horizontal loop EM | Time Domain (fixed wing, helicopter) |
| | | | | | Vertical loop EM | Frequency Domain (helicopter) |
| | | | | | Tilt angle method | |
| | | | | | Some TDEM systems | |
| | | | | | Coincident loop | |
| | | | | | Borehole configurations | |
| | Large Loop | | | | Large loop systems | Time Domain (Flairtem) |
| | | | | | Turam | Frequency Domain (Turair) |
| | | | | | Many TDEM systems | |
| | | | | | Borehole configurations | |
| | Plane Wave | Vertical Antennae | | VLF-resistivity | VLF | VLF |
| Passive | | Natural geomagnetic | | Telluric currents | Magnetotellurics | |

Table1.1: Electric and Electromagnetic methods (modified from Swift, 1988).
Notes: Grounded wires measure potential difference per length, thus electric field. Coils measure the time derivative of the magnetic field. Similarly, the magnetic field can be measured using a fluxgate magnetometers or a SQUID magnetometer. A small loop is a 3-D source (magnetic dipole). A long wire (or the long edge of a large loop) is a 2-D source. Natural EM sources are assumed to be 1-D sources. Receivers can be frequency-domain, time-domain (TEM), or both. This classification excludes the high-frequency techniques (i.e. radar, lidar, etc.).

ground. These eddy currents are the secondary electric field, which has an associated secondary magnetic field. This secondary magnetic field induces an electric field in the coils of the receiver that can be measured. The measurement is then interpreted to determine the electrical properties of the earth (Figure 1.1).

Electromagnetic methods typically use one of several types of magnetic field receivers available. Instruments such as fluxgate magnetometers, or the more sensitive Superconducting QUantum Interference Devices (SQUIDs), measure the magnetic field directly. However, most systems measure the time-derivative of the magnetic field. This is accomplished using a series of induction coils that will measure a voltage (V) or the change in the flux of the magnetic field with respect to time (*dB/dt)* (Telford et al., 1990). The magnetic field (*B*) measured in Teslas (T) can be then calculated by integrating the time-derivative of the measured magnetic field.

### *1.4 EM Induction Theory in the Earth*

The interlinked chain of induced electric and magnetic fields are governed by Maxwell's equations (Plonus, 1979). More specifically Maxwell's 1$^{st}$ and 3$^{rd}$ equations, Faraday's Law and Ampere's Law respectively. Faraday's Law of electromagnetic induction, states that a time-varying primary magnetic field will produce an electric field. The integral form of the law is:

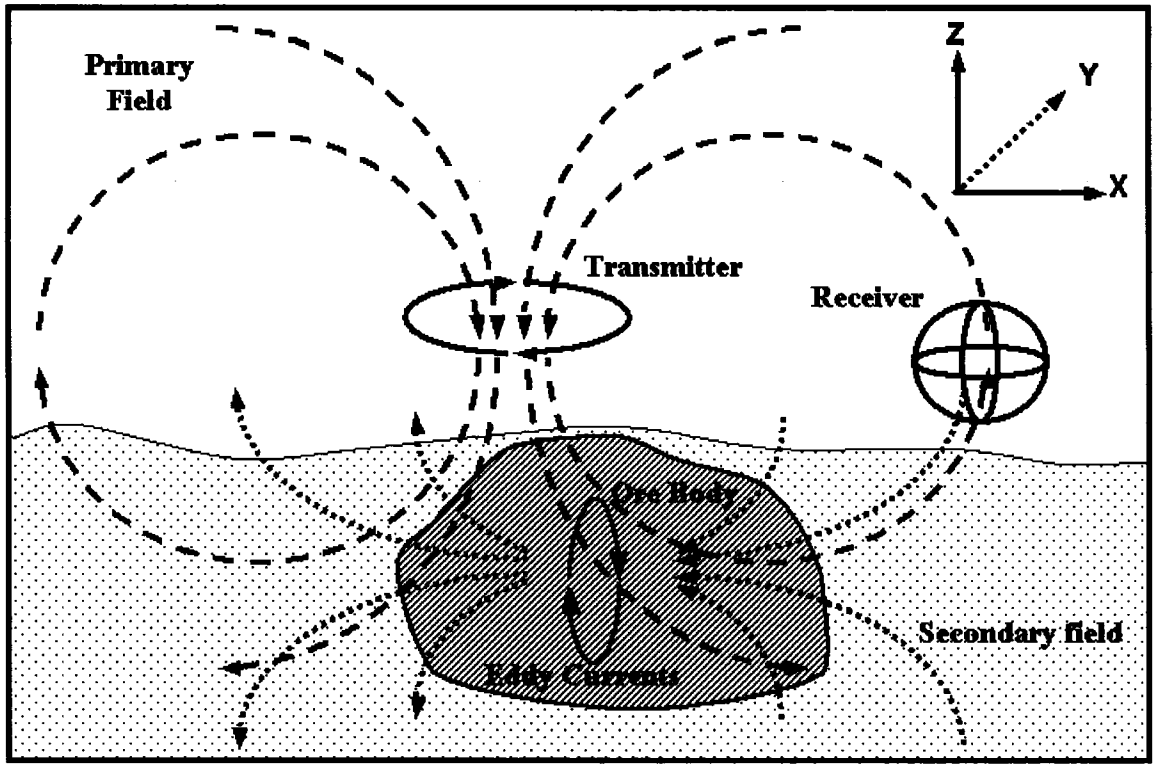


Figure 1.1: Faraday's Law of electromagnetic induction. The transmitter radiates a primary field (dashed line), which induces "eddy" currents in a grey conductive ore body. These currents in turn induce a secondary field (dotted line), which is sensed by a series of three component receiver coils as depicted in the diagram. The coordinate system used in this analysis is shown in the top right corner. The *y*-component points into the page.

$$\oint_C \boldsymbol{E} \cdot d\boldsymbol{l} = -\frac{d\Phi_B}{dt} \tag{1}$$

where $E$ is the induced electric field in Volts per metre (V/m), $dl$ is an infinitesimal element of a closed contour $C$ in metres. The magnetic flux ($\Phi_{B)}$ through a surface is the integral over the surface of the normal component of the magnetic induction expressed as Webers (Wb). The second term $d\Phi_B/dt$, is the rate of change of the magnetic flux with respect to time $t$ in seconds (s) passing through the surface bordered by the closed contour C. The differential form of the law is:

$$\nabla \times \boldsymbol{E} = -\frac{\partial \boldsymbol{B}}{\partial t} \tag{2}$$

where $B$ is the magnetic flux density in Teslas ($T$, or Wb/m$^2$). This formula shows the relationship between a time-varying magnetic field and the curl ($\nabla\times$) of the electric field.

A different relationship is formulated in Ampere's Law, which states that the integral of the magnetic field around a closed contour in space is proportional to the net currents flowing through the surface bordered by the contour. In this case, the current includes a displacement current. Ampere's Law is given by the equation:

$$\oint_C \boldsymbol{H} \cdot d\boldsymbol{l} = \int_S \boldsymbol{J} \cdot d\boldsymbol{A} + \frac{d}{dt}\int_S \boldsymbol{D} \cdot d\boldsymbol{A} \tag{3}$$

where $D=\epsilon E$ is the displacement current in coulombs per square metre ($C/m^2$) and includes a permittivity constant $\epsilon$, $H$ is the magnetic field in ampere per metre (A/m), $dl$ is an infinitesimal element, of the contour $C$, $J$ is the current density in ampere per square metre ($A/m^2$) through the surface $S$ enclosed by contour $C$. $\oint$ is the closed loop integral around contour $C$. This equation can also be stated in differential form as:

$$\nabla \times \boldsymbol{H} = \boldsymbol{J} + \frac{\partial \boldsymbol{D}}{\partial t} \tag{4}$$

where the right hand side, $\boldsymbol{J} + \frac{\partial \boldsymbol{D}}{\partial t}$, includes the current and the displacement current. However, because the frequencies used in EM exploration are relatively low, any contribution from the displacement current is negligible.

For EM systems, the receiver normally consists of an induction coil composed of a series of multiple-turn wire loops, in which a voltage will be induced. The induced voltage is proportional to the strength of the eddy currents in the ground and their rate of change with time. Typical receiver coils have axes in three of the Cartesian axis directions so that they are orthogonal to one another. Coils that have their axis in the same direction as the transmitter coil axis are most sensitive to horizontal layers and half-spaces. Coils that have their axis orthogonal to the transmitter coil axis are most sensitive to discrete or vertical conductors (Spies and Frischknecht, 1991).

### *1.5 EM Geophysical Survey Systems*

Controlled-source EM survey systems can be divided into two categories: frequency-domain and time-domain, (Grant and West, 1965). In frequency-domain systems, the transmitter signal is a sinusoidal waveform of constant frequency inducing electrical currents in the ground at the same frequency. Most systems use several constant frequencies that are treated independently. Although the secondary field has the same frequency as the primary field, it will have a different amplitude and phase. It is customary to separate the secondary response into two components, in-phase and quadrature. The in-phase component is defined as having the same phase as the transmitter waveform whilst the quadrature component is shifted in phase by 90 degrees to the in-phase component.

For time-domain systems, a time-varying field is created by a current that may be pulsed or stepped (Dobrin and Savit, 1988; Smith and Annan, 1997). The time-rate of change of the magnetic field associated with the transmitted current induces an electrical current in the ground that persists after each pulse (or step) of the primary field after the transmitter primary field is turned off. Typical time-domain receiver coils measure the rate of change of this secondary field. The time-domain transmitter current waveform repeats itself periodically (Grant and West, 1965) and can be transformed to the frequency domain where each harmonic has a specific amplitude and phase. The response from a time-domain system can also be decomposed into a "time-domain in-phase" and "time-domain quadrature" components. The time-domain in-phase component is dominated by the time-varying primary field, which repeats with a characteristic period T

(corresponding to a base frequency f =1/T) (Smith, 2001a). The transmitter signal is composed of an on-time and an off-time. The on-time is the portion of the signal that occurs when the transmitter is actively sending a pulse of current through the transmitter loop. The off-time occurs when there is no current sent through the transmitter loop. There is little in-phase response during the off-time, so most of the off-time current pulses (or transients) must be quadrature signal and therefore associated with the secondary response from the ground (Annan, 1983; Palacky and West, 1991).

Figure 1.2 illustrates a typical time-domain waveform. This diagram shows the primary signal from the transmitter and the response of the primary as it is measured at the receiver (Palacky and West, 1991). It also shows the secondary response from the ground as two components: time-domain in-phase, and time-domain quadrature. The secondary in-phase response is the same shape as the primary in-phase response. There are several methods to separate and remove the primary field from the secondary field, as discussed by Telford et al. (1990). However, these methods do not necessarily work for systems measuring on-time signal or the secondary in-phase response. For example, one such method of separating and removing the primary field from the secondary field that works for off-time systems involves removing anything with the same shape as the primary in-phase (Smith, 2001a). This method removes not only the primary in-phase response, but also the secondary in-phase response.

Geophysical electromagnetic exploration has successfully employed airborne technology throughout the world for more than 50 years (Fountain, 1998). Efficiency and speed of

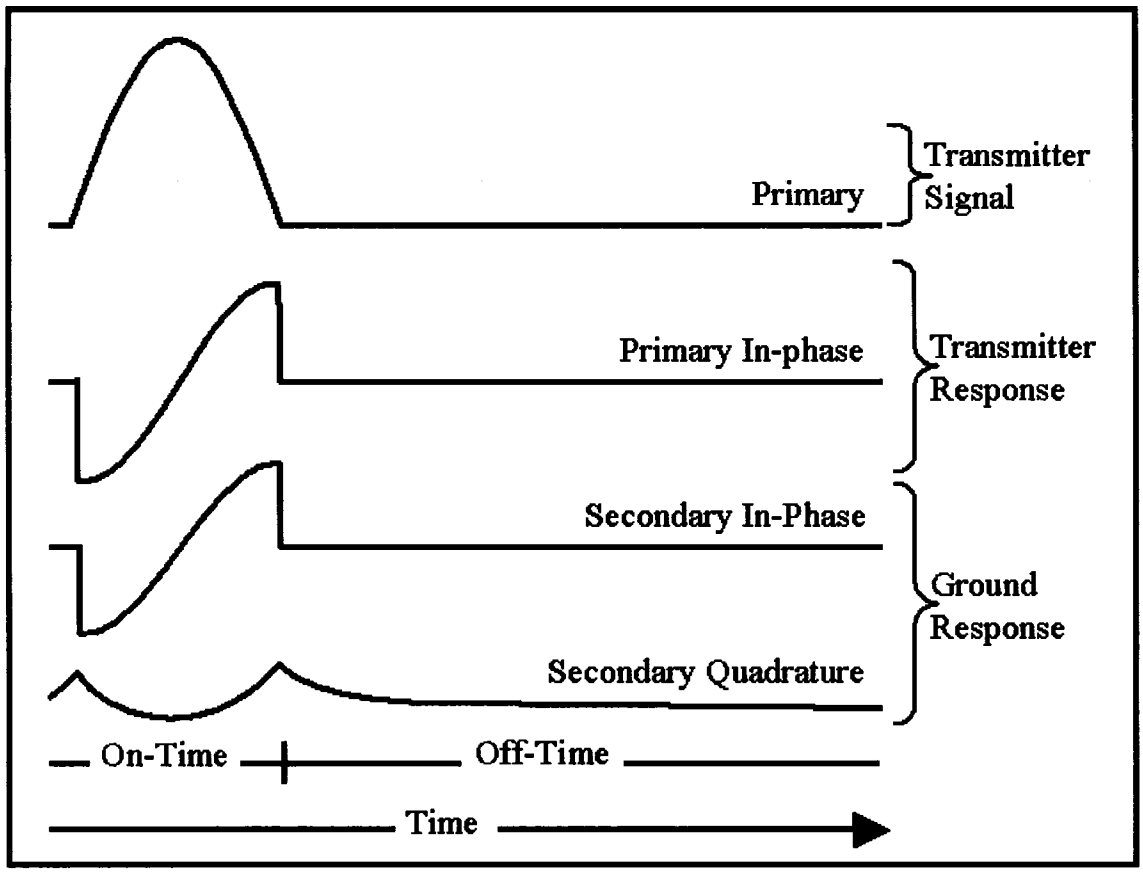


Figure 1.2: Typical time-domain half-sine "primary" waveform output from the transmitter. The "primary in-phase" is the signal from the transmitter as measured at the receiver. The "secondary in-phase" and the "secondary quadrature" are the in-phase and quadrature components of the ground response respectively.

coverage are among some advantages compared with conventional terrestrial survey techniques. After WWI and WWII, the objective of the earliest airborne systems was almost exclusively for the exploration of sulphide mineralization. Published examples of successful case histories include Wolfgram and Golden (2002), Hammack and Mabie (2002), and Smith et al. (2003). More recent systems have a greater depth of exploration, attributed to higher signal to noise ratios. These systems also offer a greater variety of derived products for interpretation that may depend on the geology of the target area. These derived products may include time constant calculations, apparent conductance/conductivity, chargeability, and conductivity depth transforms/inversions. For these reasons, the use of this technology has been extended from its traditional use in mineral exploration to a greater variety of applications ranging from petroleum exploration (Paine et al., 1997), hydrogeology (Smith et al., 2004), and environmental research (Beamish and Mattsson, 2003; Shang et al., 2001).

Currently, there are several electromagnetic geophysical airborne systems available operating in both the frequency-domain and the time-domain. Time-domain airborne surveys can be flown from a fixed-wing aircraft or a helicopter. Regardless of the specific time-domain electromagnetic system used, the movement between the transmitter and receiver creates changes in the signal at the receiver. The amount of signal depends on the system configuration and is directly related to the nominal position of the receiver with respect to the transmitter and the amount of movement between the two. In this thesis, four different systems are considered: GEOTEM, GEOTEM+, HeliGEOTEM and a Generic Concentric system. GEOTEM+ is a proposed modification

to the existing and well-established technology of GEOTEM. Both systems are fixed-wing and therefore allow for rapid data collection. The HeliGEOTEM system is new on the market and similar to the Generic Concentric configuration in that they are both helicopter systems. The Generic Concentric configuration is a fictional helicopter system that uses a common configuration and is used to allow comparison with existing concentric systems currently on the market. Time-domain helicopter systems are a fairly recent development only becoming available for commercial use in the last five or so years. There are several advantages for helicopter systems over fixed-wing systems, including slower flight speed, the ability to fly over more variable or rugged terrain and the lack of the need for a runway. Also, helicopter systems can be transferred to any number of different helicopters, whereas fixed-wing systems are permanently fixed to a specific aircraft.

The four different configurations analyzed in this thesis are considered to cover the broad spectrum of systems available on the market today. Also, this selection of systems including the largest to the smallest transmitter-receiver offset in order to investigate the relationship between the primary field and geometric noise in a more general way. These four systems were also chosen to allow comparison between existing and well-established technology with cutting-edge developments in geophysics exploration.

### 1.5.1 The GEOTEM System

GEOTEM is the most widely used time-domain electromagnetic airborne survey systems. It is operated by Fugro Airborne Surveys[1] of Ottawa, Ontario, Canada. First introduced in 1985, it has continually been updated to provide an airborne geophysical exploration system with proven success worldwide (Fountain, 1998). The system is installed on a CASA C-212 aircraft as shown in Figure 1.3. The transmitter is attached directly to both wing tips and the nose and tail of the aircraft, and consists of a series of six turns of aluminum loop wires. The receiver is towed below and behind the aircraft on a reinforced cable. It consists of three coils; one coil has a vertical axis and two have a horizontal axis, all of which are enclosed in a hard aerodynamic casing. One horizontal axis coil points in the flight direction, and the other is 90 degrees from it so as to complete the orthogonal set. The transmitter has the flexibility to permit variation of the base frequency, pulse width and off-time period. Also, the location of the measurement times (windows) can be adjusted. This flexibility allows the GEOTEM system to adapt to various ground conditions and gather responses diagnostic of the intended target. The nominal transmitter-receiver distance for the GEOTEM system is estimated to be 130 metres behind the transmitter loop and 50 metres below. The transmitter is in the shape of a non-equilateral hexagon with an area of approximately 230 square metres ($m^2$).

### 1.5.2 The GEOTEM+ System

GEOTEM+ is a hypothetical configuration intended to be a cost-effective improvement with very little change to the existing GEOTEM system. The thought is that with a

[1] www.fugroairborne.com


Figure 1.3: GEOTEM operated by Fugro Airborne Surveys. The transmitter consists of a series of 6 loops that are attached directly to the aircraft. The receiver is towed behind on a long cable. (From www.fugroairborne.com)

longer cable the error due to geometrical variations between the transmitter and the receiver will have significantly less impact. The proposed GEOTEM+ system has the same aircraft, transmitter and receiver as the GEOTEM system but the relative distance between the transmitter and the receiver is greater. Hence, it is subject to a similar type of error associated with the transmitter and receiver geometry as for the GEOTEM system. Although the GEOTEM+ system would use the same aircraft and transmitter as the GEOTEM system, the receiver would be 250 metres behind and 70 metres below the aircraft.

### 1.5.2 The GEOTEM+ System

The proposed GEOTEM+ system has the same aircraft, transmitter and receiver as the GEOTEM system but the relative distance between the transmitter and the receiver is greater (the receiver would be 250 metres behind and 70 metres below the aircraft). Hence, it is subject to a similar type of error associated with the transmitter and receiver geometry as for the GEOTEM system.

### 1.5.3 The HeliGEOTEM System

Although still under development, HeliGEOTEM is designed to combine the capability of GEOTEM with the flexibility of a helicopter system. HeliGEOTEM (Figure 1.4) is configured quite differently from the GEOTEM and GEOTEM+ systems. Besides being a helicopter system, the most apparent difference is that the receiver is above and in front of the transmitter instead of below and behind. This geometry positions the transmitter

closer to the ground than the receiver, and therefore, is able to excite the ground with a stronger magnetic field using a smaller current. Part of the motivation for positioning the much heavier transmitter below the receiver is to stabilize both the transmitter and receiver with respect to one another and minimize transmitter-receiver geometric variations.

Although the transmitter and the receiver are separated, the distance is not a great as in the GEOTEM or GEOTEM+ systems. The transmitter is powered by a generator that is contained within the loop unlike both fixed-wing systems that draw their power from the aircraft generators. The estimated position of the receiver for the HeliGEOTEM system is 20 metres in front of and 35 metres above the centre of the transmitter. The transmitter loop is two circular turns of aluminum pipe with a radius of 5.5 metres

### 1.5.4 The Generic Concentric System

Although there are several time-domain helicopter systems commercially available, most are configured with the transmitter and the receiver loops having coincident centre points. Although the specifications vary from system to system, the transmitter loop typically has a diameter between 5 and 15 metres. For the purposes of this analysis, a representative system has been selected to compare a Generic Concentric configuration with the other systems analyzed. A transmitter of 5 metres radius and a dipole receiver have been selected. These values are representative of the concentric systems currently available on the market. However, the exact diameter is not important for the purposes of this analysis. AeroTEM (Figure 1.5) is an example of a concentric system that is operated by

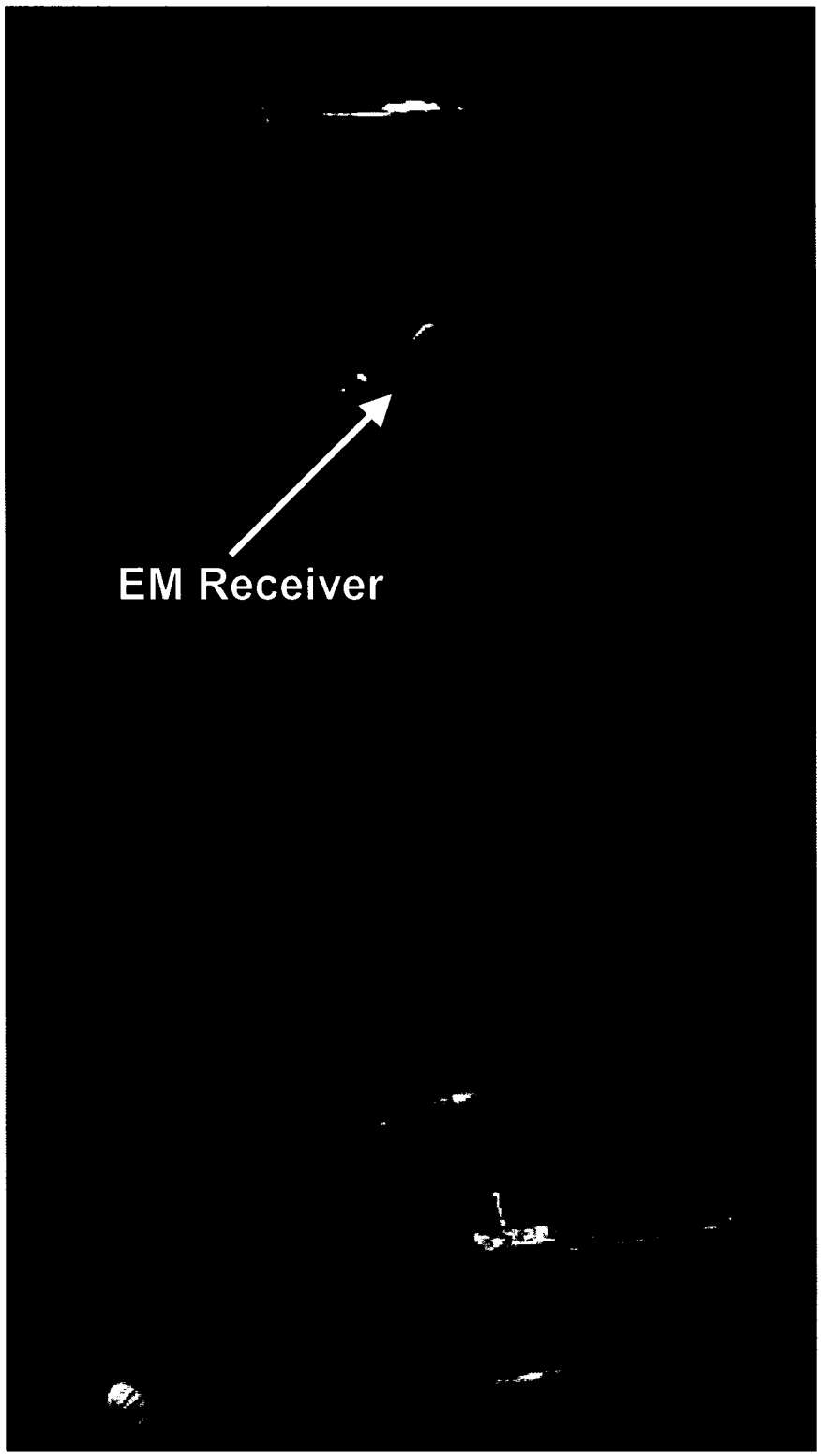


Figure 1.4: HeliGEOTEM operated by Fugro Airborne Surveys. The transmitter is suspended from a long cable. The small receiver is suspended between the aircraft and the transmitter (bottom), on the same cable that supports the transmitter. (From www.fugroairborne.com.)

Aeroquest Limited[2] from Milton, Ontario, Canada. Another example is the VTEM system (Figure 1.6) operated by Geotech Limited[3] from Aurora, Ontario, Canada.

### *1.6 Structure of Thesis*

This thesis investigates the effect on the primary field from changes in the transmitter and receiver geometry of the various airborne electromagnetic systems presented above. Since the subject matter of the thesis is concerned with a very specific aspect of electromagnetic geophysics, Chapter One is a brief introduction.

Chapter Two states the problem addressed in the thesis. This chapter describes the general and specific objectives of the thesis and offers a comprehensive justification of the causes and complexities of the problem. The problem section describes the geometric variations and offers an explanation as to why this impairs the ability of an electromagnetic system to detect targets of high conductance.

Chapter Three is dedicated to describing, in detail, how the analysis was accomplished. The methodology presents the framework of the analysis starting from the theory and the software utilized. This chapter gives a breakdown of the various calculations and presents the verification procedures that ensure the results are accurate.

---

[2] www.aeroquestsurveys.com
[3] www.geotechairborne.com

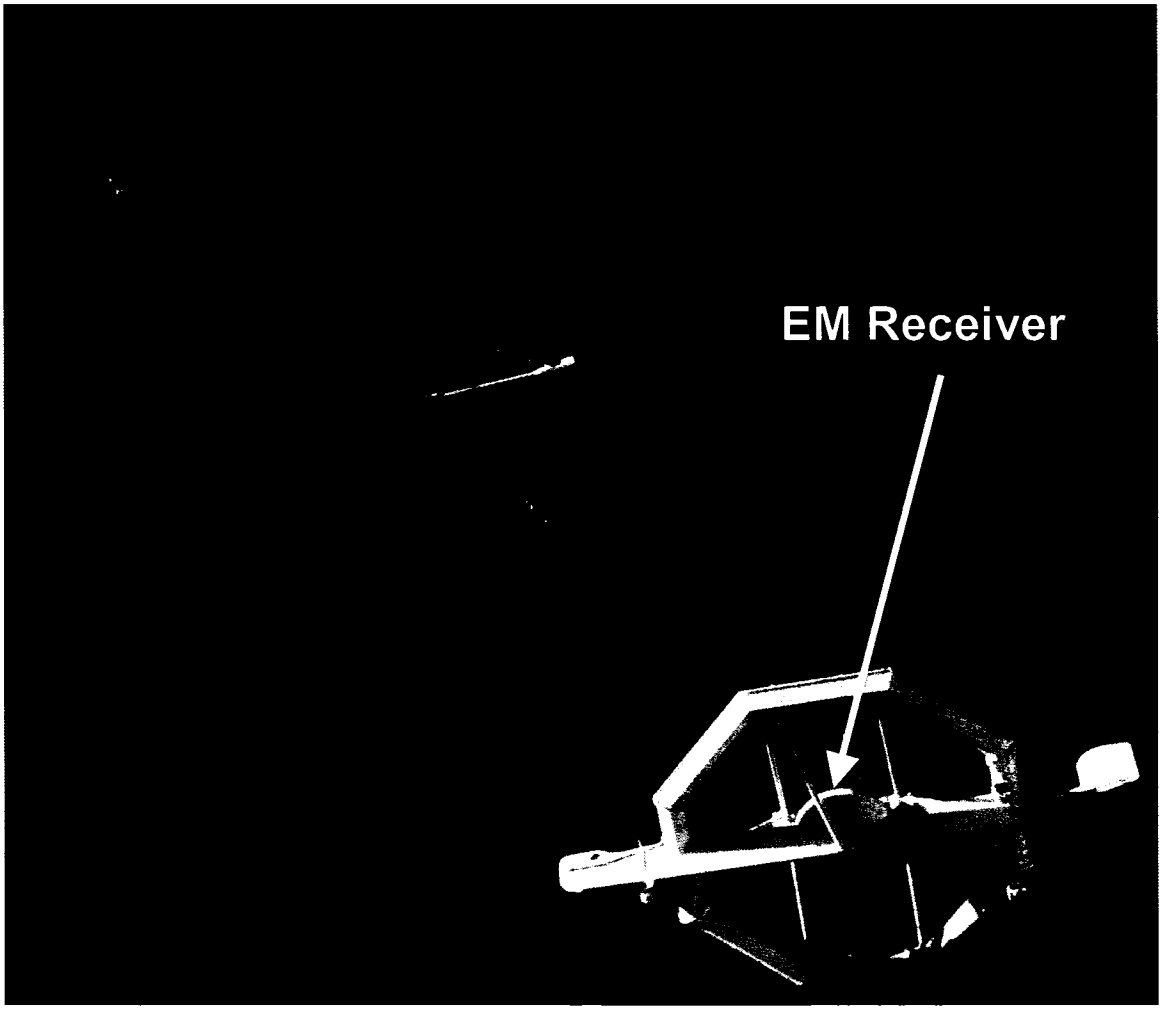


Figure 1.5: AeroTEM operated by Aeroquest Limited. The receiver is located in the centre of the transmitter loop. A magnetic sensor is located partway up the cable that supports the transmitter and receiver. (Photo courtesy of Sean Scrivens.)

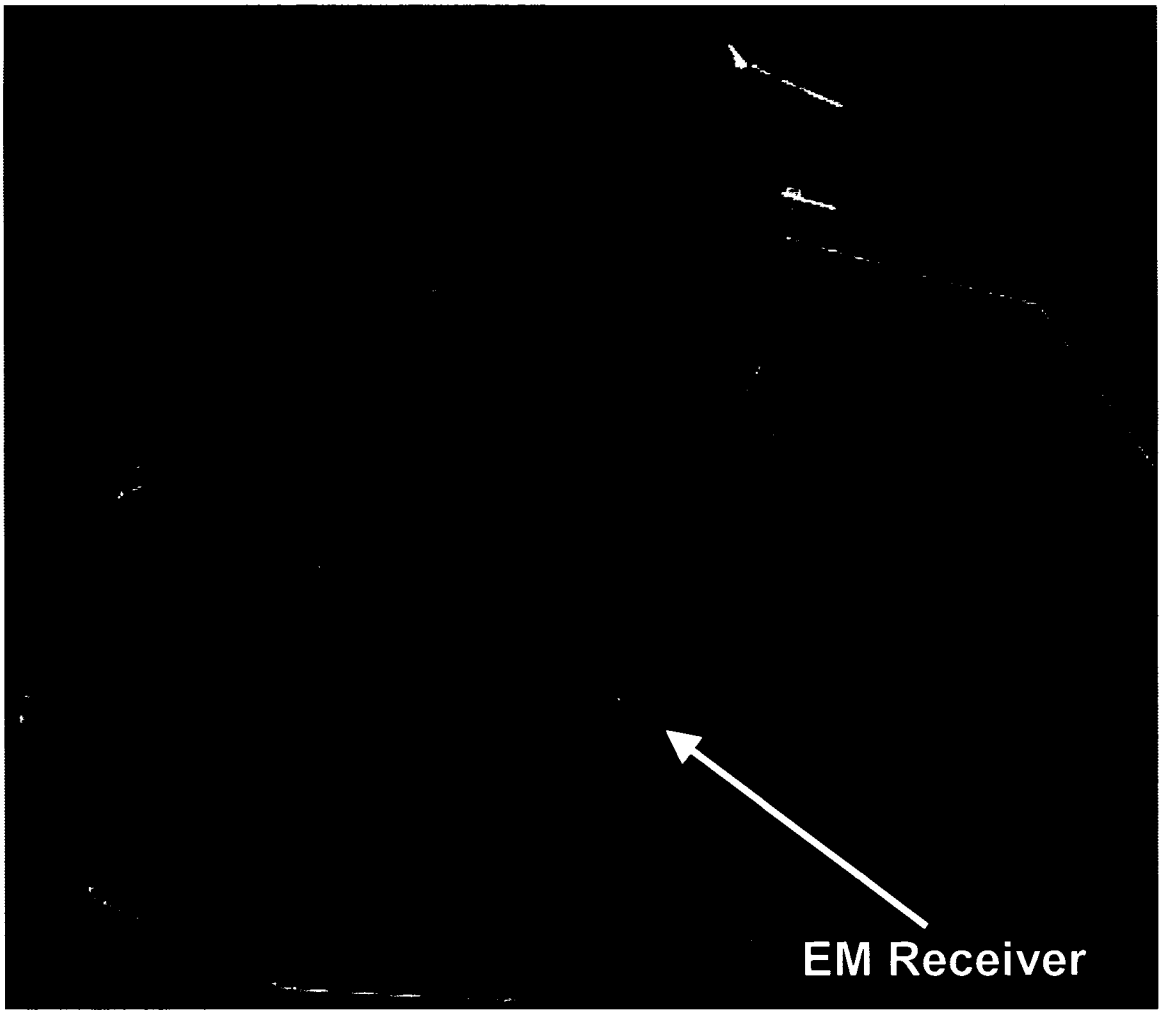


Figure 1.6: VTEM operated by GEOTECH limited. The small receiver coil is located in the centre of the larger transmitter loop. A magnetic sensor is located partway up the cable that supports the transmitter and the receiver. (From www.geotechairborne.com)

In Chapter Four, the results for the variations in receiver position, variations in transmitter attitude, and transmitter loop deformation are presented for each system.

Chapter Five includes an analysis of the results for each system, and concludes with a comparison of all the systems. It also introduces potential solutions to the problem of geometric variations.

Chapter Six summarizes and highlights the key findings of this research project.

## 2. Statement of problem[4]

### *2.1 Objective*

This thesis investigates the effect that changes in the transmitter and receiver geometry of various electromagnetic systems have on the primary field (which is, by definition, in-phase). The receiver measures both the transmitted primary field and the secondary field. The secondary field is determined by subtracting the primary field from the measured total response at the receiver. However, the primary field at the receiver varies with the transmitter and receiver geometry. Therefore, the ability to monitor these geometric changes would offer the capability of predicting the changes in the primary field and hence estimating the residual secondary in-phase response. The ability to estimate this secondary in-phase would improve our ability to locate highly conductive targets below the ground surface.

The objective of this thesis is to show how the transmitter and receiver move with respect to one another; demonstrate why movement between the transmitter and the receiver compromises a system's ability to detect targets of high conductance; and estimate the necessary accuracy for the movements to be known in order to detect targets of high conductance. Ultimately, the goal of this analysis is to provide guidelines on the accuracy needed to measure the variations in transmitter-receiver geometry for successful measurement of the in-phase response and hence detection of very high conductance targets. For the analyses presented in this thesis, the origin of the coordinate system for

[4] The material presented in this chapter is adapted from Hefford et al. (2006). Hefford is the first author and the main contributor to the material in this paper.

each system is set to the centre of the transmitter with the following orientation conventions; $x$ as horizontal and positive in the direction opposite to the flight direction; $z$ as vertical and positive upwards; and $y$ as horizontal and directed to form a right-hand coordinate system (Figure 1.1). The attitude of the aircraft is characterized by the roll, pitch and yaw, where these are defined as the rotation angles about the $x$-, $y$- and $z$- axes, respectively. By convention, the rotations are positive if they are clockwise when viewed along the axis of rotation pointing towards the origin.

### *2.2 Variations in system geometry*

During survey flying, each system attempts to maintain a nominal transmitter altitude. As the terrain changes, the aircraft must adjust to maintain constant altitude, which as a consequence causes temporal and spatial changes in the speed and attitude of the aircraft. As the aircraft adjusts according to the terrain, the transmitter and the receiver also move with respect to one another (Annan, 1983). Data collected by the GEOTEM system acts as a good example of how variations in the relative position of the transmitter and the receiver affect data. Figure 2.1 shows the estimated receiver locations for a short straight flight by the GEOTEM system for a segment of 240 seconds (Smith, 2001b). The receiver typically moves by ± 5 metres in all three directions. It is seen that occasionally, the receiver varies its position by as much as 20 metres in the $x$- and $z$-directions and by as much as ~35 metres in the $y$-direction. For this segment of the test flight, the receiver was also affected by strong crosswinds, which cause a bias in the $y$-offset.

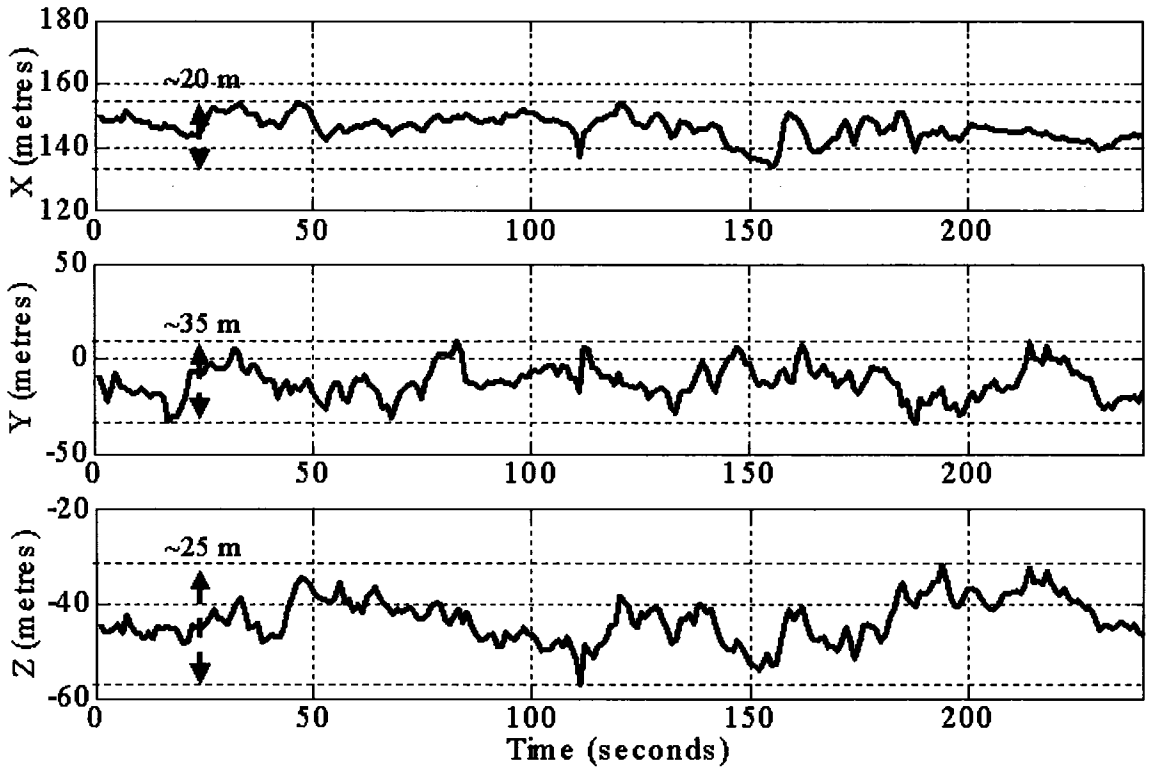


Figure 2.1: Estimated $x$, $y$, and $z$-positions of the receiver with respect to the transmitter centre for a typical GEOTEM straight flight segment. Variation in the $x$-distance is ~20 metres, variation in the $y$-distance is ~35 metres, and variation in the $z$-distance is ~25 metres.

The variation of the transmitter attitude during the same flight segment as reported by the aircraft navigation instruments are illustrated in Figure 2.2. It can be seen that the roll and pitch of the aircraft varies by ~17 degrees compared to ~5 degrees for the yaw. This relative motion means that the in-phase primary field response varies considerably. Changes in the attitude of the transmitter have an effect similar to moving the position of the receiver as seen in Figure 2.2. For example, if the transmitter was to pitch its front down, it would have a similar effect on the primary field as moving the receiver some distance closer to the transmitter along the $x$-direction thereby changing the amount of primary field measured at the receiver. The complexity associated with the roll, pitch, and yaw of the receiver coils is removed from this analysis by combining them into a total component that is independent of orientation.

Changing the speed and the attitude of the transmitter also leads to deformation of the transmitter loop segments. The amount of deformation of the transmitter loop segments is dependent on the material and configuration of the transmitter loop itself as well as the flying conditions. Variations in transmitter loop shape not only alter the area of the loop but also are similar to changing the aircraft attitude. Certain types of loop deformation are analogous to movement of the receiver. For example, a movement that involves the front and rear loop segments moving in opposite $z$-directions is equivalent to the aircraft changing pitch. Similarly, if the loop segments on one side of the aircraft move down while those on the other side move up, the resultant effect would be equivalent to an aircraft roll. Changing the speed and the attitude of the transmitter also leads to

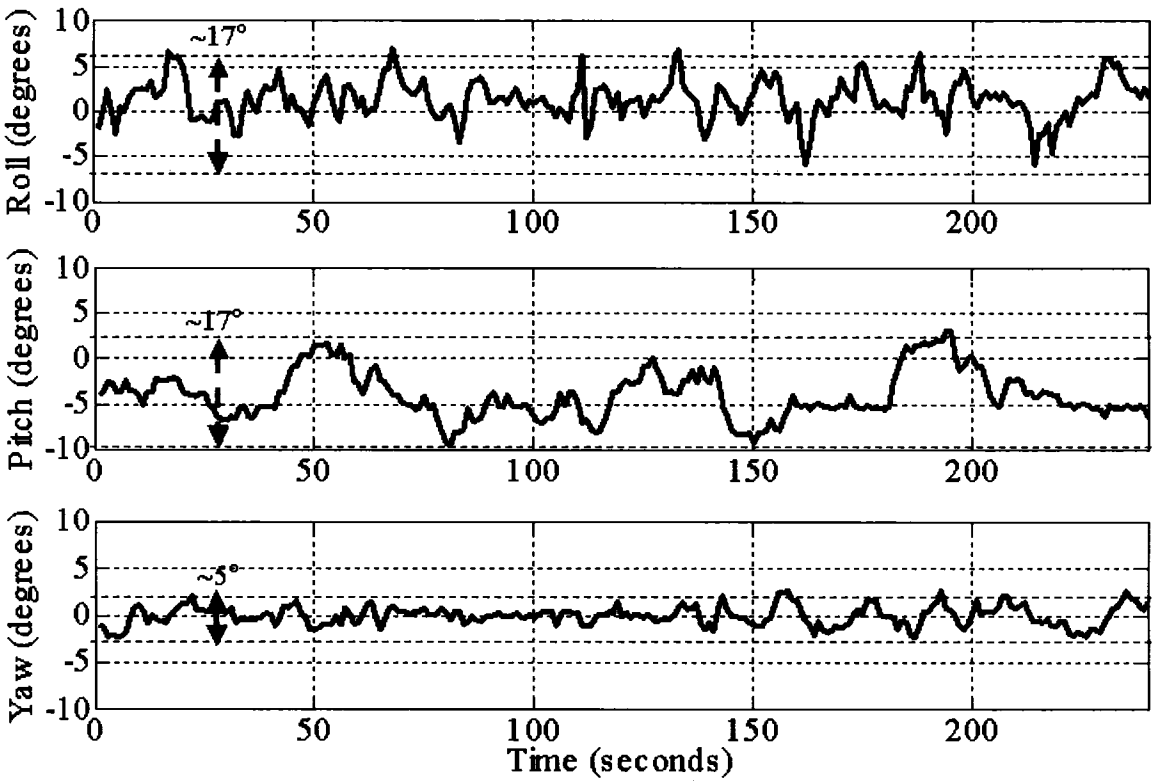


Figure 2.2: Transmitter attitude during the same flight segment as in Figure 2.1, as reported by the aircraft navigation instruments. The roll varies by ~17°, the pitch varies by ~17° and the yaw varies by ~5°.

deformation of the transmitter loop segments. The amount of deformation of the transmitter loop segments is dependent on the material and configuration of the transmitter loop itself as well as the flying conditions. Variations in transmitter loop shape not only alter the area of the loop but also are similar to changing the aircraft attitude. Certain types of loop deformation are analogous to movement of the receiver. For example, a movement that involves the front and rear loop segments moving in opposite $z$-directions is equivalent to the aircraft changing pitch. Similarly, if the loop segments on one side of the aircraft move down and on the other side move up, the resultant effect would be equivalent to an aircraft roll.

For the analyses presented in this thesis, the fixed-wing systems (GEOTEM and GEOTEM+) have a nominal altitude of 120 metres. This positions the receiver at a nominal altitude of 70 and 50 metres above the topography for each system, respectively. Since the transmitter is mounted on the aircraft for a fixed-wing system, its attitude is approximately the same as the aircraft attitude. The nominal pitch of the aircraft and transmitter is 4 degrees nose up at survey altitude during straight and level flying. The nominal roll and yaw are zero under the same conditions. The configurations for the GEOTEM and GEOTEM+ systems are summarized in Table 2.1. The helicopter systems (HeliGEOTEM, Generic Concentric) use a mean transmitter altitude of 35 metres and the nominal attitude of the transmitter is assumed to be zero for roll, pitch and yaw. The configurations of the HeliGEOTEM and Generic Concentric systems are summarized in Table 2.2. Table 2.3 provides the specifications for various other systems currently available.

| | | Fixed Wing | |
|---|---|---|---|
| | | GEOTEM | GEOTEM+ (Long Cable) |
| Platform | Flying height | 120 m | 120 m |
| | Flying speed | 200 km/h | 200 km/h |
| | Tow cable length | 135 m | 270 m |
| | Total area | 230 $m^2$ | 230 $m^2$ |
| | Loop turns | 6 | 6 |
| | Current | 500 A | 500 A |
| Transmitter | Peak dipole moment | 690,000 $Am^2$ | 690,000 $Am^2$ |
| | Height above ground | 120 | 120 |
| | Number of coils | 3 | 3 |
| | Orientation | Orthogonal *X, Y, Z* -Coils | Orthogonal *X, Y, Z* -Coils |
| | Vertical separation | 50 | 70 |
| Receiver | Horizontal separation | 130 | 250 |
| | Height above ground | 70 | 50 |
| | Shape | Half-Sine | Half-Sine |
| Waveform | Time-derivative | Half-Cosine | Half-Cosine |
| | Operating frequency | Selectable (12.5-150 Hz) | Selectable (12.5-150 Hz) |
| | Pulse width | 1 - 8 ms | 1 - 8 ms |
| | Length of off-time | Up to 36 ms | Up to 36 ms |
| | Sampling rate | 384 kHz | 384 kHz |

Table 2.1: Specifications for the fixed-wing systems analyzed in this thesis (GEOTEM and GEOTEM+).

| | | Helicopter | |
|---|---|---|---|
| | | HeliGEOTEM | Generic Concentric |
| Platform | Flying height | 80 m | 80 m |
| | Flying speed | 60 km/h | 60 km/h |
| | Tow cable length | 60 m | 60 m |
| | Total area | 190 $m^2$ | 160 $m^2$ |
| | Loop turns | 2 | 2 |
| | Current | ? | ? |
| Transmitter | Peak dipole moment | 230,000 $Am^2$ | ? |
| | Height above ground | 35-40 m | 35 m |
| | Number of coils | 3 | 3 |
| | Orientation | Orthogonal *X, Y, Z* -Coils | Orthogonal *X, Y, Z* -Coils |
| | Vertical separation | 35 | 0 |
| | Loop Radius | 5.5 metres | ? |
| Receiver | Horizontal separation | 20 | 0 |
| | Height above ground | 80 | 35 |
| | Shape | Half-Sine | ? |
| Waveform | Time-derivative | Half-Cosine | ? |
| | Operating frequency | Selectable (12,5 - 150 Hz) | ? |
| | Pulse width | 1 - 8 ms | ? |
| | Length of off-time | Up to 36 ms | ? |
| | Sampling rate | 384 kHz | ? |

Table 2.2: Specifications of helicopter systems analyzed in this thesis (HeliGEOTEM and a Generic Concentric system).

| | | Helicopter | | |
|---|---|---|---|---|
| | | VTEM | Generic Concentric | AeroTEM |
| | Type | Helicopter | Helicopter | Helicopter |
| Platform | Flying height | ? | 80 m | 80 m |
| | Flying speed | up to120 km/h | 60 km/h | 60 km/h |
| | Tow cable length | ? | 60 m | 50 m |
| Transmitter | Total area | 500 $m^2$ | 160 $m^2$ | 19.8 $m^2$ |
| | Loop turns | 3 | 2 | 8 |
| | Current | 250 A | ? | 250 A |
| | Peak dipole moment | up to 500,000 NIA | ? | 40,000 $Am^2$ |
| | Height above ground | 30 m | 35 m | 30 m |
| | Number of coils | 1 | 3 | 2 |
| | Loop Radius | 7.5 metres | ? | 2.5-6 metres |
| Receiver | Orientation | Vertical Z | Orthogonal *X, Y, Z* -Coils | Orthogonal *X, Z* -Coils |
| | Vertical separation | 0 | 0 | 2.5 m |
| | Horizontal separation | 0 | 0 | 0 |
| | Height above ground | 30 | 35 | 30 |
| Waveform | Shape | Trapezoid | ? | Triangular |
| | Time-derivative | ? | ? | Step Response |
| | Operating frequency | 25-200 Hz | ? | 150 Hz |
| | Pulse width | 1-10 msec | ? | 1.1 ms |
| | Length of off-time | ? | ? | 2.2 ms |
| | Sampling rate | up to 200 kHz | ? | 128 |

Table 2.3: Specifications of various concentric helicopter systems currently available for commercial service.

Figure 2.3 shows the total primary field response as measured at the receiver for the same flight segment as in Figures 2.1 and 2.2. During this flight segment, the system is flown at a very high altitude so as to minimize the ground response. This enables us to consider the secondary field (i.e. ground response) negligible. The amount of variation is ~240000 parts per million (PPM) and can be attributed primarily to variations in the transmitter-receiver geometry. The measured response consists of the primary field (or transmitted signal) plus the secondary in-phase component (or ground response). Without the capability to accurately measure the primary field, the ability to correctly separate the primary field from the in-phase secondary field component is severely diminished.

At present, there is no direct method to accurately determine the geometric variations between the transmitter and the receiver (Samson et al., 2004) or determine the transmitter loop deformation. Recent work by Yin and Fraser (2004) and Fitterman and Yin (2004) discusses how variable receiver altitude modulates the ground response as measured by a frequency-domain helicopter airborne system. However, unlike current time-domain airborne systems, the transmitter and receiver in a frequency-domain helicopter system are at a fixed distance from one another and the primary field is easily accounted for. As the main focus in this analysis is the primary field, the secondary field (i.e. the ground response) is not considered. Zandee et al. (1985) has suggested a method to remove receiver motion for TDEM systems. However, this method has met with limited success, as it does not account for all geometric variations between the transmitter and the receiver or for transmitter deformations.

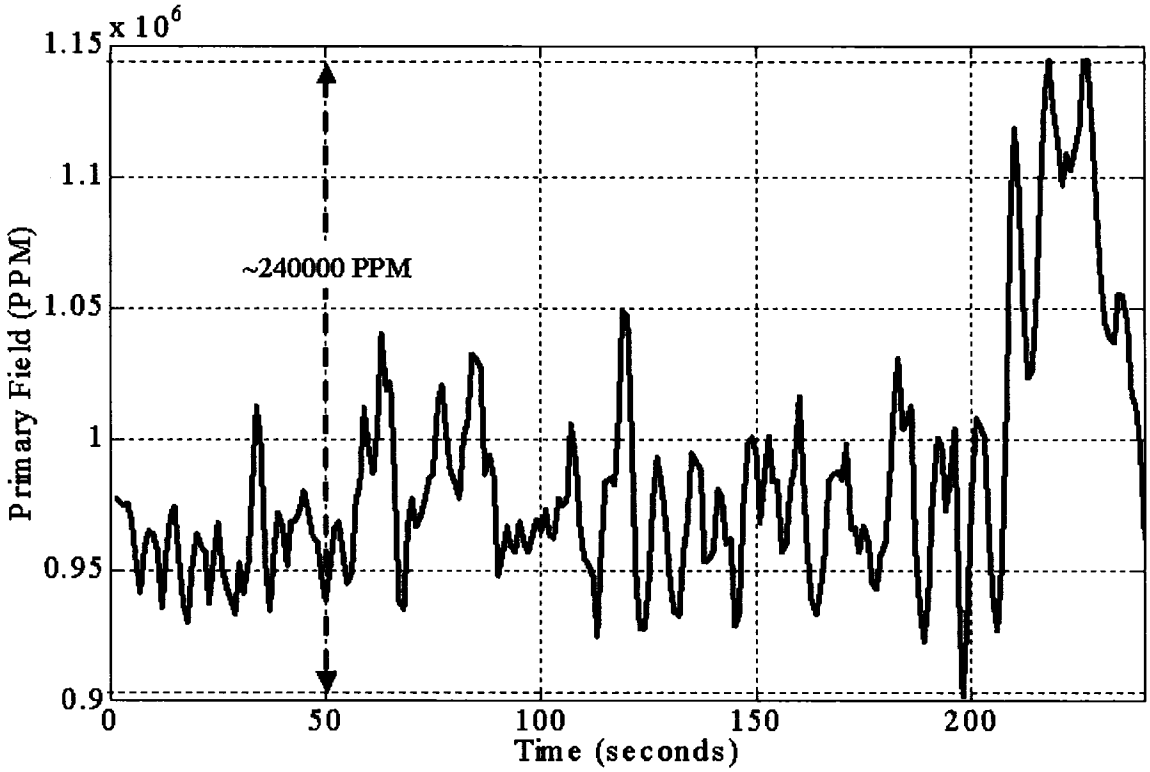


Figure 2.3: Total primary field for the flight segment presented in Figures 2.1 and 2.2 as measured from a high altitude to negate any ground effects. The primary field measured at the receiver varies by ~240000 PPM for this sample data.

Several considerations of minimizing and removing the primary field are outlined by Palacky and West (1991). This includes the method currently utilized by the GEOTEM system where the system first flies at a high altitude, free from a secondary field, to determine the characteristic waveform of the primary field. This characteristic waveform is subsequently used as a template of the primary field of which to remove from the data collected during survey flying. Additional detail on this method is presented by Smith (2001a), which also outlines some of the potential problems encountered with separating and removing the primary field and determination of the receiver location. Subsequent work by Smith (2001b) offers a method to estimate the relative positions but does not take into account the effects of the transmitter loop shape.

The aforementioned methods to estimate receiver position assume a resistive environment or that there is no secondary field response and therefore, breakdown over conductive areas. Consideration to the receiver position in conductive environments is presented in Vrbancich and Smith (2005). This thesis compares the receiver offsets obtained from both uncorrected (free-space) and corrected (inductive-limit) primary fields from survey data recorded over seawater, in order to understand the limitations of these two methods.

Currently there is no literature that discusses the effect of variations of the transmitter and receiver offset, transmitter loop deformation, or transmitter attitude for the different time-domain EM survey systems currently available on the market. This is the key problem addressed in this thesis and its original contribution. It is important to note that the

objective is to compare the effect that each movement has on the primary field measured at the receiver and not the amount of movement between the transmitter and receiver for the different configurations.

### *2.3 Detection of highly conductive targets*

Examples given by Balch (2000) illustrate the ability of various electromagnetic systems to detect and identify the Voisey's Bay Ni-sulphide deposit. It is shown that although the GEOTEM system was successful in the detection of the deposit, it did not discriminate it as a highly conductive target. This inability to discriminate between moderate and highly conductive targets is partly due to a common limitation of most electromagnetic exploration systems, namely the necessity for a constant (or known) relative geometry of the transmitter and receiver. Frischknecht et al. (1991) briefly discusses the error associated with the geometric variation of various electromagnetic system configurations.

Figure 2.4 illustrates the GEOTEM in-phase and quadrature responses as a function of transmitter frequency, for a thin vertical plate conductor with infinite lateral extent cropping out at surface and extending to a depth of 300 metres. The response is calculated for a target of three different conductances: from 100 Siemens (medium conductance) such as a disseminated sulphide deposit; 1000 Siemens (good conductance) such as a massive sulphide deposit; and 10000 Siemens (very high conductance) such as a massive sulphide deposit that contains significant nickel (e.g. the Voisey's Bay deposit) (Balch, 2000). These responses were calculated using the EMIGMA modeling package

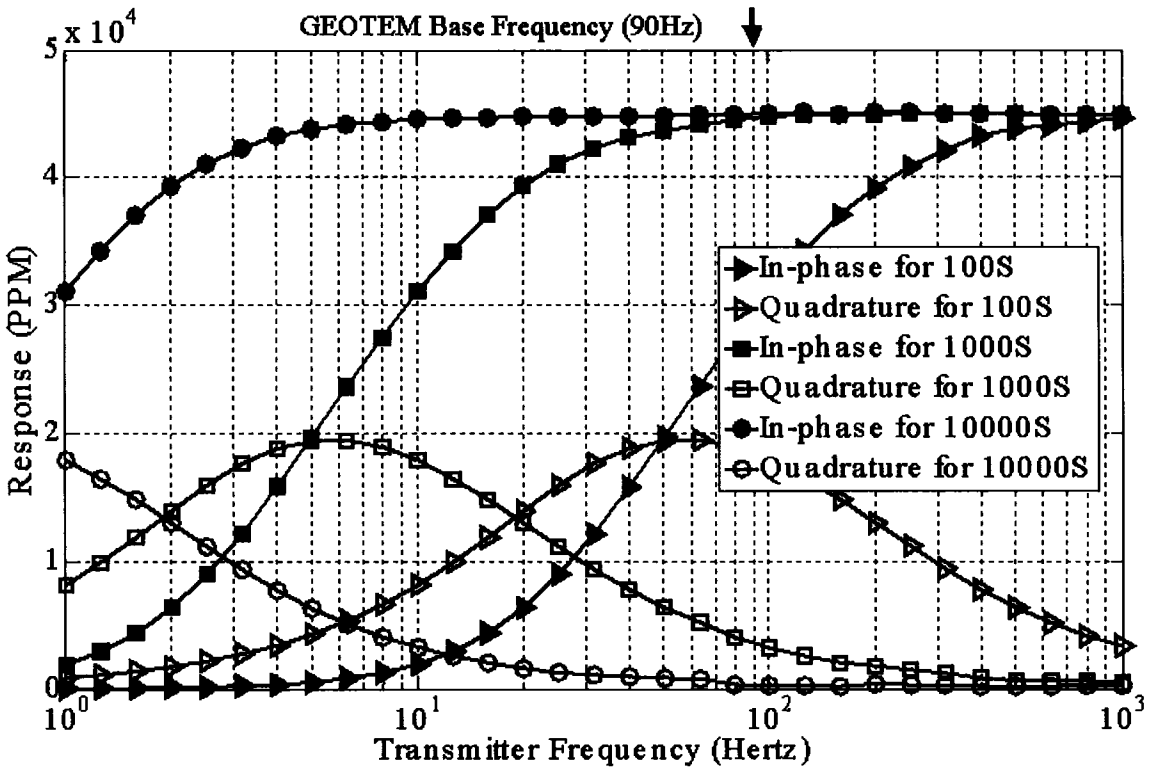


Figure 2.4: The frequency-domain in-phase and quadrature responses for 100 Siemens, 1000 Siemens, and 10000 Siemens conductors as a function of transmitter frequency. GEOTEM normally operates at a base frequency of 90 Hertz (marked by the arrow), which is dominated by the in-phase response for the very conductive targets.

developed by PetRos EiKon Ltd[5] of Concord, Ontario. EMIGMA is an EM modeling package that has been designed to model the response for a variety of targets for a variety of different survey systems and configurations. Deposits with very high conductance are of considerable economic interest and are prime exploration targets. For any given frequency, the response becomes dominated by the in-phase component as the conductance of the body increases. Figure 2.4 shows the GEOTEM in-phase and quadrature responses at a transmitter base frequency of 90 Hertz for a target with a range of conductances. If we consider a target with a conductance of 10000 Siemens, at the nominal GEOTEM base frequency of 90 Hertz, we can see that the response is dominated by the in-phase component and the response from the quadrature component is almost zero. Similar responses can be shown for each of the other configurations. Hence, the in-phase component is more responsive than the quadrature component over highly conductive bodies and the quadrature component is more responsive over weaker conductive bodies (Smith, 2001a). This illustrates the importance of measuring the in-phase response to detect highly conductive bodies in the subsurface.

[5] www.petroseikon.com

# 3. Methodology[6]

## *3.1 Experimental Approach*

The specific geometric variations examined are changes in the position of the receiver with respect to the transmitter, variations in transmitter attitude, and transmitter loop deformation. Each of the variations investigated are specific for the system configurations outlined in Tables 2.1 and 2.2. It is important to note that for this analysis of instrument geometry, any induced field in the ground is ignored, as we are only interested in the changes created in the primary field due to the geometric variations. To reduce the complexity associated with variation in roll, pitch and yaw of the receiver coil, only the total component independent of orientation is calculated at the receiver.

There are several analytical formulae used to calculate the primary field from the transmitter at the receiver. For all the analyses it was important that the formulae chosen have the versatility to calculate the primary field in each of the three Cartesian directions and to perform rotations about these axes. For the analyses of loop deformation, it was also necessary that the formula have the capability to handle various transmitter loop shapes.

All calculations and theoretical analysis has been carried out using the MATLAB program. MATLAB is a high-level technical computing language and interactive environment for algorithm development, data visualization, data analysis, and numeric

[6] The material presented in this chapter is adapted from Hefford et al. (2006). Hefford is the first author and the main contributor to the material in this paper.

computation. This application enabled the programming and calculation of the various parameters spanning an assortment of circumstances. MATLAB also facilitated the manipulation of the data to display and compare the results of each analysis.

### *3.2 Dipole Approximation*

One approximation is to assume that the transmitter can be represented by a dipole, which has a field given by the formula (Smith, 2001b):

$$\boldsymbol{H}(\boldsymbol{r}) = \frac{|M|}{4\pi r^3}\left(\frac{3\boldsymbol{m}\cdot\boldsymbol{r}}{r^2}\boldsymbol{r} - \boldsymbol{m}\right) \tag{1}$$

where $\boldsymbol{H}$ is the primary magnetic field vector as measured in Ampere per metre (A/m), $|M|$ is the magnitude of the dipole moment in $Am^2$, $\boldsymbol{m}$ is the unit vector describing the direction of the transmitter dipole, and the vector $\boldsymbol{r} = (x,y,z)$ is the distance between the receiver and the transmitter centre in metres. This equation assumes that the transmitter is a dipole and therefore does not take into account the size and shape of the transmitter loop.

### *3.3 Roll, Pitch, and Yaw Rotations*

The added complexity of transmitter loop attitude is analyzed by introducing matrices to describe the rotation about each axis, to the formula. The matrices governing rotation are:

$$R_x(\alpha)=\begin{bmatrix}1 & 0 & 0\\ 0 & \cos\alpha & \sin\alpha\\ 0 & -\sin\alpha & \cos\alpha\end{bmatrix},\ R_y(\beta)=\begin{bmatrix}\cos\beta & 0 & -\sin\beta\\ 0 & 1 & 0\\ \sin\beta & 0 & \cos\beta\end{bmatrix},\ \text{and}$$

$$R_z(\gamma)=\begin{bmatrix}\cos\gamma & \sin\gamma & 0\\ -\sin\gamma & \cos\gamma & 0\\ 0 & 0 & 1\end{bmatrix} \quad (2)$$

where $R_x$, $R_y$, and $R_z$ are rotation matrices about their respective axes, and $\alpha$, $\beta$, and $\gamma$ are the aircraft roll, pitch and yaw, respectively measured in degrees. These rotation matrices can be applied to the vector ***m*** describing the orientation of the transmitter.

### *3.4 Biot-Savart Law*

In the case of the GEOTEM and GEOTEM+ systems, the transmitter loop is mounted on the aircraft and is composed of thick aluminum wires. For the HeliGEOTEM system, the loop is a more rigid design of aluminum tubing. A concentric system may have either type of loop. Regardless of the material used, the loop is not completely rigid and is subject to some deformation. In the case of the fixed-wing systems, at several points along the loop, it is free to move over a range of the order of one metre. In the analysis of the Generic Concentric system, it was also important that the formula work for calculating the field within the transmitter loop. To determine the variations of the primary field response for changes in the transmitter loop shape and area, Equation (1) is not suitable as it assumes a dipolar transmitter that implies a fixed shape. By assuming a dipole, Equation (1) also requires that the radius of the transmitter loop is much smaller than the distance between the transmitter and the receiver. A different approach is

necessary to allow for the finite size, finite separation and for variations in the shape and area of the loop. The loop deformation analysis is a static analysis and does not take into account any vibrations that may exist between multiple loop wires. Accounting for the individual transmitter loop wire motions involves a level of complexity beyond the objective of this thesis.

The Biot-Savart Law states that if a wire carries a steady current $I$ in Ampere (A), the magnetic field $d\boldsymbol{B}$ in Tesla ($T$) at a point $P$ associated with a small element, $d\boldsymbol{s}$, is given by the formula:

$$d\boldsymbol{B} = \frac{\mu_o I}{4\pi} \frac{d\boldsymbol{s} \times \boldsymbol{r}}{r^3} \tag{3}$$

where $\mu_o = 4\pi 10^{-7} \mathrm{T \cdot m^2/A}$ and $r$ is the distance, in metres, between the current element $d\boldsymbol{s}$ and the point $P$. This formula, like Equation (1), is a specific form of Ampere's Law.

The primary field at the receiver was calculated by dividing the loop into many small segments and then summing the contributions of each loop segment using the Biot-Savart Law. Although this approach is more computationally intensive, it allows for virtually any shape of the transmitter to be modeled at virtually any offset.

Figure 3.1 shows a comparison between the results from Equation (1) (dipole approximation) and Equation (3) (Biot-Savart Law) for a variety of distances using the GEOTEM configuration. For the Biot-Savart calculations presented in this comparison, a

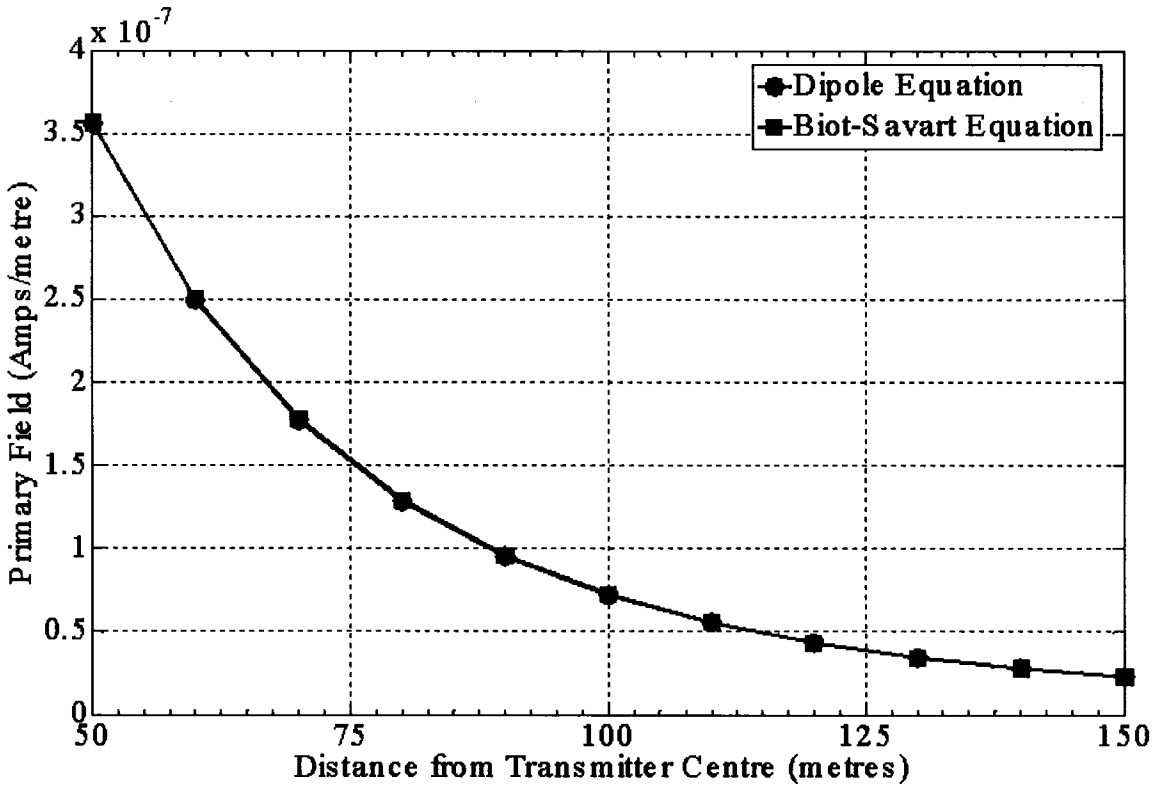


Figure 3.1: The measured primary field response at the receiver for various transmitter-receiver offsets. The response is calculated using two methods, which yield virtually identical results over the range of distances plotted.

square transmitter loop with a small area with respect to the distance between the transmitter and the receiver is used. This figure (Figure 3.1) shows that over a range of distances including distances typical of the GEOTEM system (~130 metres between the transmitter loop centre and the receiver), both formulae yield the same results. Therefore, it is concluded that both formulas are reliable when the distance between the transmitter centre and the receiver is large with respect to the radius of the transmitting loop. Figure 3.2 illustrates that, when the distance between the transmitter and the receiver is much less (distance between transmitter centre and receiver < 25 metres), there is a deviation in the results from the two equations. This deviation is attributed to the breakdown of the dipole formula to correctly calculate the primary field at close proximities of the transmitter loop. For distances closer than ~15 metres, Equation (3) is more reliable and should be used. It is therefore acceptable to use Equation (1) for the GEOTEM, GEOTEM+ and the HeliGEOTEM configurations and necessary to use Equation (3) for the Generic Concentric configuration.

Equation (3) is also used to determine the effect of the transmitter loop deformation on the primary field calculations. For this analysis, the calculation requires a finite number of loop segments. Although this is reasonable for the GEOTEM and the GEOTEM+ configurations since they both have a finite number of loop segments, the HeliGEOTEM and Generic Concentric configurations are circular (i.e. an infinite number of segments are required to model a perfect circle). For these calculations, a polygon with sixteen segments has been used to approximate the circular shape of the transmitter loop. This number of segments was chosen as it provides reasonable accuracy and is not

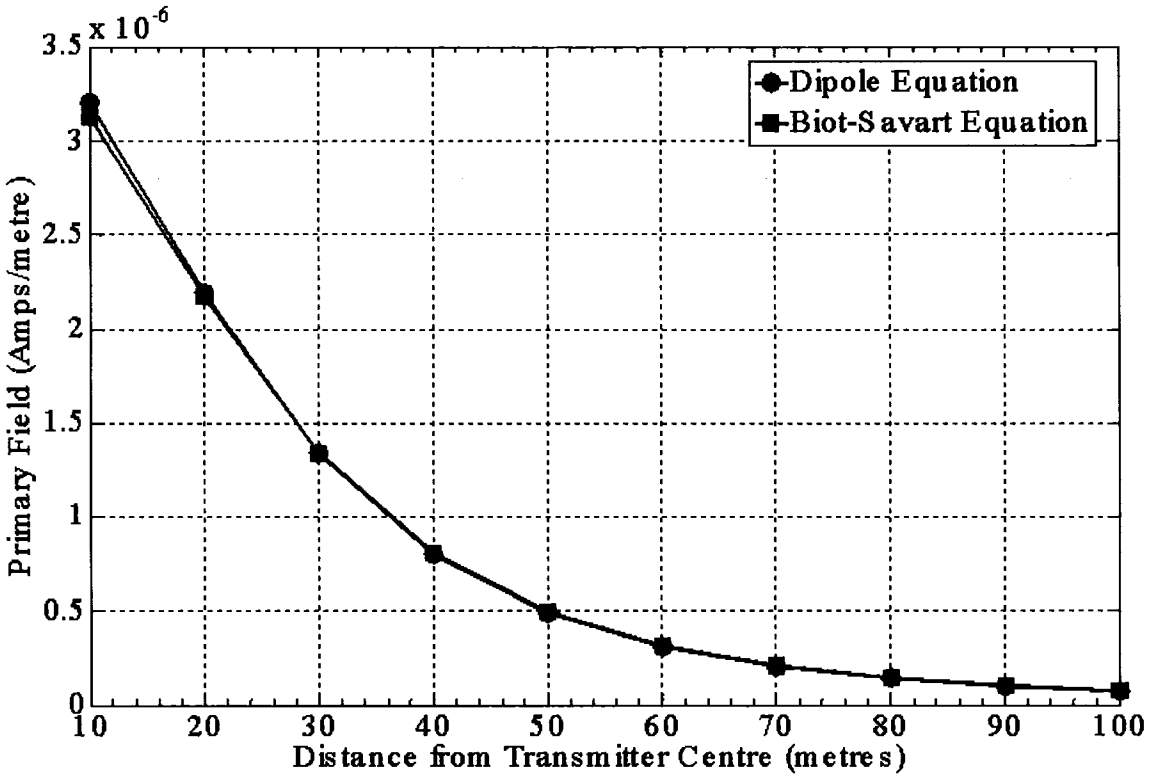


Figure 3.2: The measured response at the receiver for various transmitter-receiver offsets from the nominal position for the GEOTEM configuration. The response is calculated using two methods, which yield virtually identical results over a range of distances greater than ~20 metres.

overwhelmingly computationally intensive. Figure 3.3 is a comparison of the primary field as a function of the number of segments used in the calculation. The greater the number of segments, the closer the polygon resembles a circle. This figure (Figure 3.3) shows how increasing the number of loop segments has little impact on the primary field calculation beyond ~15 segments.

### *3.5 Theoretical Response*

As a second part of the study, the EMIGMA software was used to determine the theoretical in-phase response of each system over a variety of targets. This program is capable of calculating responses in the time or frequency domain. For simplicity, the response at the base frequency of 90 Hertz was calculated in the frequency domain. 90 Hertz is chosen as a reference frequency as it is a typical operating frequency of airborne TEM systems. The target used is a vertical plate 600 metres by 300 metres with a conductance of 10000 Siemens (Figure 3.4). The target was placed at increasing depths ranging from 0 to 350 metres in increments of 25 metres. Figure 3.5 shows the response for each system, as a function of depth, using the theoretical target and a base frequency of 90 Hertz. The objective of this analysis was to determine the in-phase response from the target at various depths so as to compare them to changes in the in-phase response when introducing variations in transmitter-receiver geometry. This analysis illustrates how variations in system geometry compromise the ability of each system to detect and distinguish a highly conductive target at various depths. The criteria for successful target detection has been set when the in-phase response is at least 3 times greater than the noise level caused by geometric variations, that is, when the signal-to-noise ratio is S/N $\geq$3.

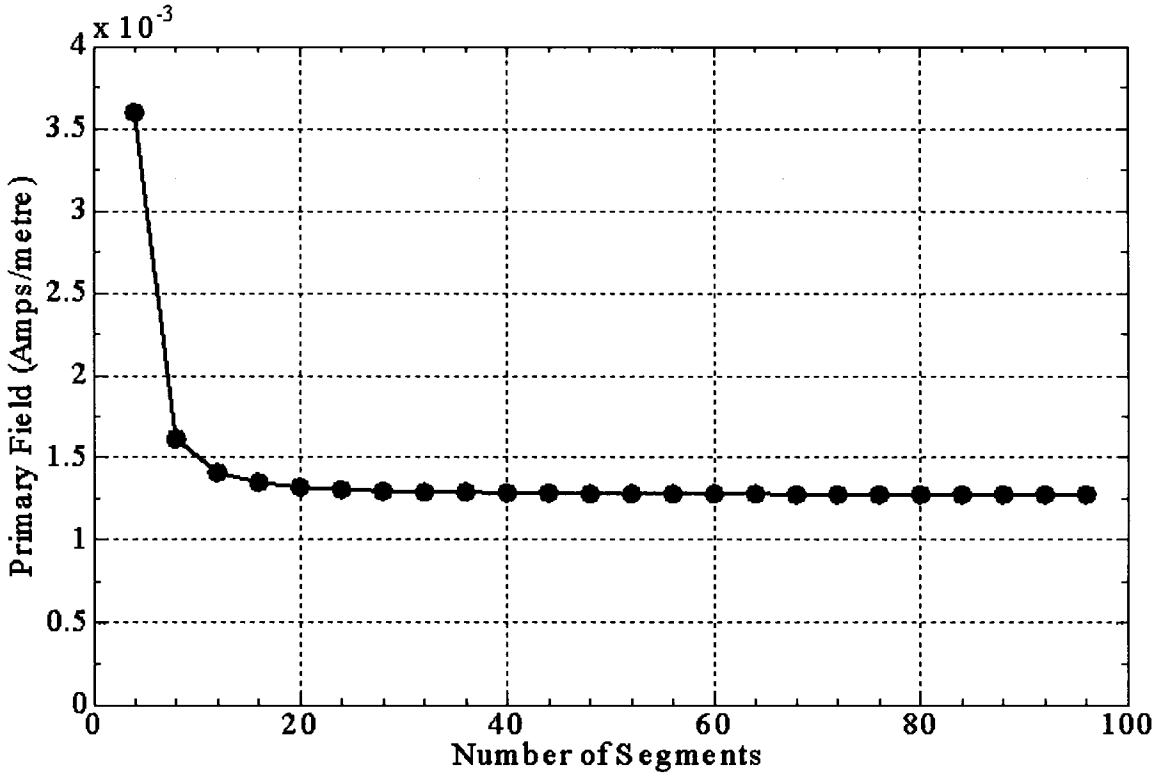


Figure 3.3: Comparison of primary field responses measured plotted as a function of the number of segments constituting the transmitter polygon. This was calculated using the Biot-Savart equation and a Generic Concentric transmitter-receiver configuration.

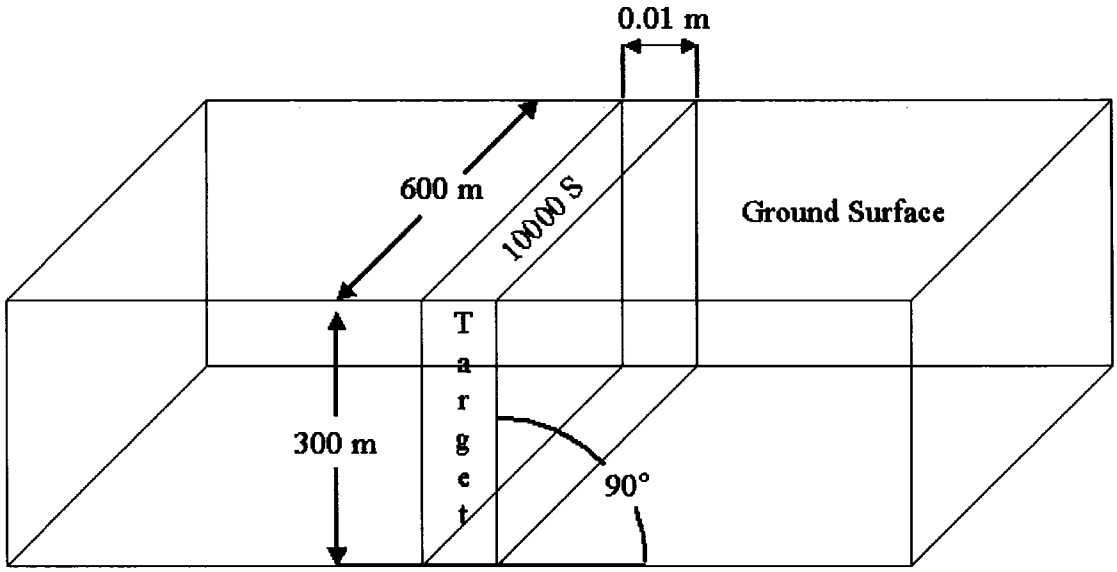


Figure 3.4: Theoretical target used to calculate the response for the various configurations. The target is of very high conductance and the surrounding ground is highly resistive.

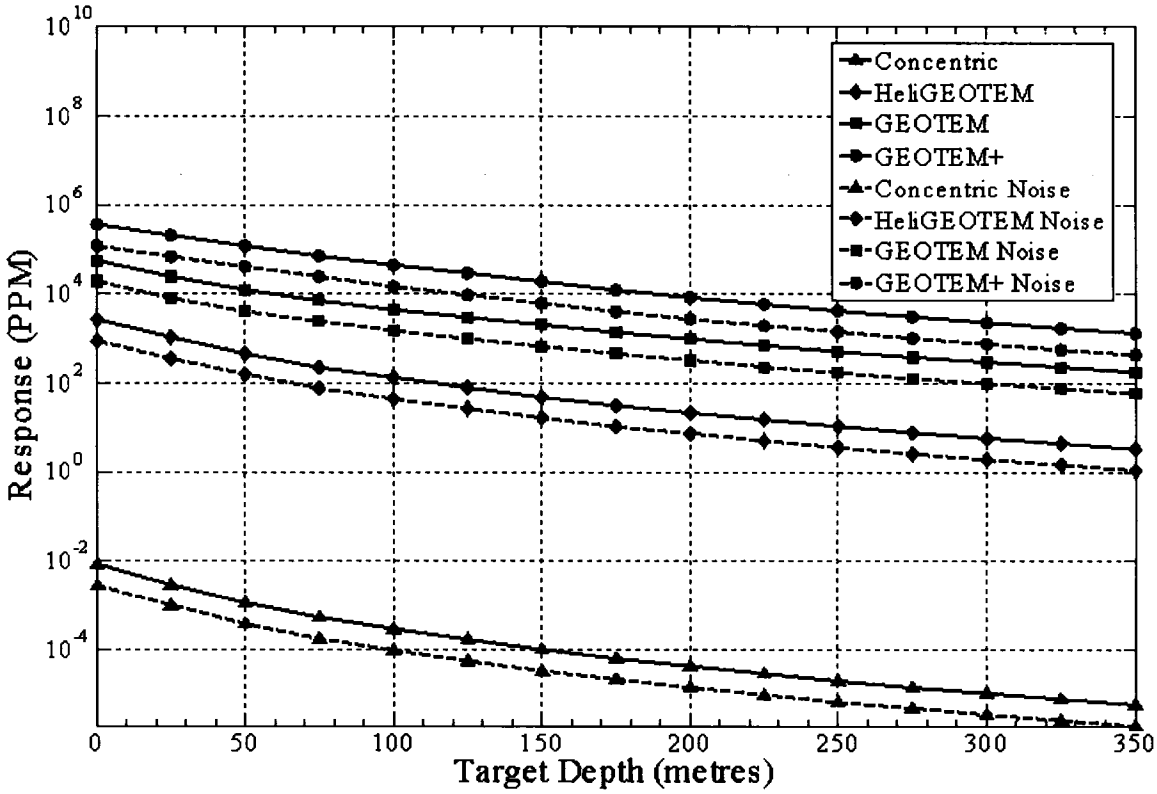


Figure 3.5: The solid lines show the theoretical response of each system as a function of target depth for the target in Figure 3.4 and a base frequency of 90 Hertz. The dashed lines represent the maximum tolerable noise levels caused by geometric variations given a S/N $\geq$3.

Based on experience, this noise level offers a satisfactory confidence level in identifying geological signal over geometric noise. This means that the noise caused by geometric variations for each depth cannot exceed more than a third of the values plotted in Figure 3.5 for each respective depth.

# 4. Results

## *4.1 GEOTEM*

### 4.1.1 Variations in Receiver Position

Theoretical calculations were carried out using Equation (1) to estimate the change in the magnitude of the primary field at the receiver resulting from various offsets of the receiver from the nominal position of 130 metres behind and 50 metres below the transmitter centre as illustrated in Figure 4.1. Values tested were within the range of ±5 metres from the nominal position in each of the three *x*-, *y*-, and *z*-directions. This range of values corresponds to typical receiver variations encountered during survey flying. Each calculation was subtracted from and then normalized by the expected primary field at the nominal transmitter-receiver geometry. Results are therefore expressed in parts per million of the nominal primary field. The results are plotted in Figure 4.2 to compare the effect of the offsets in each direction individually.

The greatest deviation from the nominal response occurs when the receiver moves in the ±*x*-direction, that is, in the direction of flight. It is possible to convert these deviations into the accuracy at which the transmitter-receiver offset must be known for successful target detection. For example, if the response of the conductive target at 0 metres depth is $0.6\times10^5$ PPM (as is the case for the GEOTEM system), then the noise associated with offset variations should be, at most, equal to a third of this value or $0.2\times10^5$ PPM. For

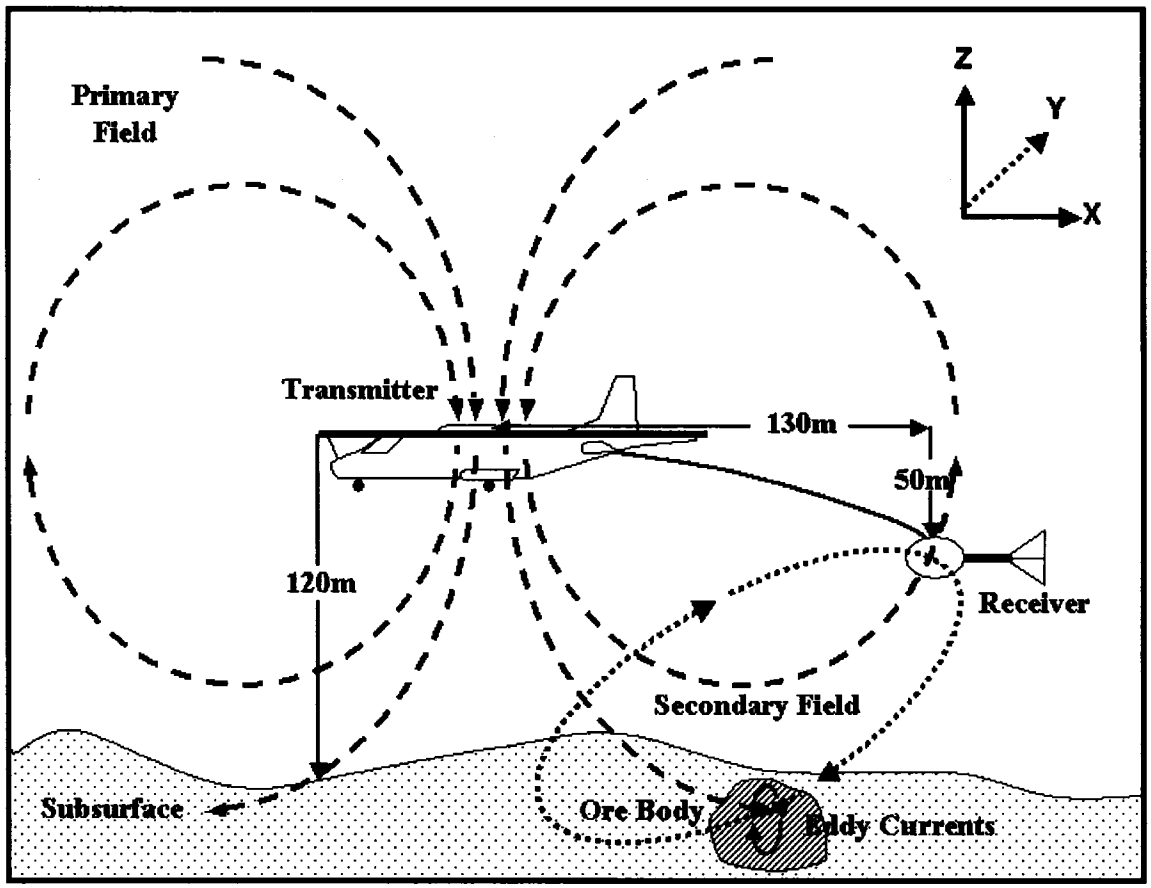


Figure 4.1: Schematic diagram of the GEOTEM system. The mean altitude for the aircraft and transmitter is 120 metres. The receiver is located 130 metres behind and 50 metres below the centre of the transmitter loop.

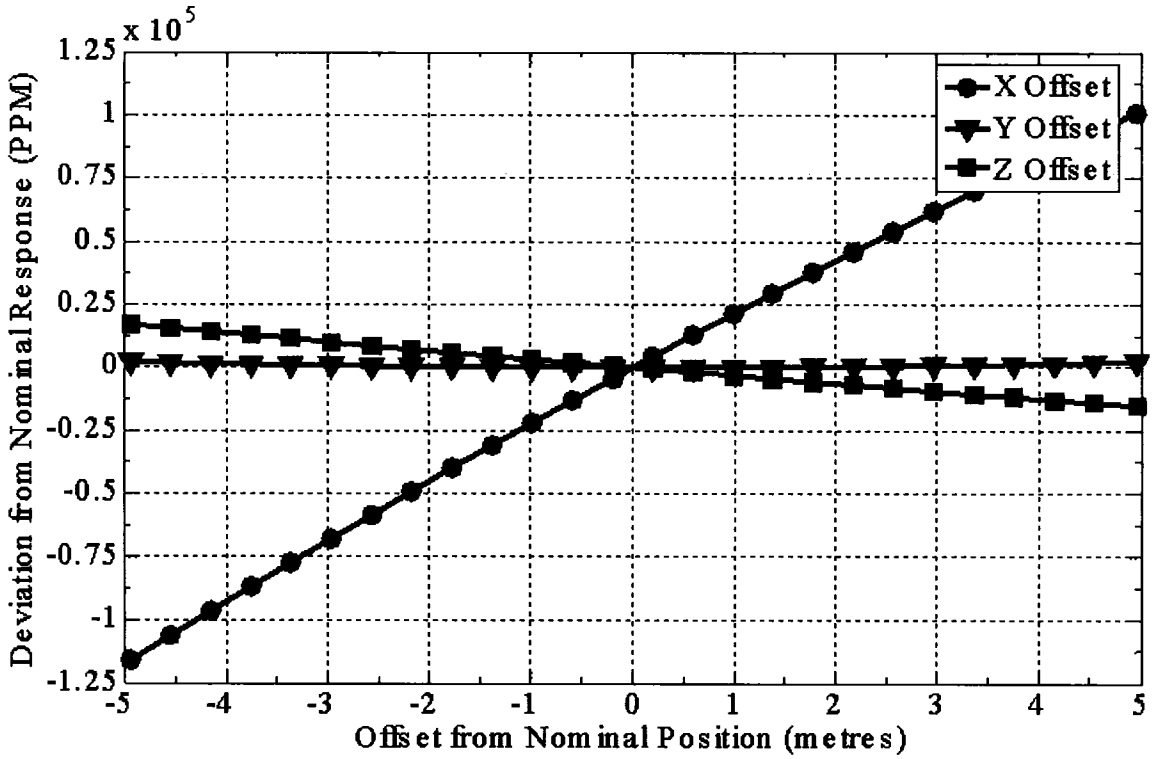


Figure 4.2: Deviation of the primary field from its nominal value as a function of variations in the receiver positions along the *x*-, *y*-, and *z*-directions for the GEOTEM configuration.

movements in the $x$-direction, this requires that the receiver moves no more than ±1.0 metre away from the nominal position. Similar calculations have been done for all directions of receiver movement and multiple target depths and are summarized in Figure 4.3. When the target depth increases, the maximum tolerable receiver offset from the nominal position decreases. The accuracy requirements are more stringent in the direction of flight. For example, to successfully detect and identify the target described above a depth of 100 metres, the receiver offset in the direction of flight ($x$) must be known to an accuracy of ~7 centimetres, whereas the tolerance is ~46 centimetres in the vertical direction ($z$) and ~4.2 metres in and out of the $x$-$z$ plane ($y$-direction offset). This is indicated in Figure 4.3.

### 4.1.2 Variations in Transmitter Attitude

The impact of transmitter attitude variations was calculated using Equation (2) to rotate the unit vector $\boldsymbol{m}$ in Equation (1). The primary field at the receiver was calculated for transmitter attitude variations between ±5 degrees from the nominal roll, pitch, and yaw. This range of values corresponds to typical attitude variations of the aircraft and transmitter during survey flying. Each calculation was subtracted from and then normalized by the expected primary field at the nominal transmitter-receiver geometry. The results are plotted in Figure 4.4 to compare the effect of each angle individually.

Figure 4.5 shows the maximum tolerable variations in attitude, for a S/N $\geq$3 and the target described above. The results in Figure 4.5 show more stringent accuracy

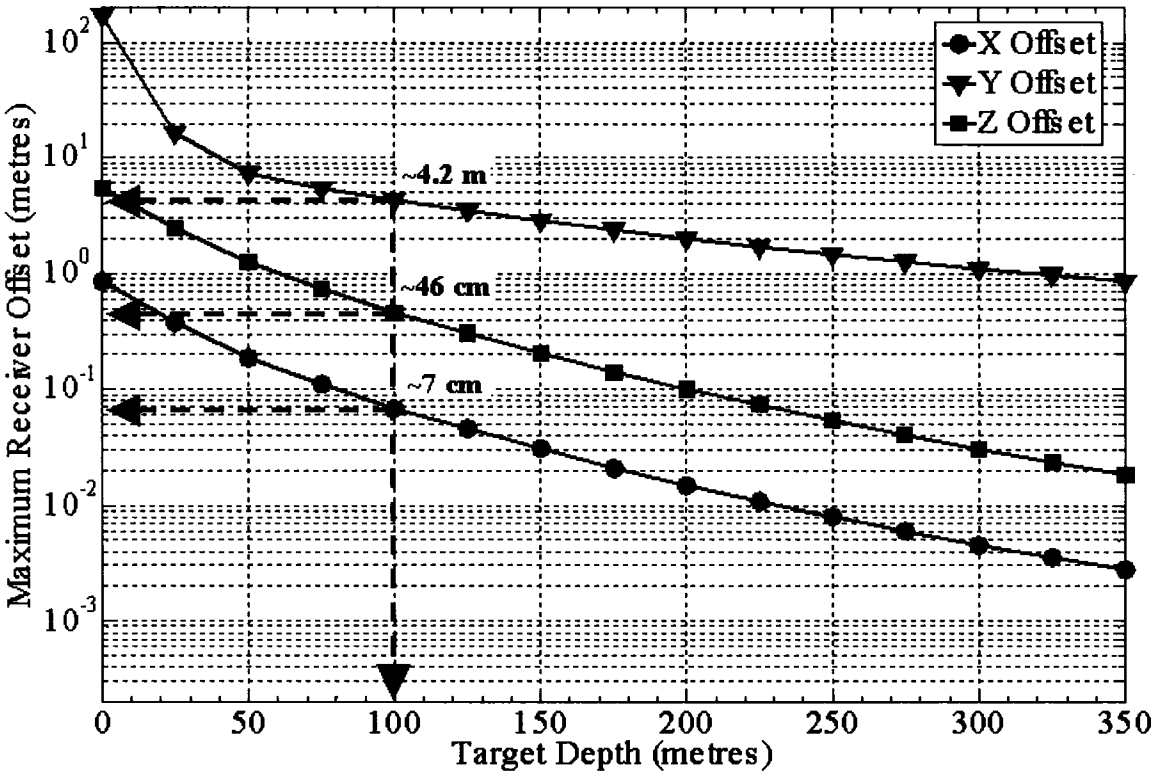


Figure 4.3: Maximum tolerable receiver offsets permitted to successfully detect and identify a vertical plate with a conductance of 10000 Siemens as a function of the depth to the target for the GEOTEM configuration. For example, for a target depth of 100 metres, the required accuracy in the $z$-direction is ~4.2 metres, the required accuracy in the $y$-direction is ~46 centimetres, and the required accuracy in the $x$-direction is ~7 centimetres.

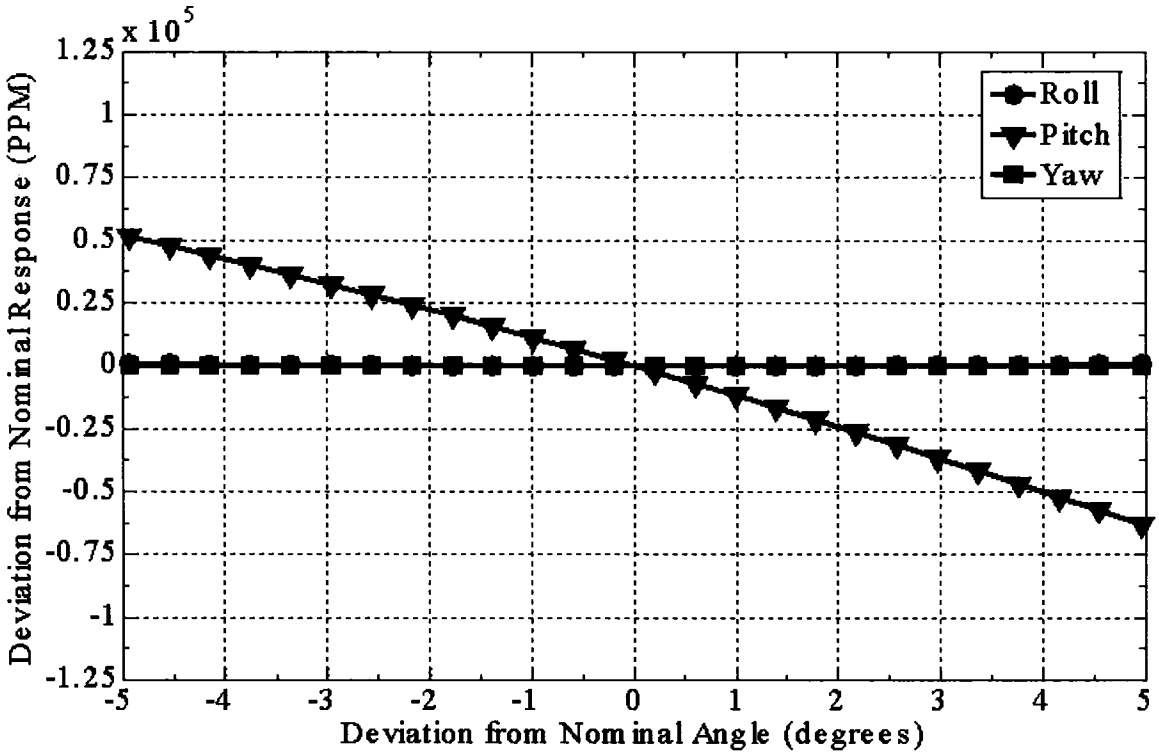


Figure 4.4: Deviation of the primary field from its nominal value as a function of variations in the transmitter attitude for the GEOTEM configuration. Note: The roll and yaw have such a minimal influence that they overlap close to zero.

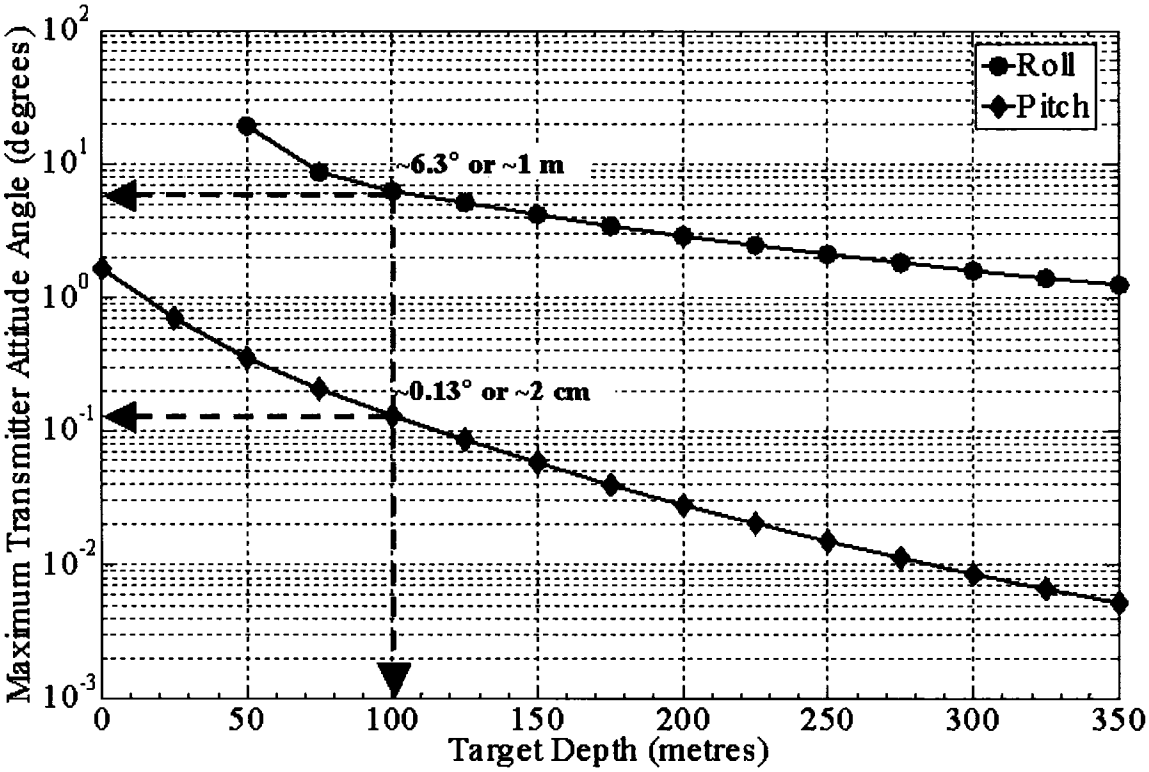


Figure 4.5: Maximum tolerable transmitter attitude angle variations permitted to successfully detect and identify a vertical plate with a conductance of 10000 Siemens as a function of the depth to the target for the GEOTEM system. Yaw has a negligible effect and is therefore omitted. For a target depth of 100 metres, roll requires an accuracy of ~6.3°; pitch requires variation less than ~0.13°. These angles are equivalent to movements of ~1 metre at the wingtips and ~2 centimetres at the nose of the aircraft respectively.

requirements for pitch. Figure 4.5 also indicates that to successfully detect and identify the target at a depth of 100 metres, the transmitter pitch must be stable within approximately ±0.13 degrees, which equates to about ±2.0 centimetres from the nominal position at the nose of the aircraft. The tolerance is significantly greater for roll, which can vary by approximately ±6.3 degrees, which equates to about ±1.0 metre from the nominal position at the lateral edge of the transmitter or the tip of the wing. Yaw has a negligible effect since it is equivalent to the transmitter rotating about the vertical axis, which does not change the primary field.

### 4.1.3 Transmitter Loop Deformation

The GEOTEM transmitter loop is attached at each of the wing tips, at a long extension at the tail of the aircraft and at two smaller extensions at the nose, as shown in Figure 4.6. For this analysis, the wing tips, nose and tail are considered fixed in the aircraft frame of reference. Although at the present time there is virtually no way to determine the amount each of the loop segments actually moves during flight, it is estimated that the segments in between these attachment points are free to move by as much as one metre. By moving the loop at positions between the attachment points, the shape of the loop and its area vary. Equation (3) was used to calculate the primary field contribution of each segment in all possible orientations, at the receiver. For this analysis, the four mobile points indicated in Figure 4.6 along the loop were varied by ±0.1, ±0.2, ±0.3, ±0.4, and ±0.5 metres in each of the $x$-, $y$-, and $z$-directions. This configuration yields $3^{12}$

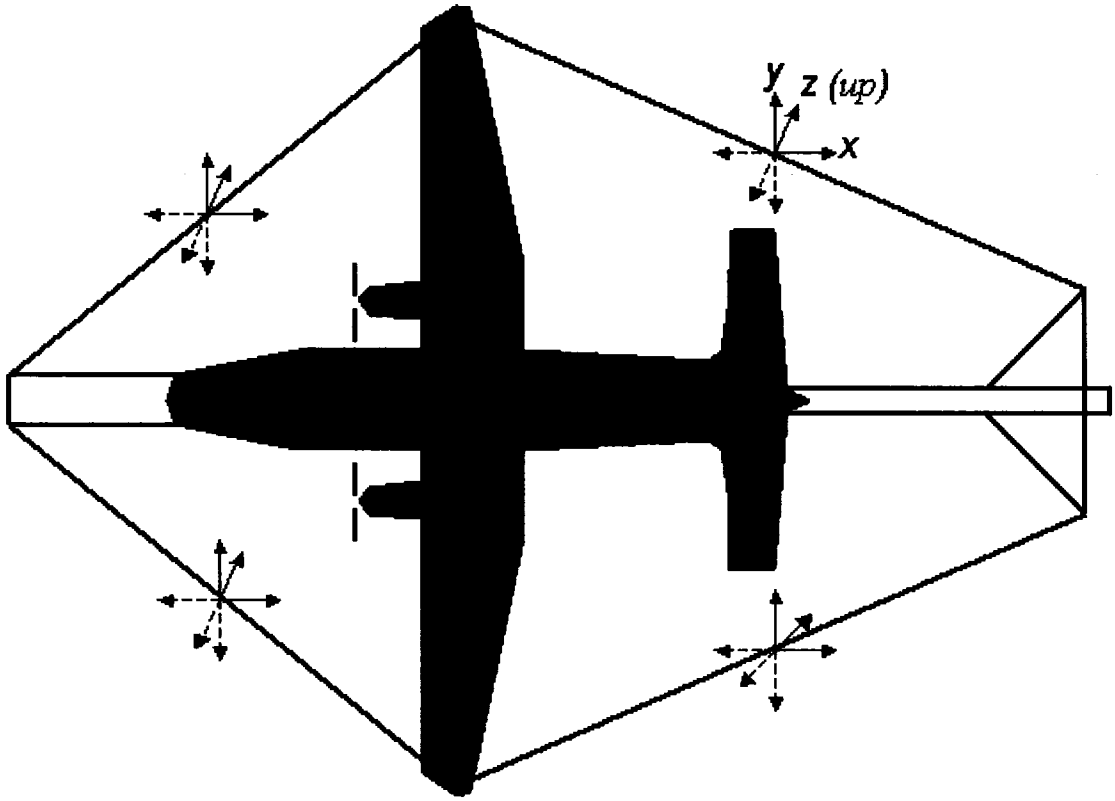


Figure 4.6: Top view of the aircraft and the transmitter loop. The loop is attached at the wing tips and at a long extension at the tail and at two smaller extensions at the front. The four marked points along the loop are those that are varied in the directions shown for the GEOTEM and GEOTEM+ analysis.

different combinations of potential loop deformations. For each of the different combinations, the maximum, minimum, average and standard deviation were calculated and presented in Figure 4.7. As expected, the minimum is always zero since the nominal position is one of the potential arrangements. The scenario that yields the maximum deviation occurs twice; when the points are arranged so as to minimize the size of the loop and pitch it nose up; and when the points are arranged so as to maximize the size of the loop and pitch it nose down. However, these are considered extreme situations and the mean is more likely representative of the actual loop deformation during flight. Considering the average pitch of the aircraft and wind drag on the loop, it is more appropriate to simulate a situation in which all points move towards the receiver and stay within the plane of the aircraft. This would, in effect, bring the transmitter closer to the receiver thereby increasing the primary field measured at the receiver. This situation yields a deviation consistent with the mean values in the results.

The deviations as a function of displacement shown on Figure 4.7 were converted to the maximum variations allowed for successful target detection and plotted in Figure 4.8 assuming S/N $\geq$3. From this figure, we can determine that to successfully detect the target described above at a depth of 100 metres in the case of the maximum deviation scenario, the loop can only deform by a maximum of $\pm$0.7 centimetres. However, if the mean values are representative of the actual loop movement, the maximum allowable deformation is $\pm$3.5 centimetres.

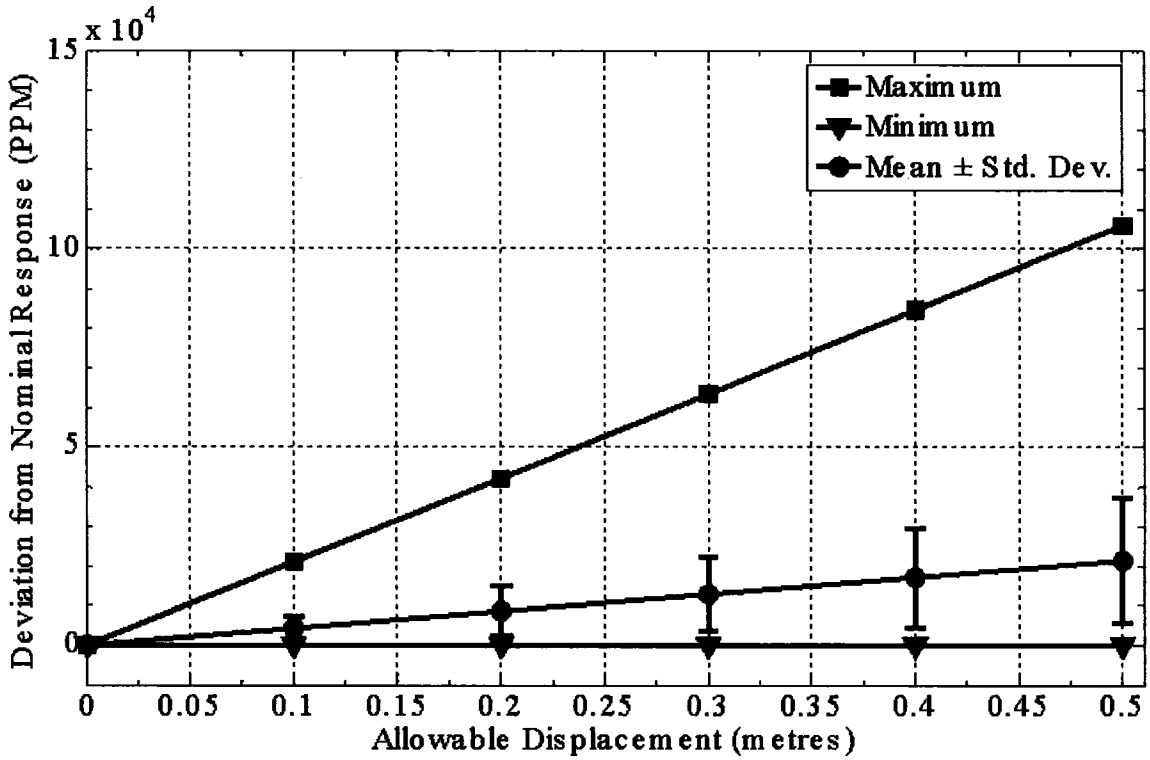


Figure 4.7: Deviation of the primary field from its nominal value as a function of displacement of the four mobile points midway between the attachment points along the transmitter loop shown in the previous figure for the GEOTEM configuration.

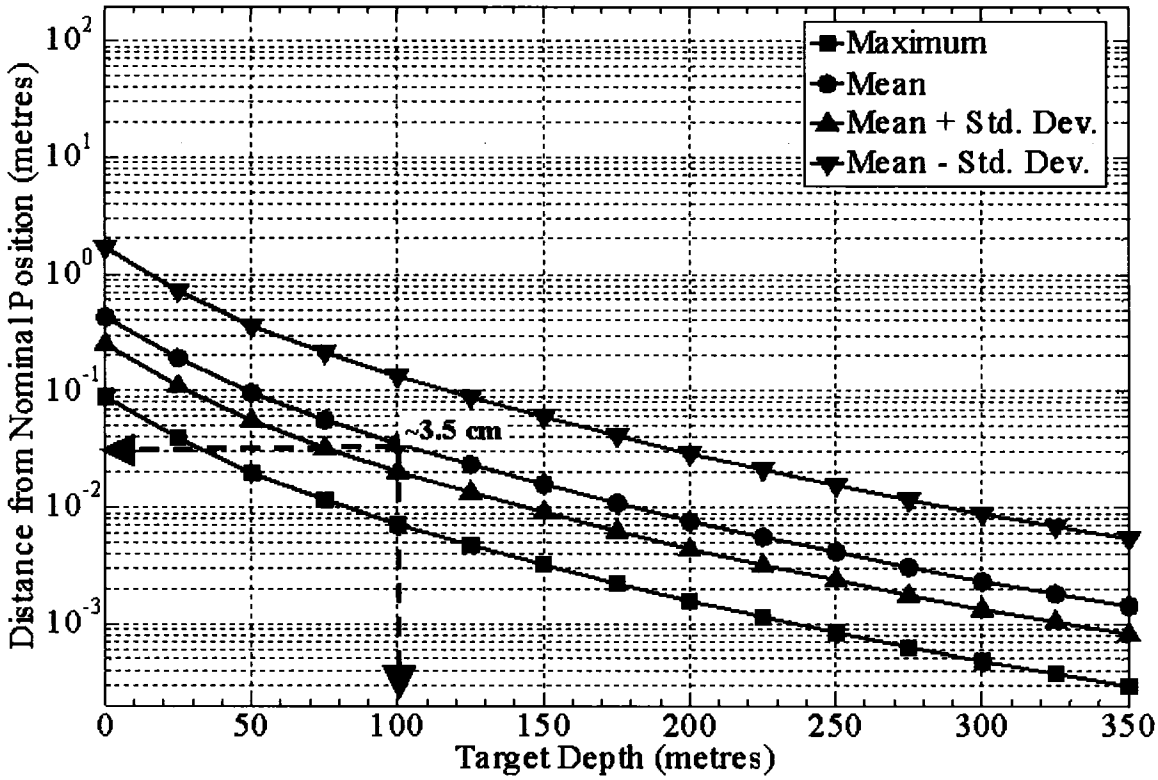


Figure 4.8: Maximum tolerable variations in order to successfully detect and identify a vertical plate with a conductance of 10000 Siemens as a function target depth, for each statistical parameter derived in the loop deformation analysis for the GEOTEM configuration. For a target depth of 100 metres, the mean acceptable movement requires 3.5 centimetres accuracy. For the case representing larger deviation from the nominal response (mean plus one standard deviation), the accuracy requirement is more stringent and equal to 2 centimetres at a target depth of 100 metres.

### 4.1.4 GEOTEM Summary

The results for variations in receiver position and transmitter attitude, and for transmitter loop deformation, for the GEOTEM system, are presented in Figure 4.9. The values for transmitter attitude have been converted to a distance measurement at the respective outer position of the transmitter. This presentation of the results allows for an easy determination of which component has the greatest impact for this configuration. It can now be determined that the measurements of pitch require the greatest amount of accuracy, followed by loop deformation, *x*-distance, *z*-distance, roll and *y*-distance.

## *4.2 GEOTEM+*

### 4.2.1 Variations in Receiver Position

Using the same methodology as the analysis of the GEOTEM system, theoretical calculations were carried out for the proposed GEOTEM+ system. However, variations in the magnitude of the primary field were for deviations from the nominal position of 250 metres behind and 70 metres below the transmitter centre as illustrated in Figure 4.10. As in the GEOTEM example, the values tested were within the range ±5 metres from the nominal position in each of the three *x*-, *y*-, and *z*-directions. This ensures consistency in the analysis and enables straightforward comparison between the results for each system. The results are plotted in Figure 4.11 to compare the effect of the offsets in each direction individually.

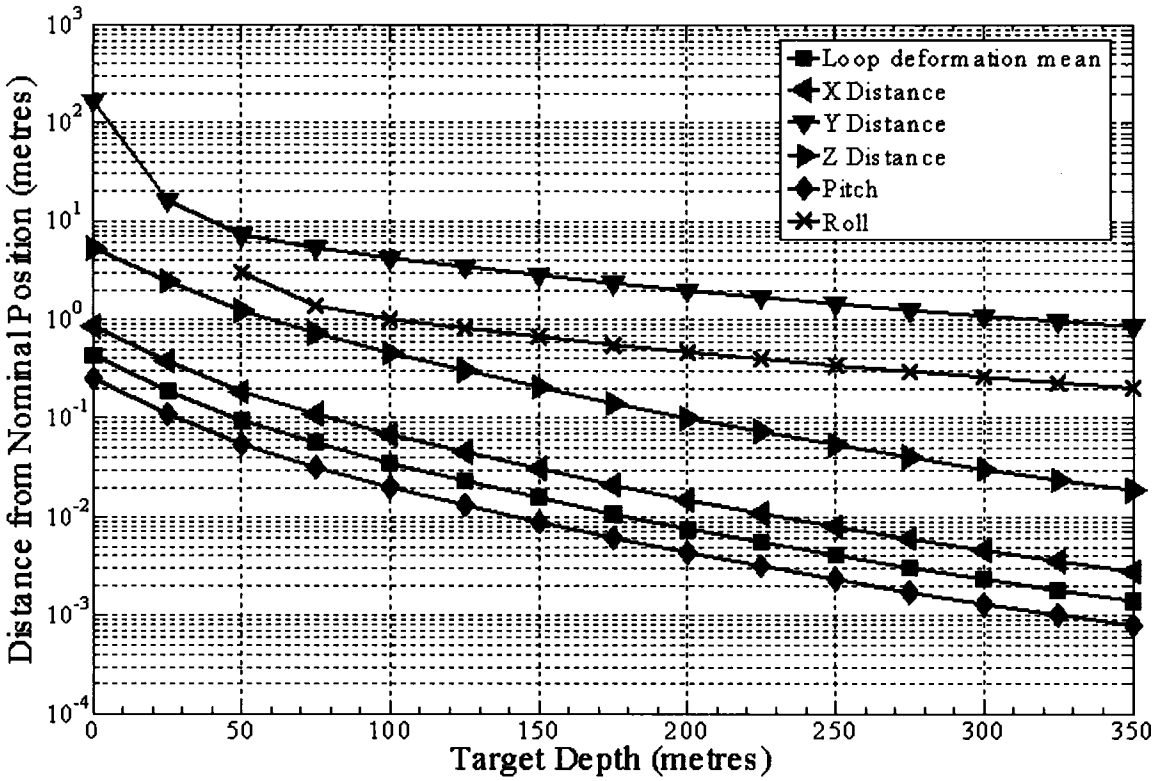


Figure 4.9: Comparison of all the variables for the GEOTEM configuration. Units for the pitch and roll have been converted to a distance measurement at the nose and the wing tip respectively.

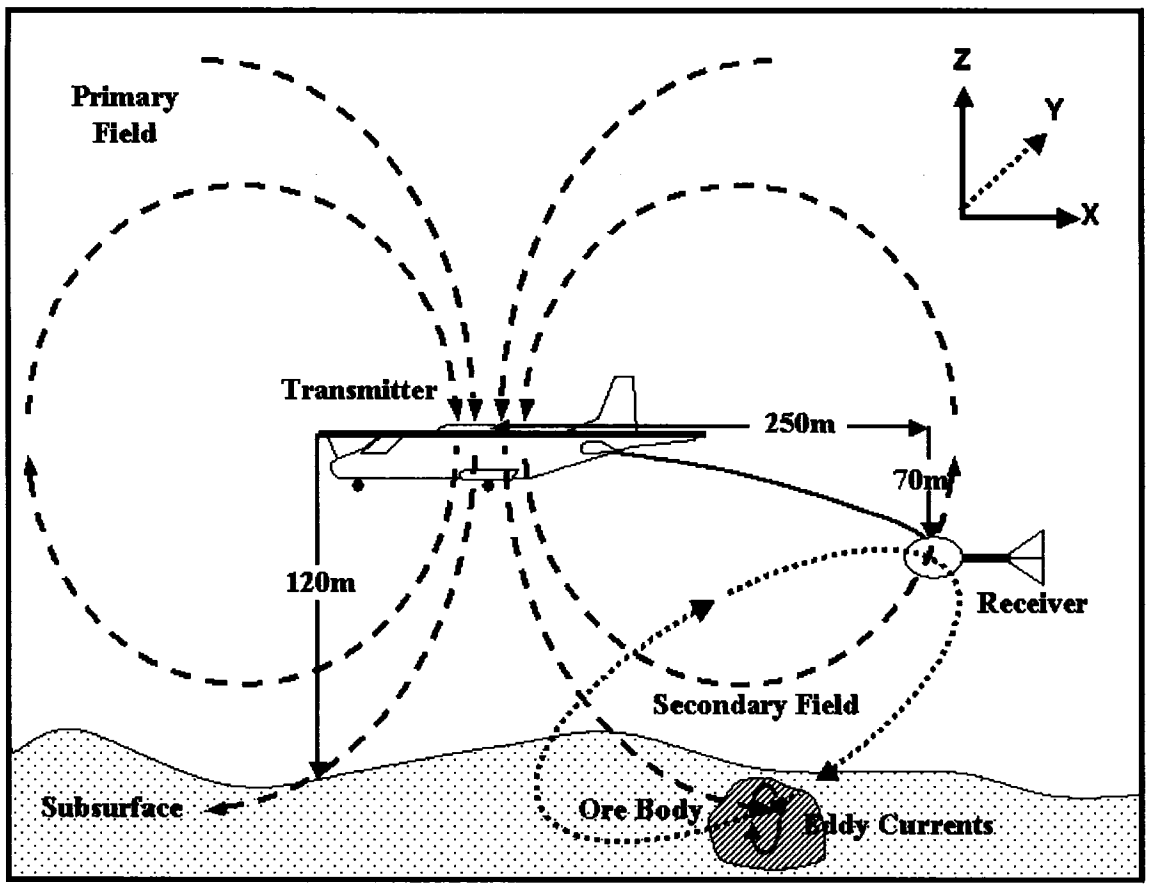


Figure 4.10: Schematic diagram of the GEOTEM+ configuration. The mean altitude for the aircraft and transmitter is 120 metres. The receiver is located 250 metres behind and 70 metres below the centre of the transmitter loop.

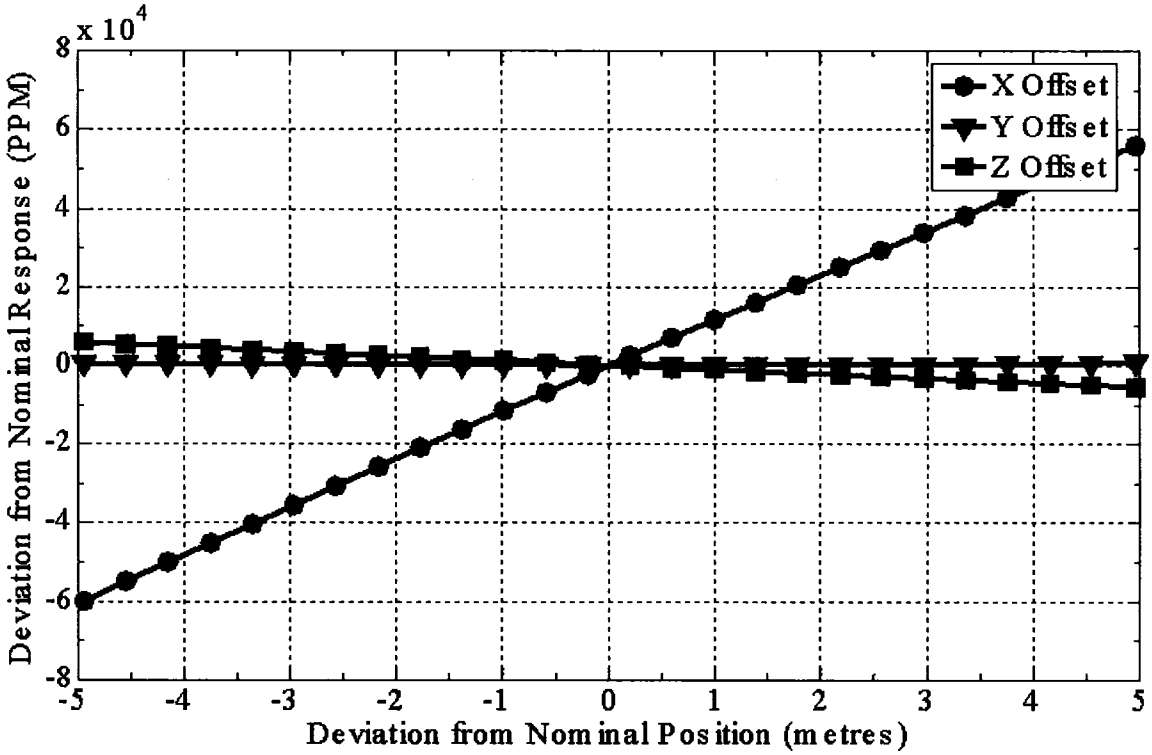


Figure 4.11: Deviation of the primary field from its nominal value as a function of variations in receiver positions for the GEOTEM+ configuration.

The greatest source of deviation from the nominal response occurs when the receiver moves in the $\pm x$ direction, that is, in the direction of flight, which is similar to the GEOTEM system. Figure 4.12 shows the accuracy for which the transmitter-receiver offset must be known for successful target detection. When the target depth increases, the maximum tolerable receiver offset from the nominal position decreases. As for the GEOTEM system, the accuracy requirements are more stringent in the direction of flight. To use the same example as above for the GEOTEM system, to successfully detect and identify the same target at a depth of 100 metres, the receiver offset in the direction of flight ($x$) must be known to an accuracy of ~1.3 metres, whereas the tolerance is ~ 11.9 metres in the vertical direction ($z$) and ~5132 metres in and out of the $x$-$z$ plane ($y$-direction). These tolerances are more than an order of magnitude greater that the tolerances required for the GEOTEM system.

### 4.2.2 Variations in Transmitter Attitude

The same methodology used for the GEOTEM configuration was also used to determine the impact of transmitter attitude variations on the primary field measured at the receiver. The transmitter attitude was varied between ±5 degrees from the nominal roll, pitch, and yaw and the primary field at the receiver was calculated. The results are plotted in Figure 4.13 to compare the effect of each variation individually. For a S/N $\geq$3, Figure 4.14 shows a graph of the maximum tolerable attitude angles. This graph shows more

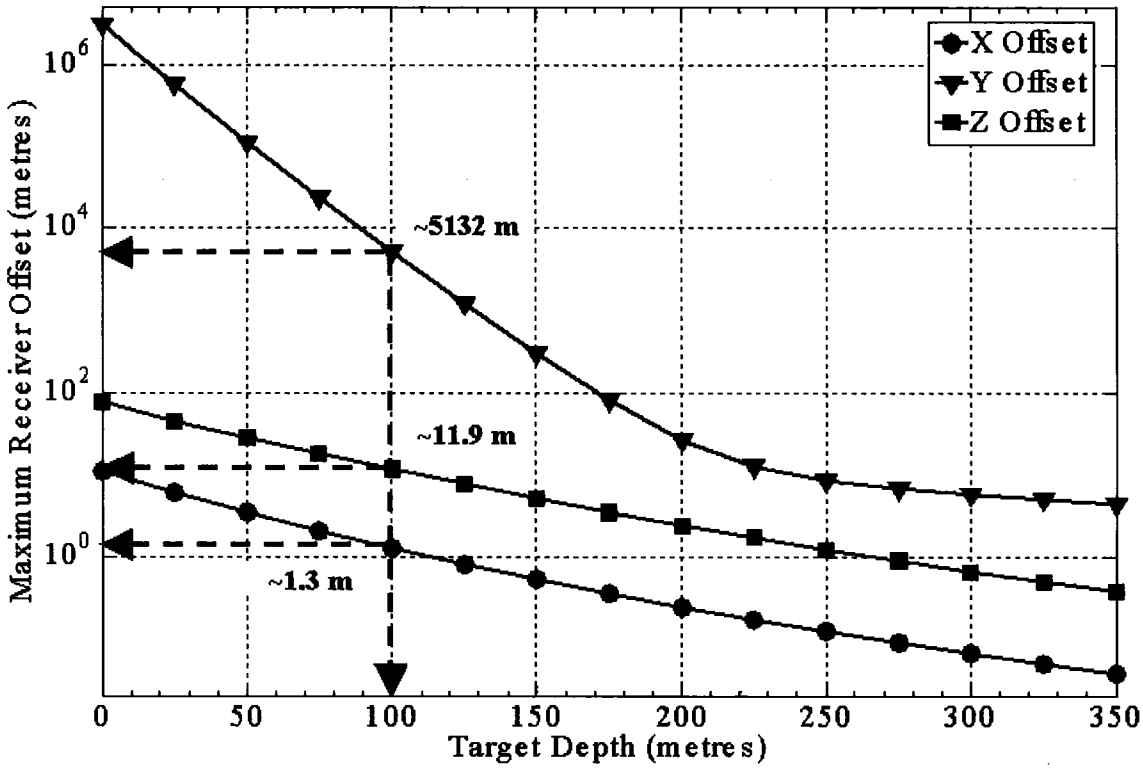


Figure 4.12: Maximum tolerable receiver offsets permitted to successfully detect and identify a vertical plate with a conductance of 10000 Siemens as a function of target depth for the GEOTEM+ configuration. For a target depth of 100 metres, the required accuracy in the $z$-direction is ~11.9 metres, the required accuracy in the $y$-direction is ~5132 metres, and the required accuracy in the $x$-direction is ~1.3 metres.

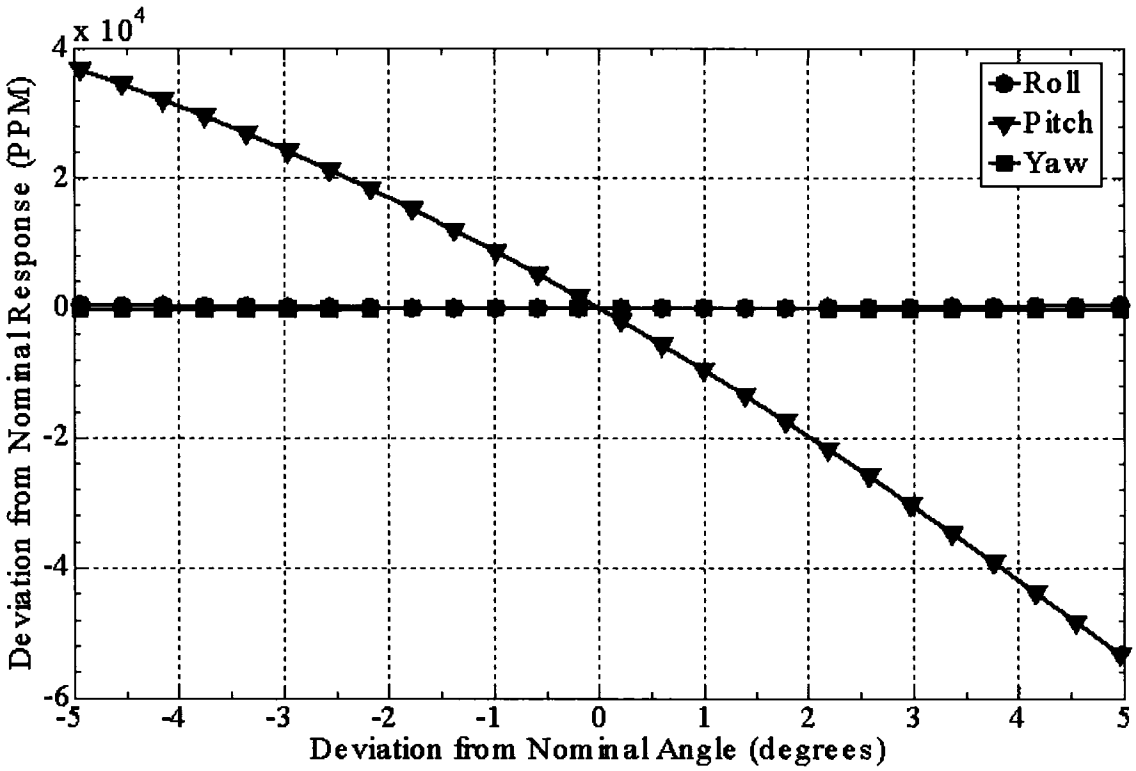


Figure 4.13: Deviation of the primary field from its nominal value as a function of variations in transmitter attitude for the GEOTEM+ configuration. Note: The roll and yaw have such a minimal influence that they overlap close to zero.

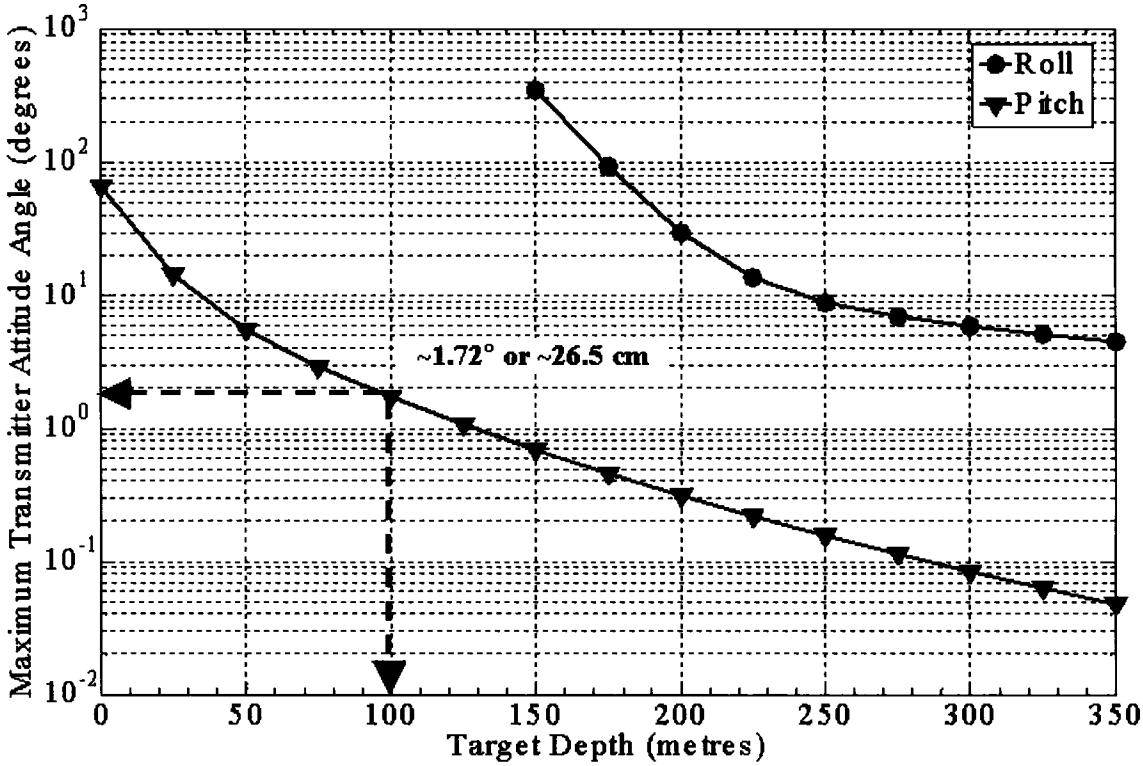


Figure 4.14: Maximum tolerable transmitter attitude angle variations permitted to successfully detect and identify a vertical plate with a conductance of 10000 Siemens as a function of target depth for the GEOTEM+ system. Yaw and roll have a negligible effect and are therefore omitted. For a target depth of 100 metres, pitch requires variation less than ~1.72° which is equivalent to a displacement of ~26.5 centimetres at the nose of the aircraft.

stringent accuracy requirements for pitch. The graph in Figure 4.14 also indicates that to successfully detect and identify the target at a depth of 100 metres, the aircraft pitch must be stable within approximately ±1.72 degrees, which equates to about ±26.5 centimetres from the nominal position at the nose of the aircraft. Accuracy requirements for pitch are much more stringent for pitch than for roll and yaw. At shallow depths both roll and yaw have a negligible effect. However, for deeper targets, the required accuracy for roll is more stringent while yaw remains negligible. The insignificance of yaw is due to its equivalence to the transmitter rotating about its axis, which does not change the primary field. These tolerances are about an order of magnitude greater than the standard GEOTEM configuration.

### 4.2.3 Variations in Transmitter Loop Shape

Since the GEOTEM+ transmitter configuration is identical to the GEOTEM system, the analysis for variations in transmitter loop shape was carried out in the exactly same fashion. The nominal offsets between the transmitter and the receiver were the only difference. The deviations as a function of displacement are shown in Figure 4.15. With the same assumption of S/N $\geq$3, the maximum variations allowed for successful target detection are plotted in Figure 4.16 for various target depths. For the same target example as in the previous analysis at a depth of 100 metres, the maximum deviation scenario requires the loop deformation to be known or restricted by a maximum of ±7.4 centimetres. However, if the mean values are representative of the actual loop

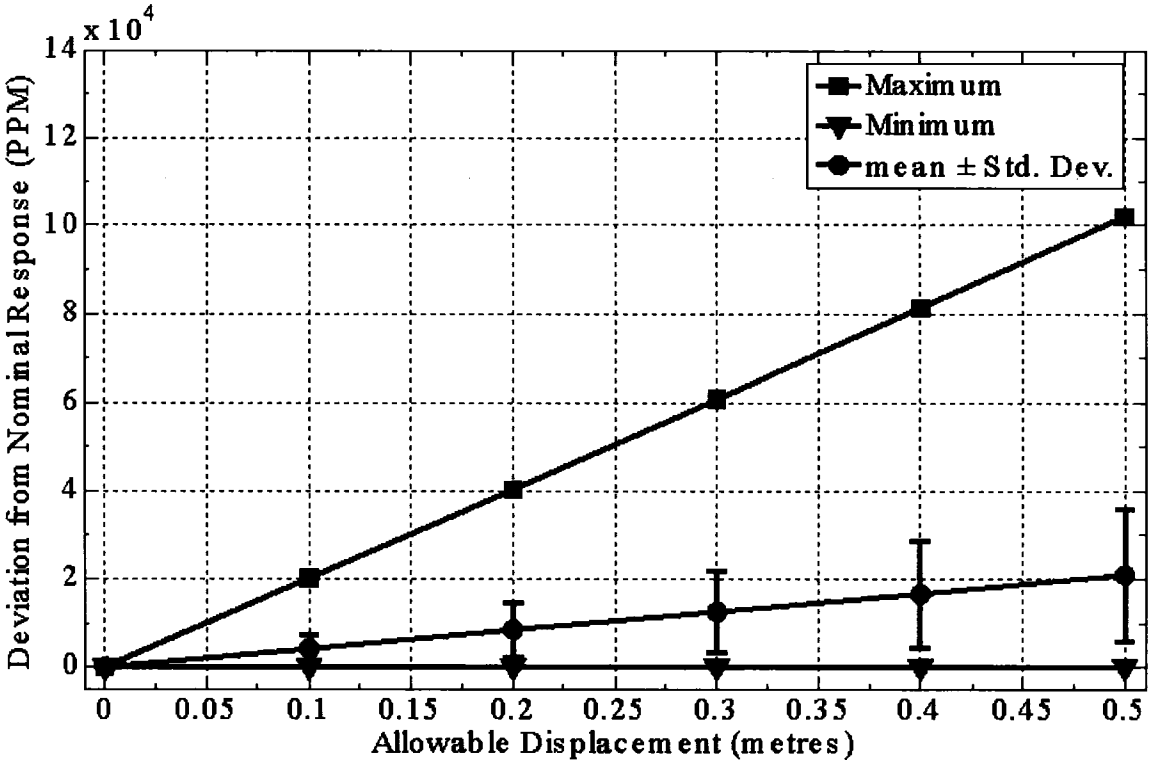


Figure 4.15: Deviation of the primary field from its nominal value as a function of displacement of the four mobile points midway between the attachment points along the transmitter loop shown in the Figure 4.6 for the GEOTEM+ configuration.

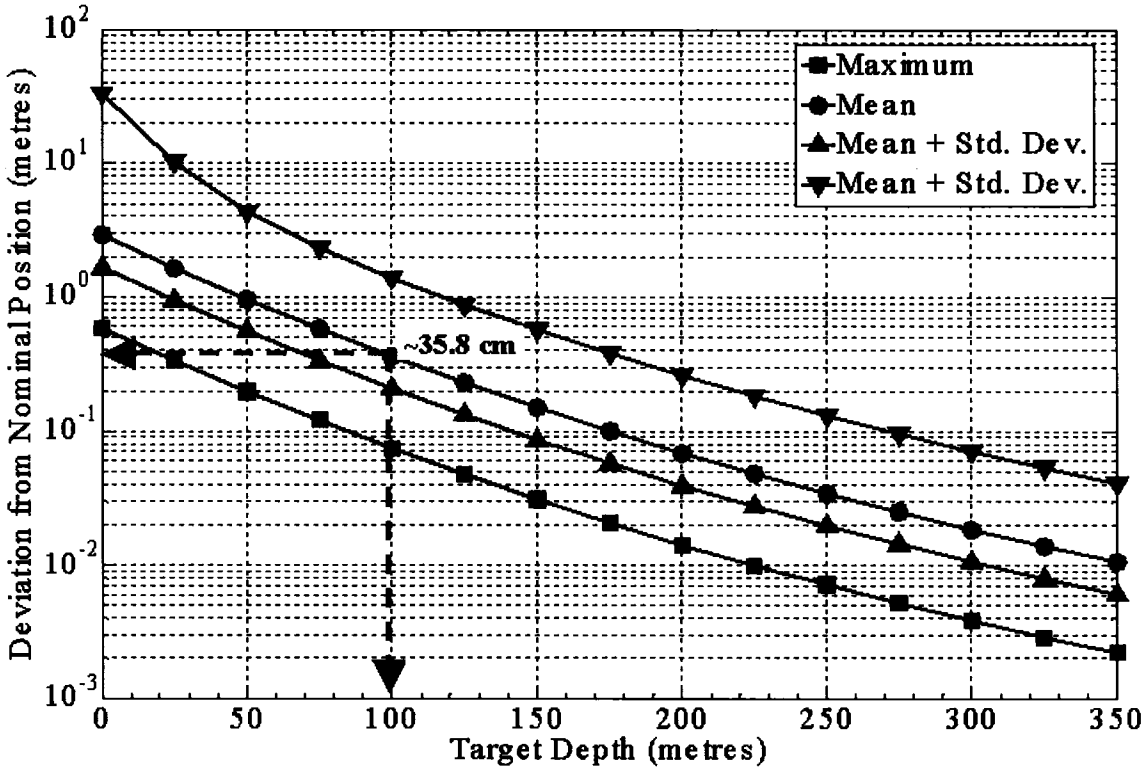


Figure 4.16: Maximum tolerable variations in order to successfully detect and identify a vertical plate with a conductance of 10000 Siemens as a function of target depth, for each statistical parameter derived in the loop deformation analysis for the GEOTEM+ configuration. For a target depth of 100 metres, the mean acceptable movement requires 35.8 centimetres accuracy. For the case representing larger deviations from the nominal response (mean plus one standard deviation), the accuracy requirement is more stringent and equal to 2 centimetres at a target depth of 100 metres.

movement, the maximum allowable deformation is ±35.8 centimetres. Similarly to the attitude variations, these tolerances are about an order of magnitude greater than the standard GEOTEM configuration.

### 4.2.4 GEOTEM+ Summary

As for the GEOTEM system, all the results are presented in the same units in Figure 4.17. This figure shows that the variables have the same relative impact on the primary field that is measured at the receiver, with pitch having the greatest impact. If the target has a depth less than ~175 metres, the roll has a negligible impact.

## *4.3 HeliGEOTEM*

### 4.3.1 Variations in Receiver Position

For the HeliGEOTEM system, the effect of receiver position was examined using the methodology described for the GEOTEM and GEOTEM+ systems. Theoretical calculations were carried out using Equation (1) to determine what the change in magnitude of the primary field is at the receiver resulting from various offsets from the nominal position of 35 metres below and 20 metres in front of the transmitter centre as illustrated in Figure 4.18. The difference in this case is that the receiver is on a more taut cable due to the weight of the transmitter beneath it (Figure 4.19). Because of this design, the receiver is expected to move around less than in the case of the GEOTEM and GEOTEM+ systems. However, for consistency with the previous examples, the range of

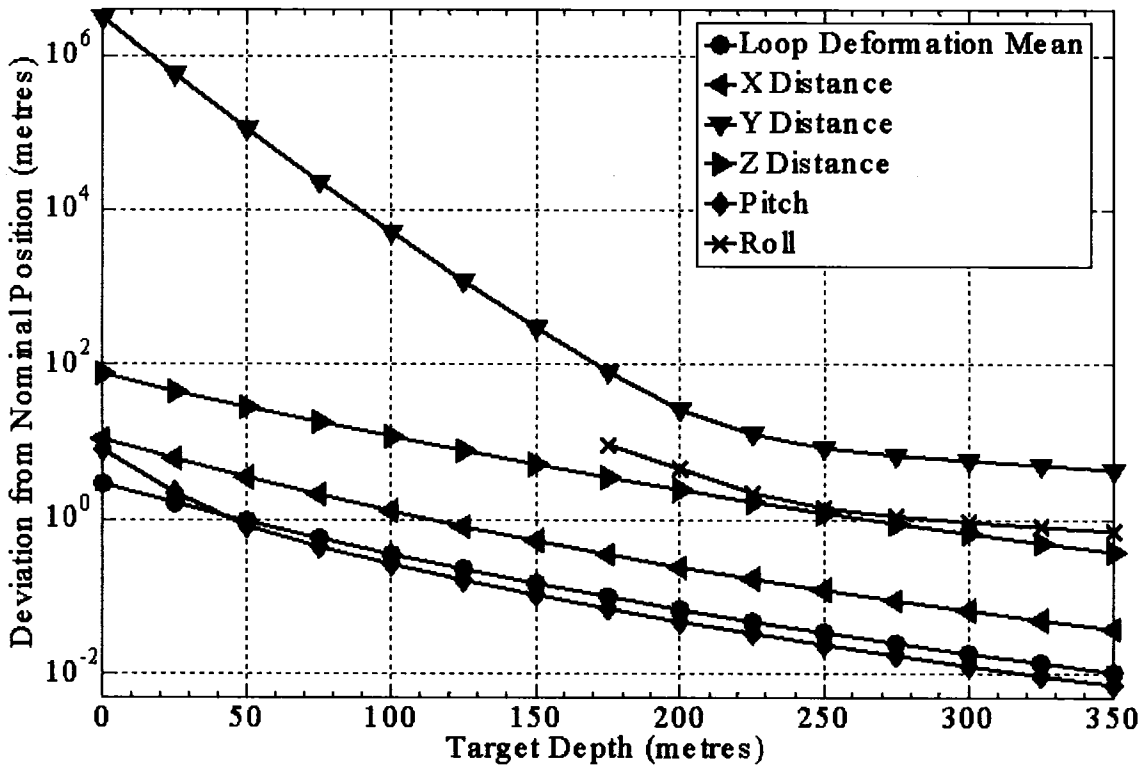


Figure 4.17: Comparison of all the variables for the GEOTEM+ configuration. Units for the pitch and roll have been converted to a distance measurement at the nose and the wing tip respectively.

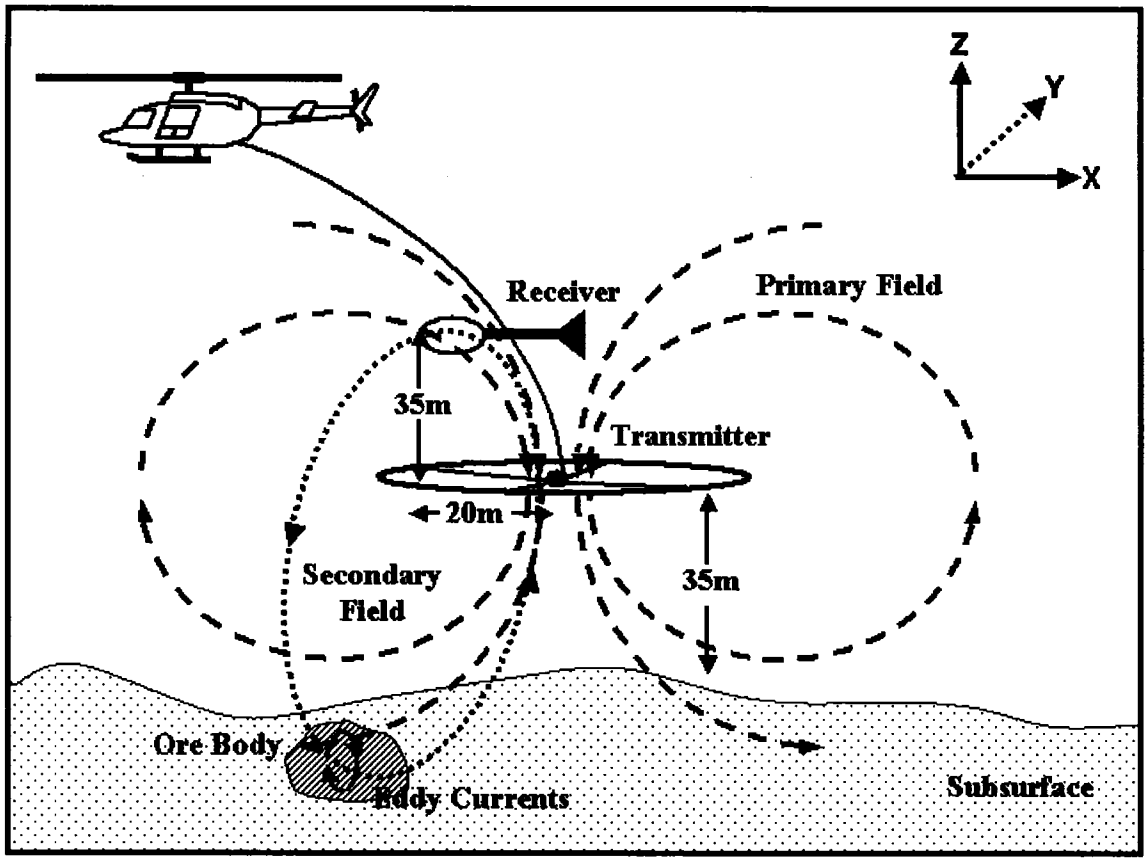


Figure 4.18: Schematic diagram of the HeliGEOTEM configuration. The mean transmitter loop altitude is 70 metres. The receiver is in front of the transmitter loop centre by 20 metres and above by 35 metres.

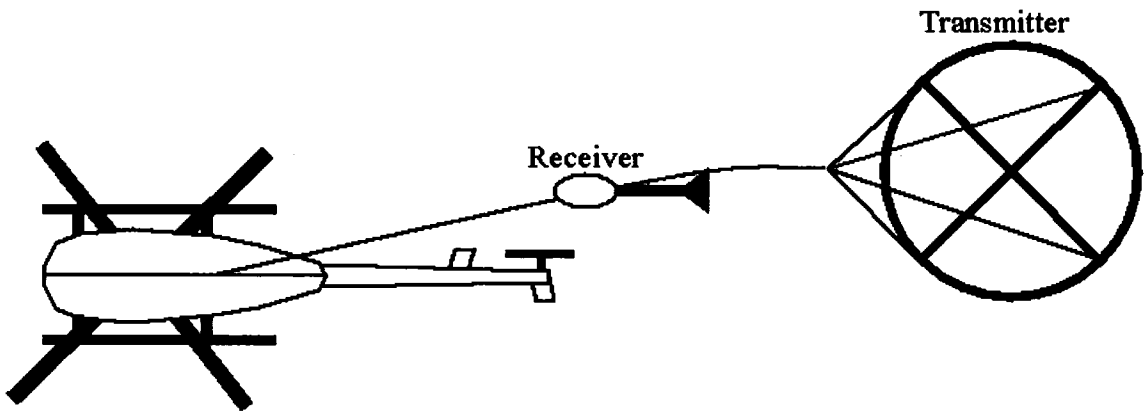


Figure 4.19: Underside view of the HeliGEOTEM configuration. Both the transmitter and the receiver are towed behind and below the aircraft. The receiver is offset from the transmitter, as it is attached part way up the tow cable.

possible variation was kept to ±5 metres. For the HeliGEOTEM system, the receiver is closer to the transmitter than for the GEOTEM or GEOTEM+ systems, so it spatially located where the field is varying rapidly as a function of distance. Hence, small changes in receiver position are expected to produce large changes in the primary field. As seen in Figure 4.20, the greatest deviation from the nominal response occurs when the receiver moves in the ±$z$-direction, that is, in the vertical direction. This is different from the two previous cases. Figure 4.21 shows the accuracy for which the transmitter-receiver offset must be known for successful target detection assuming a S/N $\geq 3$. When the target depth increases, the maximum tolerable receiver offset from the nominal position decreases. The accuracy requirements are more stringent in the $z$-direction. For example, to successfully detect and identify the target at a depth of 100 metres, the receiver offset in the $z$-direction must be know to an accuracy of 0.074 centimetres whereas along the direction of flight ($x$-direction) the offset must be know to 0.1 centimetres, and ~ 20 centimetres in and out of the $x$-$z$ plane ($y$-direction). These tolerances are nearly two orders of magnitude more stringent than in the GEOTEM case.

### 4.3.2 Variations in Transmitter Attitude

Using the same methodology as in the GEOTEM and GEOTEM+ examples, the primary field at the receiver was calculated for transmitter attitude variations between ±5 degrees from the nominal roll, pitch, and yaw. Although this may be larger than the range of motion expected in practice, this system is still experimental and there is no data available revealing how the transmitter moves during survey flying. The range of motion

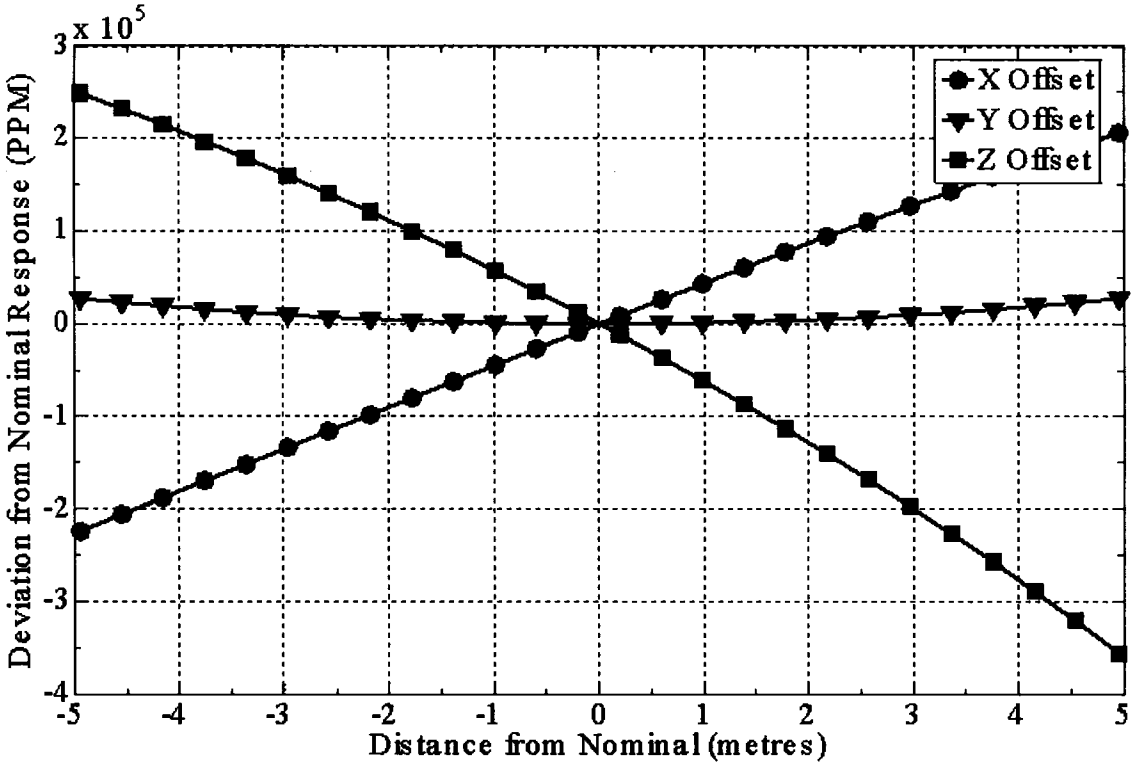


Figure 4.20: Deviation of the primary field from its nominal value as a function of variations in receiver positions for the HeliGEOTEM configuration.

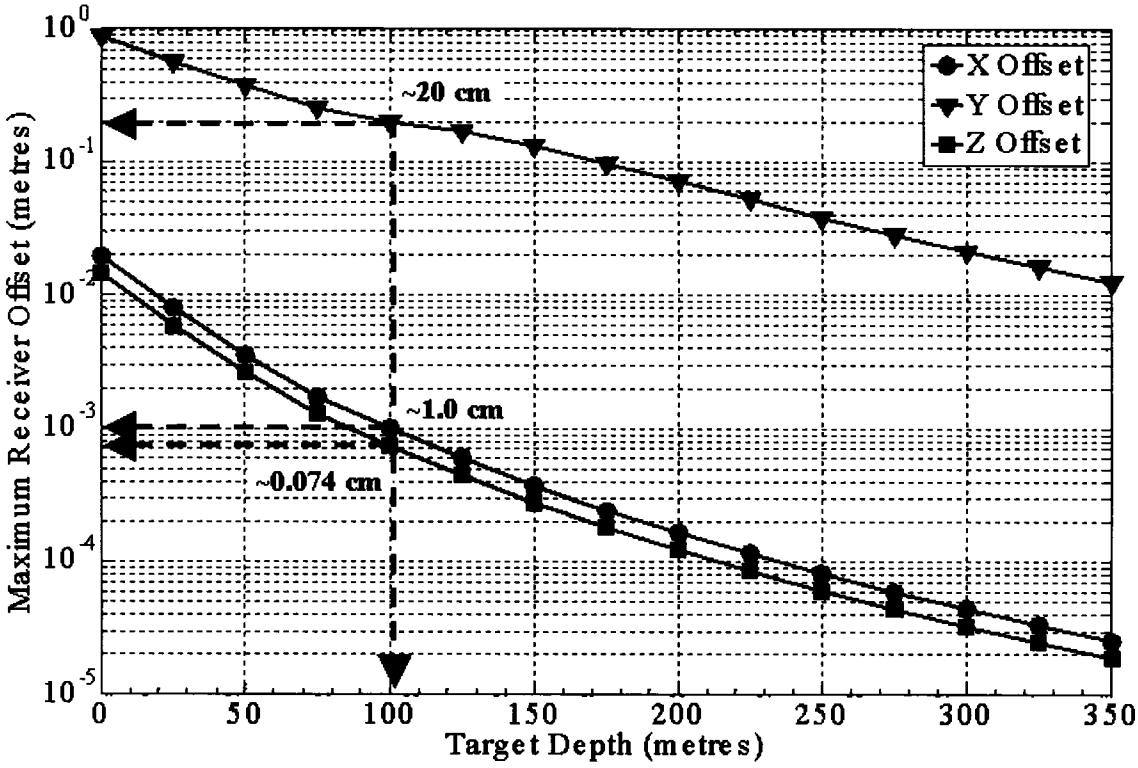


Figure 4.21: Maximum tolerable receiver offsets permitted to successfully detect and identify a vertical plate with a conductance of 10000 Siemens as a function of target depth for the HeliGEOTEM configuration. For example, for a target depth of 100 metres, the required accuracy in the $z$-direction is ~0.074 centimetres, the required accuracy in the $y$-direction is ~20 centimetres, and the required accuracy in the $x$-direction is ~1 centimetres.

for this analysis was chosen to allow a direct comparison between the other configurations. The normalized results are plotted in Figure 4.22 to allow comparison of each angle individually.

Figure 4.23 is a graph of the maximum tolerable attitude angles was produced for the target described above for a S/N $\geq 3$. As seen in Figure 4.23, the results show more stringent accuracy requirements for pitch. To successfully detect and identify the target at a depth of 100 metres, the transmitter pitch must be stable within approximately $\pm 0.0064$ degrees, which equates to about $\pm 0.062$ centimetres from the nominal position at the front edge of the transmitter loop. The tolerance is two orders of magnitude greater for roll, which can vary by approximately $\pm 0.65$ degrees. This equates to about $\pm 0.62$ centimetres from the nominal position at any side edge of the transmitter loop. Yaw has a negligible effect since it is equivalent to the transmitter rotating about its axis, which does not change the primary field.

### 4.3.3 Variations in Transmitter Loop Shape

Unlike fixed-wing systems, the transmitter for the HeliGEOTEM system is separate from the aircraft as shown in Figure 4.18 and Figure 4.19. The transmitter for the HeliGEOTEM system is very different than for the GEOTEM or the GEOTEM+ systems. The material used for its construction is much more rigid and the shape is circular. Equation (3) was used to calculate the primary field. This equation allowed the transmitter loop to be approximated as a sixteen-sided polygon.

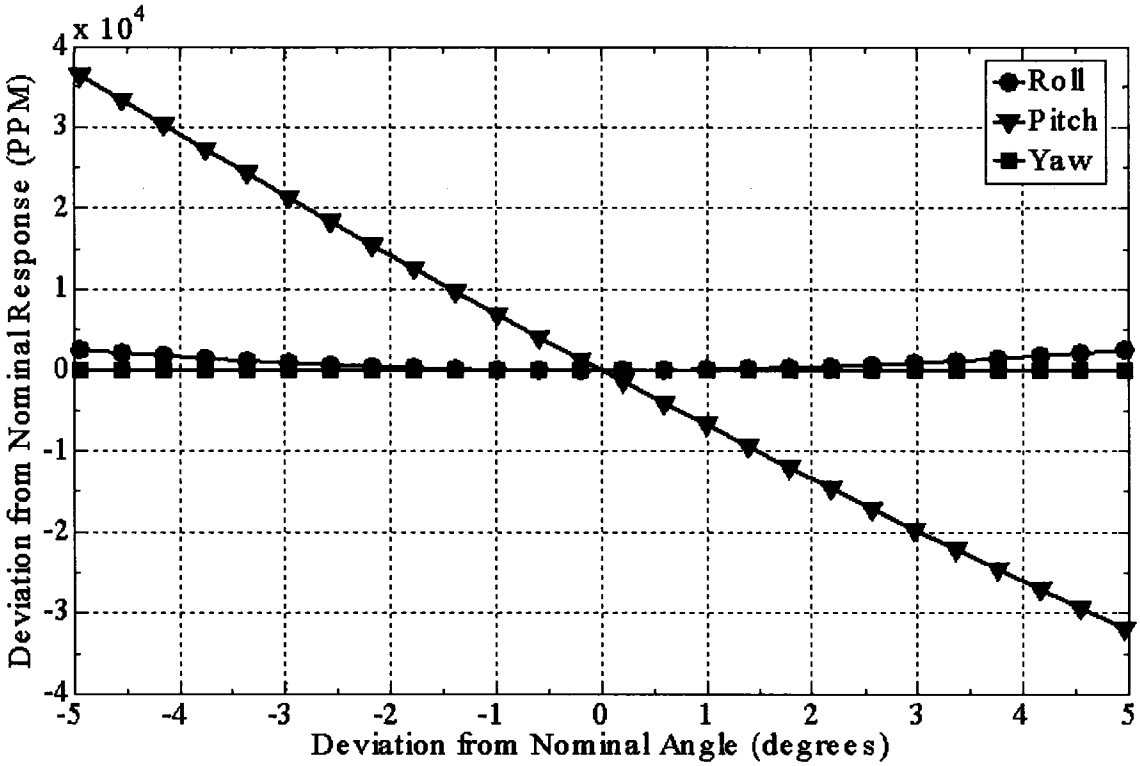


Figure 4.22: Deviation of the primary field from its nominal value as a function of variations in transmitter attitude for the HeliGEOTEM configuration. Note: The roll and yaw have such a minimal influence that they overlap close to zero.

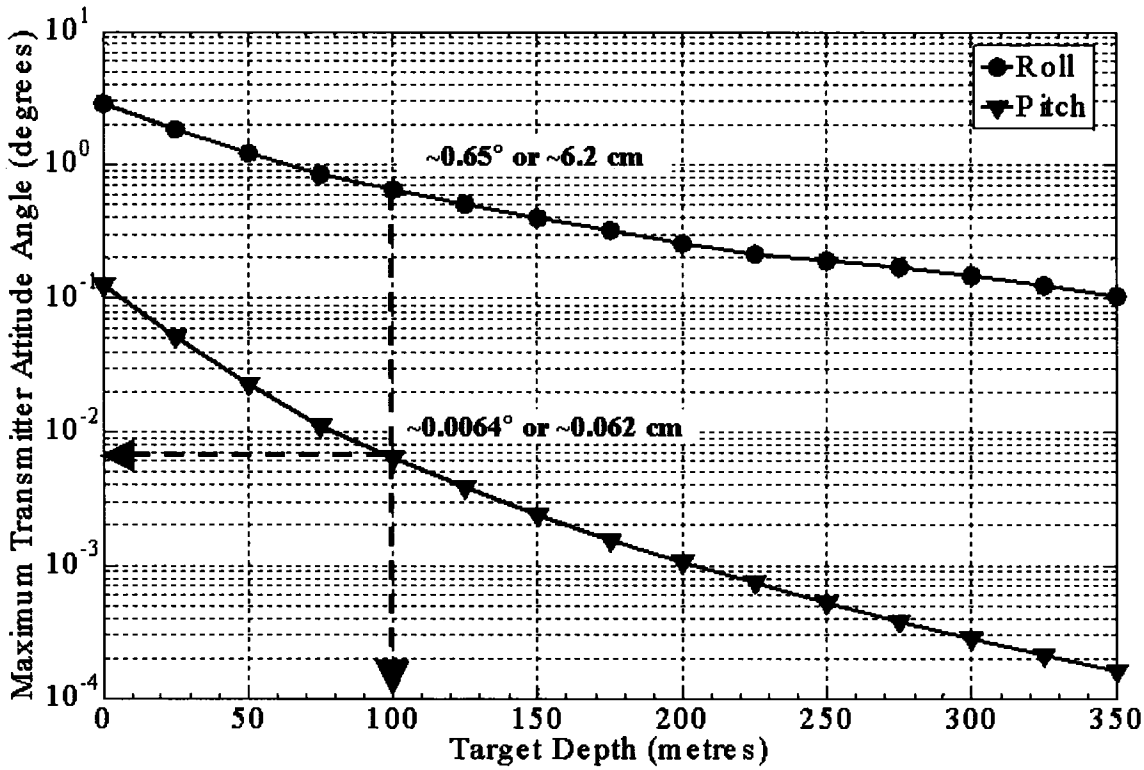


Figure 4.23: Maximum tolerable transmitter attitude angle variations permitted to successfully detect and identify a vertical plate with a conductance of 10000 Siemens plotted as a function of the depth to the target depth for the HeliGEOTEM system. Yaw has a negligible effect and is therefore omitted. For a target depth of 100 metres, roll requires an accuracy of ~0.65°; pitch requires variation less than ~0.0064°. These angles are equivalent to movements of ~6.2 centimetres at the front or back edge of the loop, and ~0.062 centimetres at the side edge of the loop.

For this analysis, four attachment points are considered fixed along the transmitter loop, one at the front, one at the rear, and one on each side as illustrated in Figure 4.24. The location of maximum deviation from the nominal is therefore midway between the attachment points. Although at the present time, there is virtually no way to determine the amount each of the loop segments actually moves during flight, it is estimated that the segments in between these attachment points are free to move by only a few centimetres as the loop is rigid. However, for the sake of comparison, the calculation was completed assuming that the maximum deviation of these mobile points is ±0.5 metres.

By the same methodology as in the GEOTEM and GEOTEM+ analysis, Equation (3) was used to calculate the primary field contribution of each segment in the various possible orientations, at the receiver. The minimum is always zero since the nominal position is one of the potential arrangements. The mean calculations may represent more movement than the actual loop deformation during flight but are still a valid comparison since at the present time there is no accurate measurement as to what the loop movement may actually be.

The statistics for the various deformations are plotted in Figure 4.25 where the deviations as a function of displacement are shown. The maximum variations allowed for successful target detection are plotted in Figure 4.26 assuming a S/N $\geq$3. From the graph

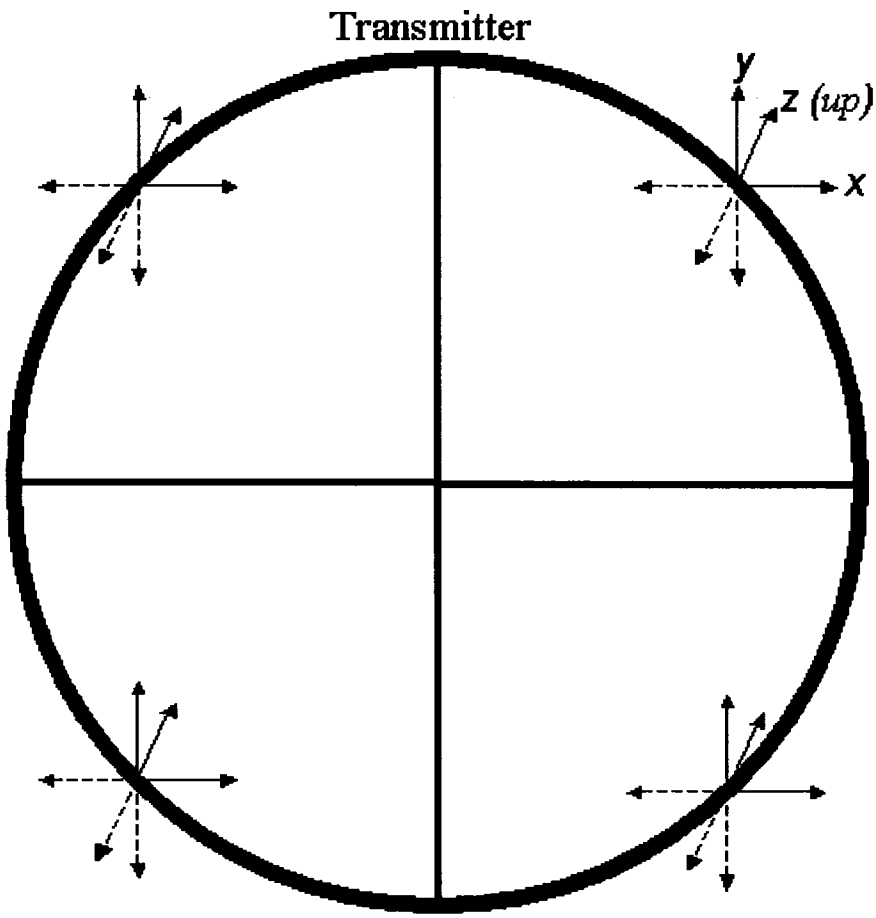


Figure 4.24: Top view of the HeliGEOTEM transmitter loop. The loop is a rigid construction and attached to the aircraft by a tow cable. The marked points along the loop are those that are varied in the directions shown for the HeliGEOTEM analysis.

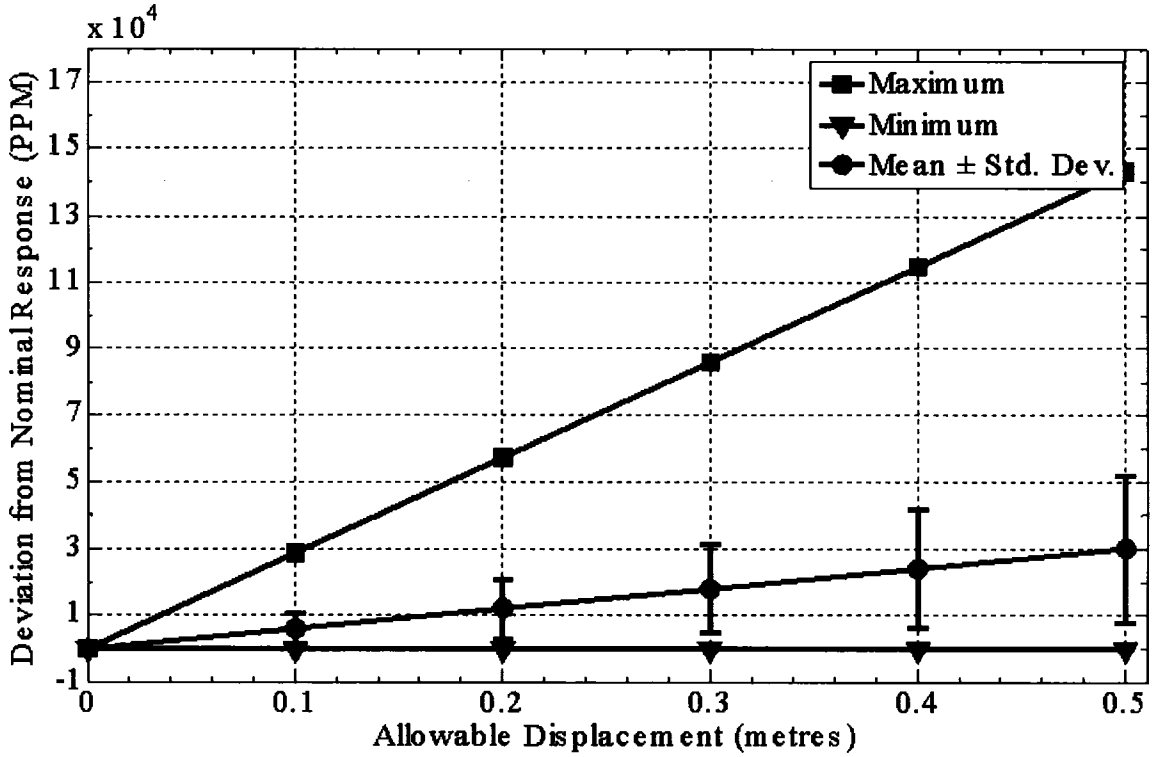


Figure 4.25: Deviation of the primary field from its nominal value as a function of displacement of the four mobile points midway between the attachment points along the transmitter loop shown in the previous figure for the HeliGEOTEM configuration.

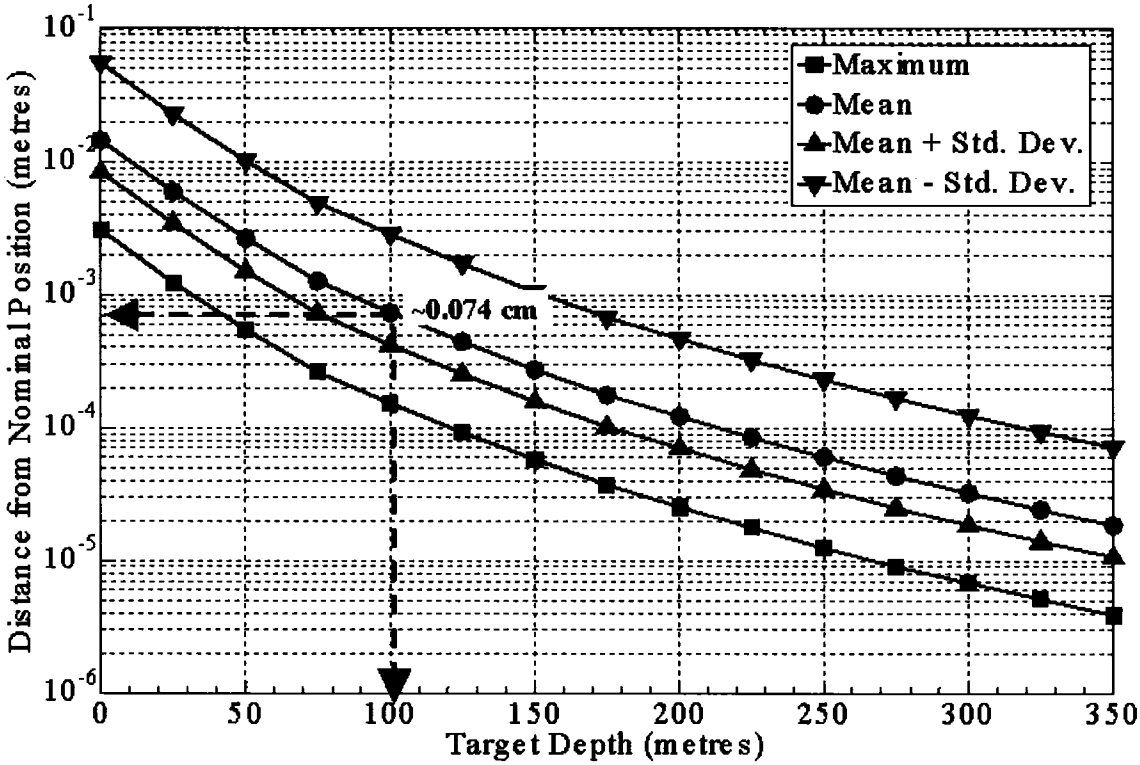


Figure 4.26: Maximum tolerable variations in order to successfully detect and identify a vertical plate with a conductance of 10000 Siemens as a function of target depth, for each statistical parameter derived in the loop deformation analysis for the HeliGEOTEM configuration. For example, for a target depth of 100 metres, the mean acceptable movement requires 0.074 centimetres accuracy. For the case representing larger loop deformation (mean plus one standard deviation), the accuracy requirement is more stringent and equal to 0.04 centimetres at a target depth of 100 metres.

in Figure 4.26, we can determine that to successfully detect the target described above at a depth of 100 metres, the maximum allowable deformation is ±0.074 centimetres given that the mean values are representative of the actual loop movement.

### 4.3.4 HeliGEOTEM Summary

The results for each of the variables for the HeliGEOTEM configuration are presented in Figure 4.27. For this configuration, as for the previous two systems, pitch has the greatest impact on the primary field measured at the receiver. However, the $z$-distance and the loop deformation play a more significant roll than the $x$-distance. The roll and the $y$-distance play a minor roll relative to the other variables.

## *4.4 Generic Concentric*

### 4.4.1 Variations in Receiver Position

The methodology for this analysis is different from the previous analyses of the GEOTEM, GEOTEM+ and the HeliGEOTEM. By definition, Equation (2) (the dipole formula) assumes that the distance between the transmitter and the receiver are much greater than the diameter of the loop. Since we are analyzing a configuration in which the receiver is inside the transmitter, the dipole formula is not applicable and would yield erroneous results. Hence, theoretical calculations were carried out using Equation (3) for all the analyses for the Generic Concentric configuration. Figure 4.28 provides a schematic illustration of the Generic Concentric configuration. The receiver is located in

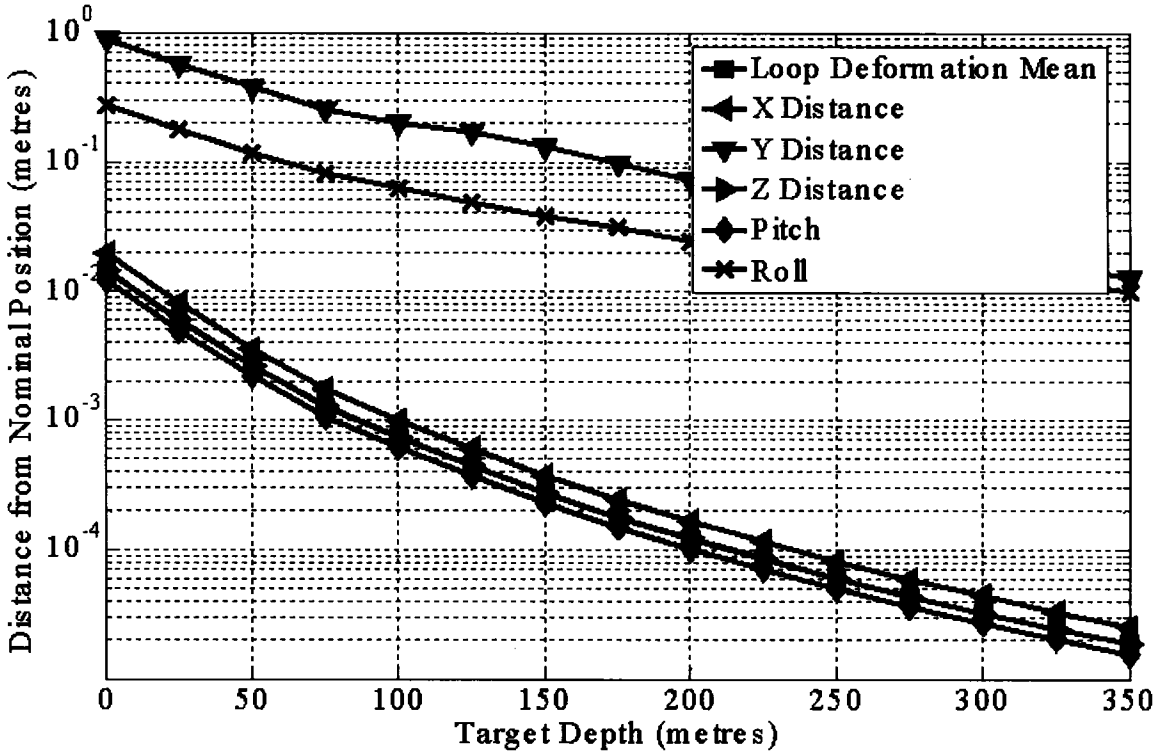


Figure 4.27: Comparison of all the variables for the HeliGEOTEM configuration. Units for the pitch and roll have been converted to a distance measurement at the nose and the wing tip respectively. The HeliGEOTEM is most sensitive to pitch followed by *z*-distance and loop deformation. When plotted, the curves for z-distance and the loop deformation overlap exactly and are very close to the pitch and the *x*-distance.

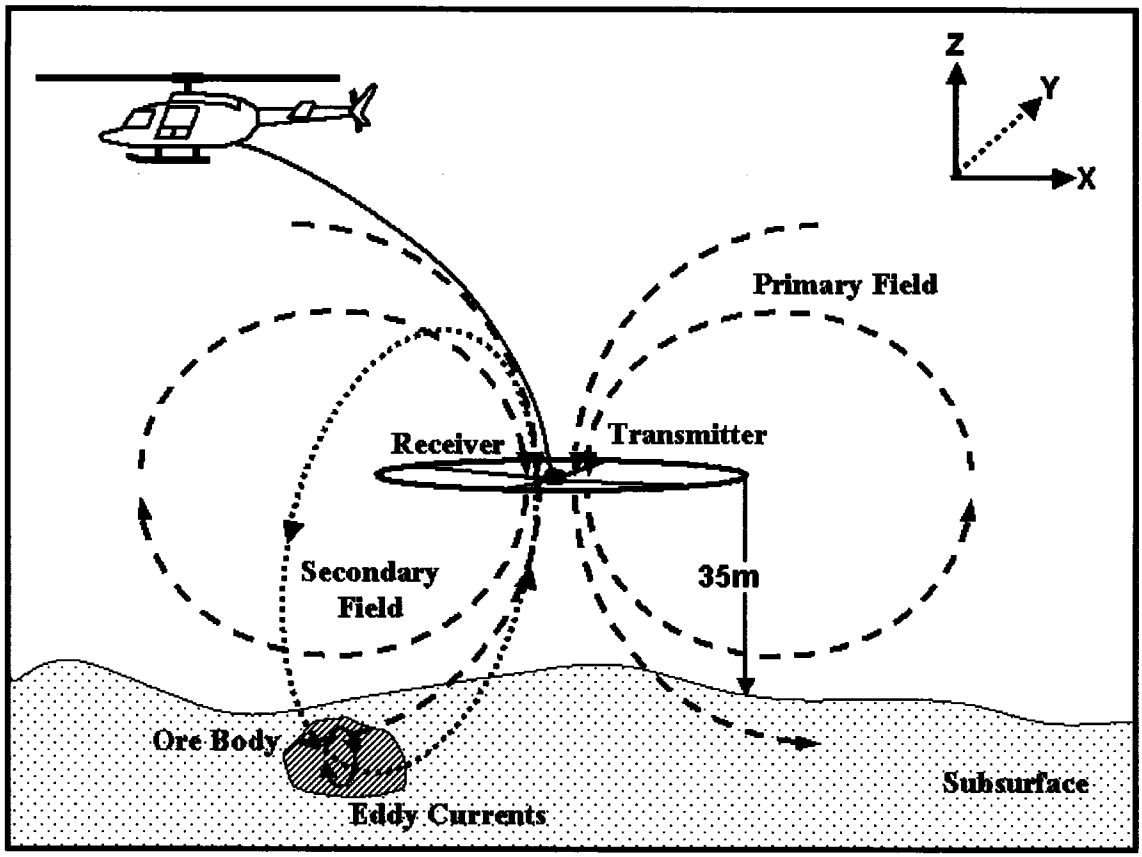


Figure 4.28: Schematic diagram of the Generic Concentric configuration. The mean transmitter loop altitude is 35 metres. The receiver and the transmitter are on the same plane.

the centre of the transmitter loop and both are suspended on a cable below the helicopter as illustrated in Figure 4.29. A sixteen-sided polygon is used to approximate the transmitter shape as in the analysis of the loop deformation of the HeliGEOTEM.

In the previous configurations, the values tested were within the range ±5 metres from the nominal position in each of the three *x*-, *y*-, and *z*-directions. For this configuration, however, that would bring the receiver across the transmitter loop. This range of motion is highly unlikely. Therefore, offsets were limited to a range of ±2.5 metres only. This range of values more than adequately spans the expected receiver variations encountered during straight and level flying. The normalized results in parts per million are plotted in Figure 4.30 to compare the effect of the offsets in each direction individually.

The greatest source of deviation from the nominal response occurs when the receiver moves in the ±*z*-direction, that is, in the vertical direction. This is different than the two fixed-wing scenarios but is similar to the HeliGEOTEM configuration. Figure 4.31 shows the accuracy for which the transmitter-receiver offset must be known for successful target detection. Using the same example as above, to successfully detect and identify the target at a depth of 100 metres, the receiver offset in the *z*-direction must be known to an accuracy of $1.96\times10^{-6}$ centimetres whereas along the direction of flight (*x*-direction) and in the *y*-direction, the offset must be known to $3.4\times10^{-6}$ centimetres.

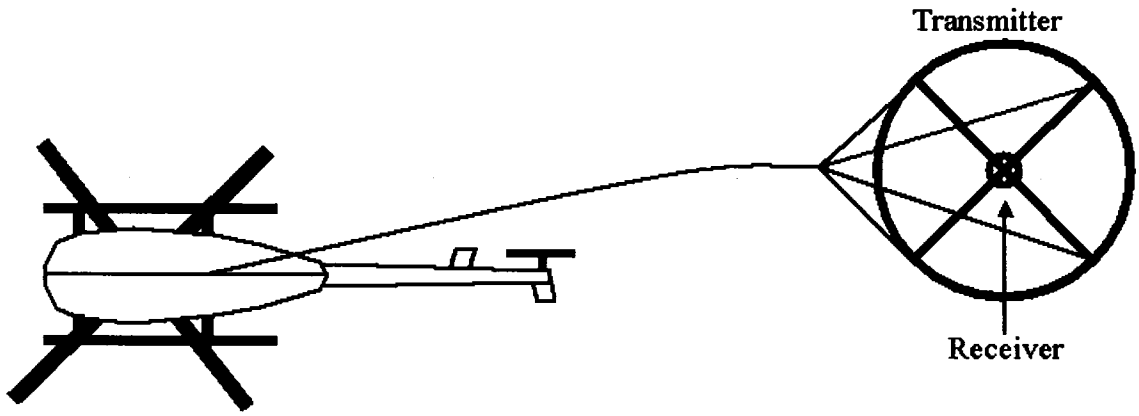


Figure 4.29: Underside view of the Generic Concentric configuration. The transmitter and the receiver are towed behind and below the aircraft. The transmitter is the larger outer loop (or series of outer loops) and the receiver is the inner loop (or series of inner loops).

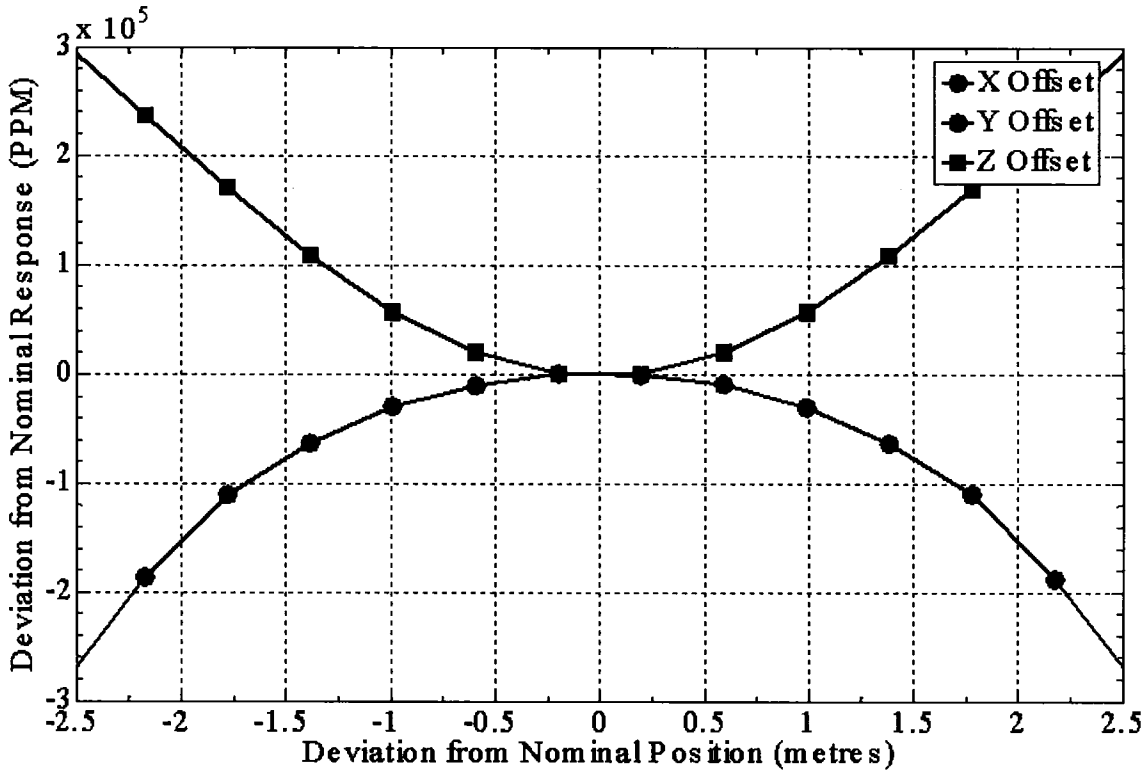


Figure 4.30: Deviation of the primary field from its nominal value as a function of variations in receiver positions for the Generic Concentric configuration.

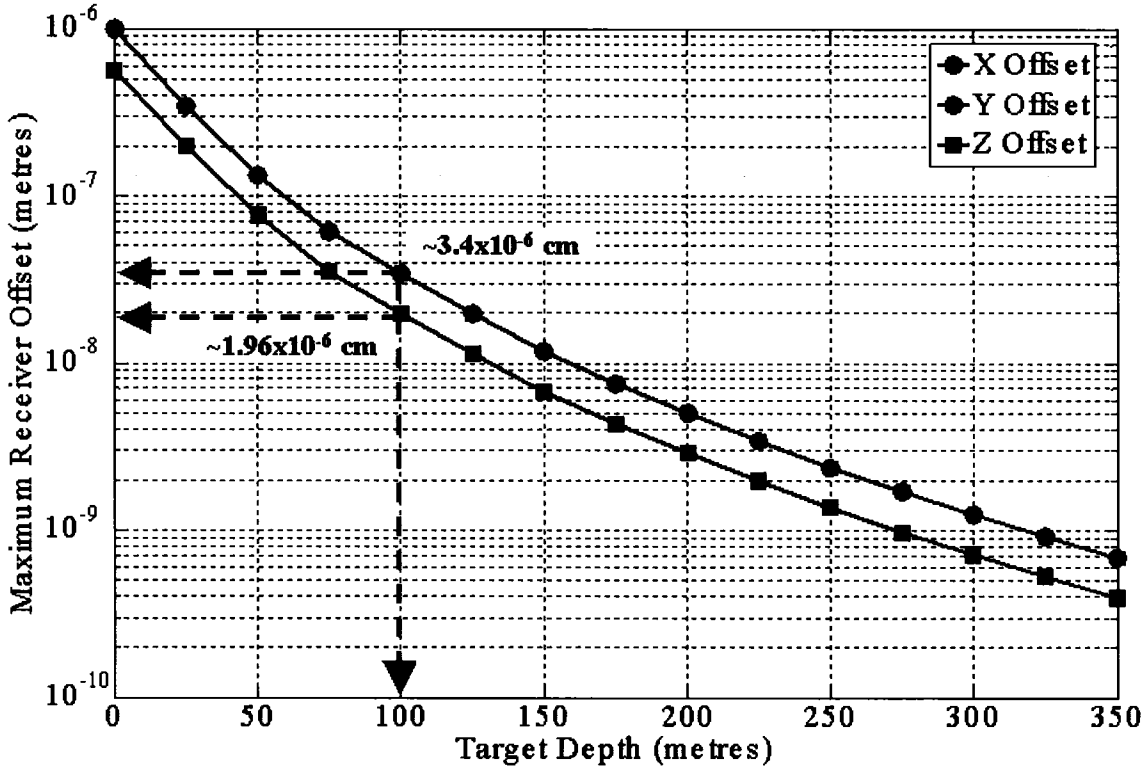


Figure 4.31: Maximum tolerable receiver offsets permitted to successfully detect and identify a vertical plate with a conductance of 10000 Siemens as a function of target depth for the Generic Concentric configuration. For example, for a target depth of 100 metres, the required accuracy in the $z$-direction is ~$1.96 \times 10^{-6}$ centimetres; the required accuracy in the $x$- and $y$-directions is ~$3.4 \times 10^{-6}$ centimetres.

### 4.4.2 Variations in Transmitter Attitude

For the same reasons as stated in the previous section, the methodology for calculating the effects of variations in transmitter attitude for the Generic Concentric configuration is using Equation (3), which is different than for the GEOTEM, GEOTEM+, and HeliGEOTEM configurations. However, the primary field at the receiver for transmitter attitude variations is still calculated for values ranging between ±5 degrees from the nominal roll, pitch, and yaw. This allows a straightforward comparison between the parameters of all the systems analyzed. The normalized results are plotted in Figure 4.32 to enable a direct comparison between the effects of variation of each angle individually.

A graph of the maximum tolerable attitude angles is shown in Figure 4.33, based on a S/N $\geq$3 detection criterion. The results show very stringent accuracy requirements for pitch and roll. Since this is a symmetric system, the pitch and the roll are identical. To successfully detect and identify the target at a depth of 100 metres, the transmitter pitch and roll must be stable within approximately $\pm 1.11 \times 10^{-5}$ degrees which equates to about $\pm 9.5 \times 10^{-5}$ centimetres from the nominal orientation at the edge of the transmitter loop. Yaw has a negligible effect since it is equivalent to the transmitter rotating about its axis, which does not change the primary field.

### 4.4.3 Variations in Transmitter Loop Shape

The methodology for the Generic Concentric configuration is similar to that used for the

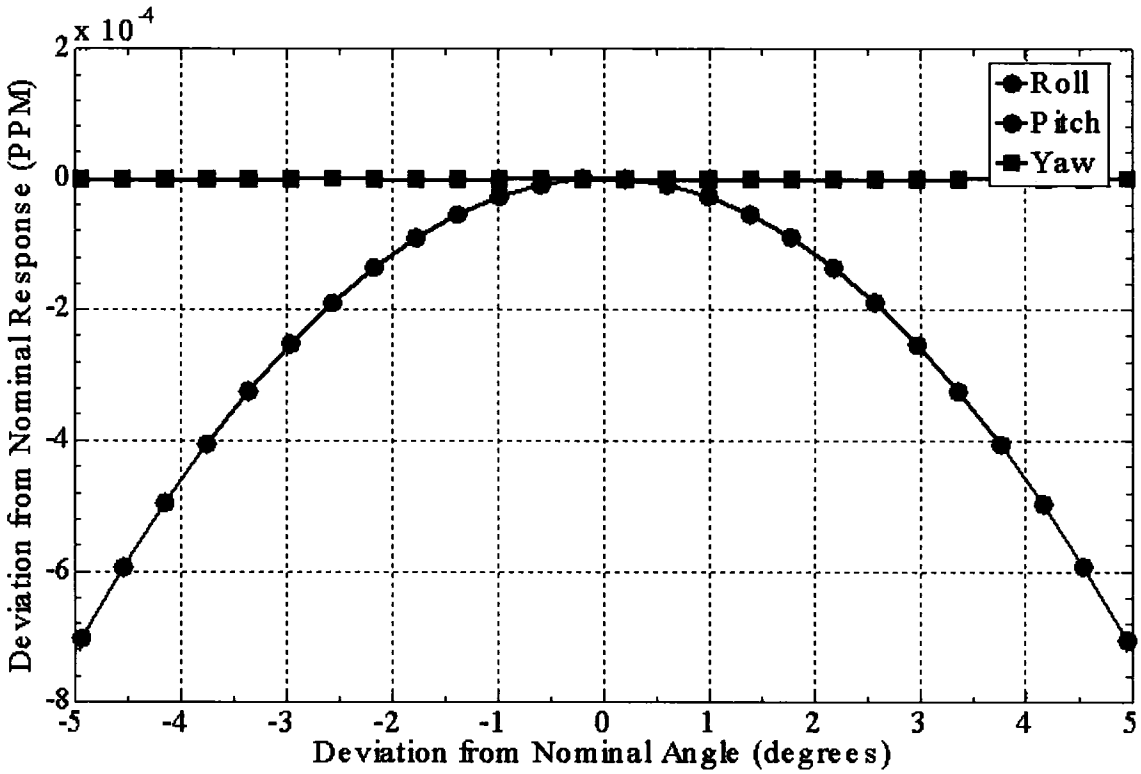


Figure 4.32: Deviation of the primary field from its nominal value as a function of variations in transmitter attitude for the Generic Concentric configuration. Note: The roll and yaw have such a minimal influence that they overlap close to zero.

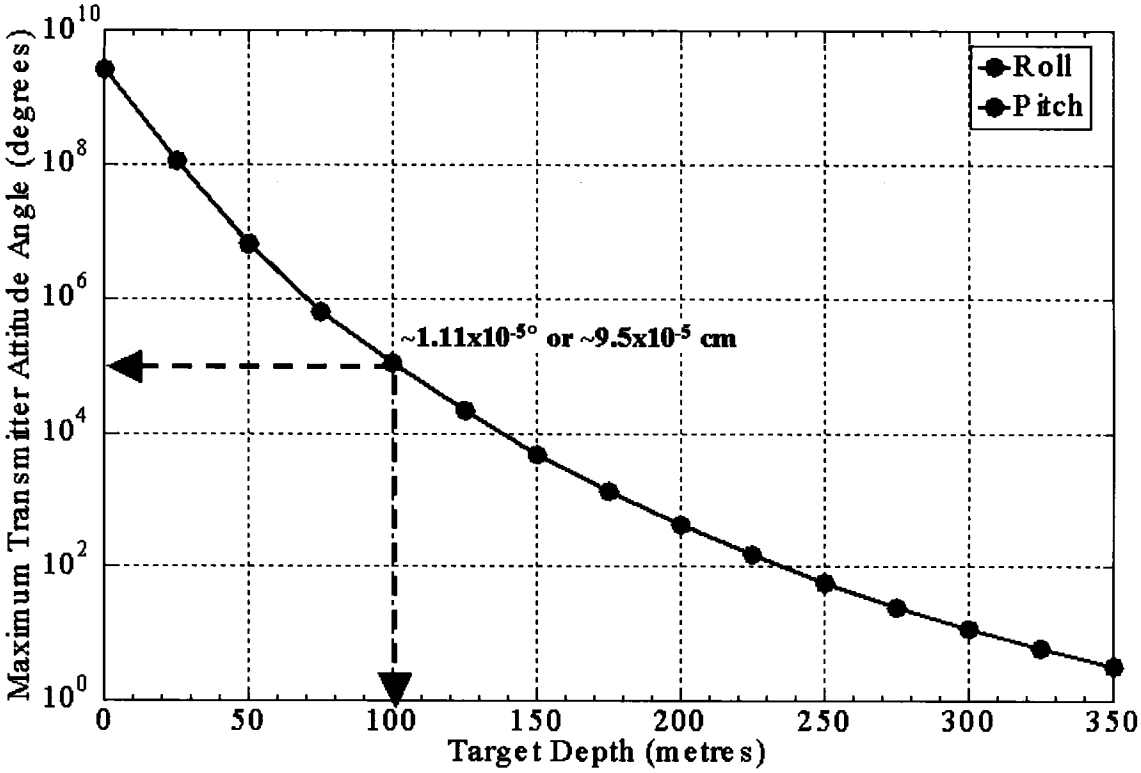


Figure 4.33: Maximum tolerable transmitter attitude angle variations permitted to successfully detect and identify a vertical plate with a conductance of 10000 Siemens as a function of target depth for the Generic Concentric system. Yaw has a negligible effect and is therefore omitted. Roll and pitch are identical for this configuration. For a target depth of 100 metres, both roll and pitch require an accuracy of $\sim 1.11 \times 10^{-5}$ degrees which is equivalent to $\sim 9.5 \times 10^{-5}$ centimetres at the edge of the transmitter loop.

HeliGEOTEM. There are four attachment points that are considered fixed along the transmitter loop, one at the front, one at the rear, and one on each side. The location of maximum deviation from the nominal is therefore midway between the attachment points as illustrated in Figure 4.34. As in the HeliGEOTEM analysis, Equation (3) was used to calculate the primary field at the receiver. This was, not only to allow for variation in movement of the transmitter segments but also to eliminate the error associated with the dipole approximation and the close proximity of the receiver to the transmitter. The calculations were completed assuming that the maximum deviation of these mobile points is ±0.5 metres as in the previous analyses. Although these values may seem large for this configuration, they allow for easy comparison with the other configurations. As before, for each of the different variations, the maximum, minimum, average and standard deviation were calculated. This is presented in Figure 4.35 where, as expected, the minimum is always zero since the nominal position is one of the potential arrangements.

Scenarios yielding the maximum deviation occur several times due to the symmetry of the system. Four of these scenarios occur when the points are arranged so as to minimize and maximize the size of the loop and pitch it both up and down; and four others occur when the points are arranged so as to minimize and maximize the size of the loop and roll it to its maximum on each side. However, these are considered extreme situations and the mean is more likely representative of the actual loop deformation during flight. Most likely deviations would probably be a wobble of the transmitter loop in which the front

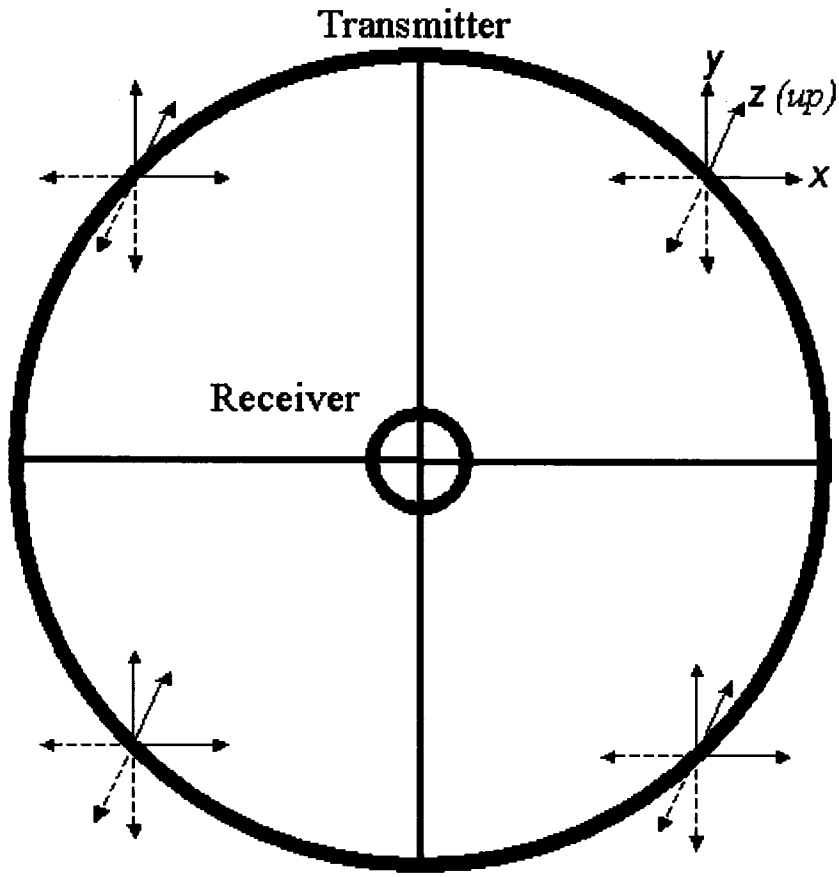


Figure 4.34: Top view of the Generic Concentric transmitter loop. The loop is a rigid construction and attached to the aircraft by a tow cable. The marked points along the loop are those that are varied in the directions shown for the concentric configuration analysis. The receiver is attached to the centre of the transmitter loop and is considered stationary for the loop deformation analysis.

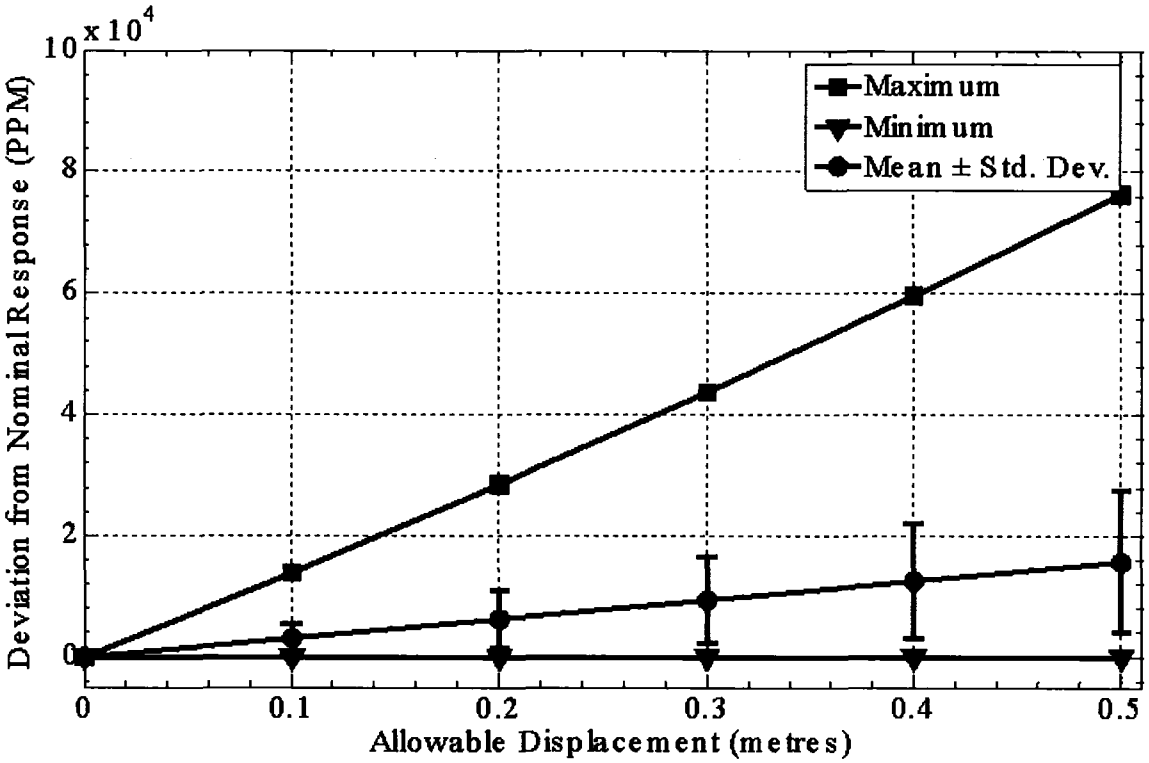


Figure 4.35: Deviation of the primary field from its nominal value as a function of displacement of the 4 mobile points midway between the attachment points along the transmitter loop shown in the previous figure for the Generic Concentric configuration.

and back or each of the sides move up and down opposite of one another. This would have a similar effect as a transmitter pitch or roll. This situation yields a deviation consistent with the mean values in the results.

The deviations as a function of displacement shown on Figure 4.35 were converted to the maximum variations allowed for successful target detection and plotted in Figure 4.36 assuming a S/N $\geq 3$. From the graph in Figure 4.36, we can determine that to successfully detect the target described above at a depth of 100 metres in the case of the maximum deviation scenario, the loop can only deform by a maximum of $\pm 7.2\times10^{-8}$ centimetres. However, if the mean values are representative of the actual loop movement, the maximum allowable deformation is $\pm 3.1\times10^{-7}$ centimetres.

### 4.4.4 Generic Concentric Summary

The results for each of the variables in the Generic Concentric configuration are presented in Figure 4.37. As with the other configurations, the attitude is presented in a distance measurement rather than an angle measurement for easy comparison. For this configuration, the loop deformation has the greatest impact on the primary field that is measured at the receiver. This variable is followed by the *z*-distance, *x*-distance, and transmitter roll and pitch, which are equal.

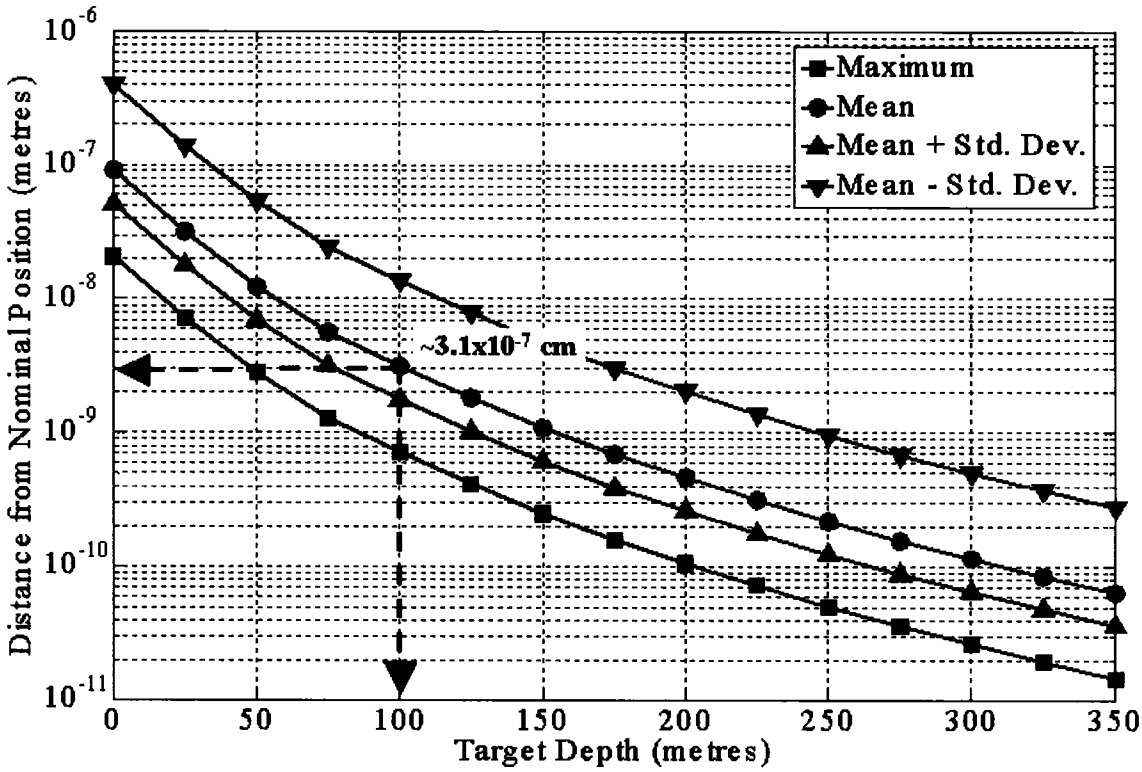


Figure 4.36: Maximum tolerable variations in order to successfully detect and identify a vertical plate with a conductance of 10000 Siemens as a function of target depth, for each statistical parameter derived in the loop deformation analysis for the Generic Concentric configuration. For example, for a target depth of 100 metres, the mean acceptable movement requires $3.1 \times 10^{-7}$ centimetre accuracy. For the case representing maximum loop deformation, the accuracy requirement is more stringent and equal to $7.2 \times 10^{-8}$ centimetres for a target depth of 100 metres.

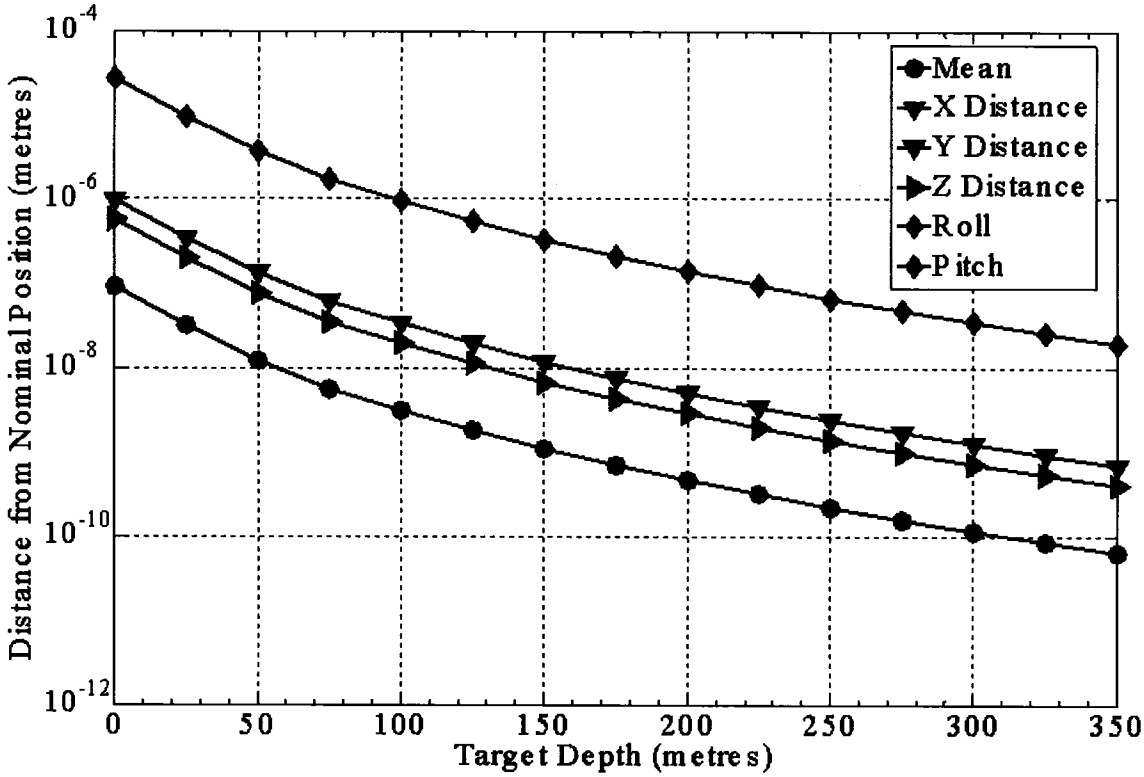


Figure 4.37: Comparison of all the variables for the Generic Concentric configuration. Units for the pitch and roll have been converted to a distance measurement at the edge of the transmitter loop.

# 5. Discussion

## *5.1 GEOTEM*

For the GEOTEM system, the transmitter-receiver geometry can vary in a number of ways: the distance between the transmitter and the receiver in each of the *x*-, *y*-, and *z*-directions can vary; there can be variations in attitude (roll, pitch, and yaw) of the transmitter; and transmitter loop deformation. All have a significant impact on the primary field measured at the receiver. The most significant variables are the transmitter pitch, followed by variations in loop shape, and by the receiver position in the direction of flight. Other variables play a less important role but are nevertheless important to accurately determine the primary field at the receiver.

The variations for each parameter for the GEOTEM system are somewhat understood as they can be measured with the exception of loop deformation. However, the parameters that can be measured can only be measured to a degree of accuracy much less than necessary to correct the problem. Several solutions have already been implemented to minimize variations in the geometry of the system. The aerodynamic design of the receiver casing, for example, is intended to help stabilize the receiver during flight, although its movement cannot be completely controlled. As the transmitter is mounted directly to the aircraft, the transmitter loop is subject to any maneuvers that the aircraft makes. This includes changes in roll, pitch, and/or yaw. Although every attempt is made to minimize these variations, their effect on the data will become exacerbated in survey areas with rough topography.

The GEOTEM has a flexible transmitter loop that may be considered a source of noise. However, since the dynamics of the transmitter loop during flight are not known, it is difficult to speculate on how great a source of noise this may be.

To minimize the geometric variations, one potential solution is to fly at a constant altitude. Without the aircraft attempting to maintain a constant elevation above ground, the relative geometry of the transmitter and the receiver would be more stable. However, this potential solution requires a method to correct for altitude variations with confidence. The data could be then mathematically corrected for the variation in altitude in post-processing.

### *5.2 GEOTEM+*

As the GEOTEM+ system is similar in configuration to the GEOTEM system, the relative geometry distortions are very much the same for both systems. Similar to the GEOTEM system, the pitch had the greatest amount of impact on the measured primary field at the receiver for target depths greater than ~50 metres. In decreasing order, loop shape deformation, $x$-distance offset, $z$-distance offset, roll and $y$-distance offset, also affect the primary field measured at the receiver.

Although the parameters are in the same order of impact as the GEOTEM system, the greater separation between the transmitter and the receiver in the GEOTEM+ system reduces the effects of the geometric variations on the data. At this time it is virtually impossible to determine how the geometry will vary since this is a hypothetical system.

It may be found that the increased distance between the transmitter and the receiver causes a large increase in system instability and the amount of geometric variation is too great and counteracts any improvement obtained from increasing the transmitter-receiver separation. Another consideration is the additional drag associated with the increase in cable length. Questions of whether or not the cable and/or winch are strong enough to bear the additional weight must be answered before implementation.

As GEOTEM+ is a hypothetical system, we can only speculate on the amount of variation expected for each parameter. This system configuration, however, does bring an interesting approach to the current primary field problem. The GEOTEM+ approach would be a cost effective and relatively easy solution. There are, however, no current plans to implement this system configuration.

### *5.3 HeliGEOTEM*

The HeliGEOTEM system is most sensitive to variations in transmitter pitch followed equally by transmitter loop deformation and variations in the $z$-direction. Movements in the $x$-direction, transmitter roll and movements in the $y$-direction have a less significant impact, respectively. The location of the transmitter loop below the receiver is unique to the HeliGEOTEM system. The very heavy weight of the transmitter is a means of stabilizing the entire transmitter-receiver unit. This system is new on the market and considered still experimental. The HeliGEOTEM configuration is not well established and therefore, the variation of the transmitter and the receiver are currently being evaluated.

### *5.4 Generic Concentric System*

The Generic Concentric system is most sensitive to variations in the transmitter loop shape. This is expected since the receiver is in close proximity to the transmitter and is attached directly to the transmitter loop. Deviations in the $z$-direction have a significant but lesser impact. Effects from variations in the $x$- and $y$-directions are slightly less than variation in the $z$-direction but are identical to one another. This is expected because the system has the receiver in the centre of the transmitter loop and the effect of any movement away from the centre is independent of direction for the total component at the receiver. Variations in the roll and the pitch are identical to one another. For the same reasons, roll and pitch have a less significant impact on the primary field measured by the receiver than all the other variables with exception of yaw. Provided that the transmitter loop maintains a vertical axis and the transmitter shape remains the same, the yaw has virtually no effect on the data.

### *5.5 System Comparison*

#### 5.5.1 Variations in Offset in the *X*- *Y*- and *Z*-Direction

Figure 5.1 shows the required accuracy necessary in the $x$-direction for various target depths. It is a good indication of how variation of the relative position of the transmitter with the receiver along the $x$-direction impact primary field measured at the receiver for each of the four systems analyzed. From this figure, it can be determined that the most sensitive system to this type of motion is the Generic Concentric system

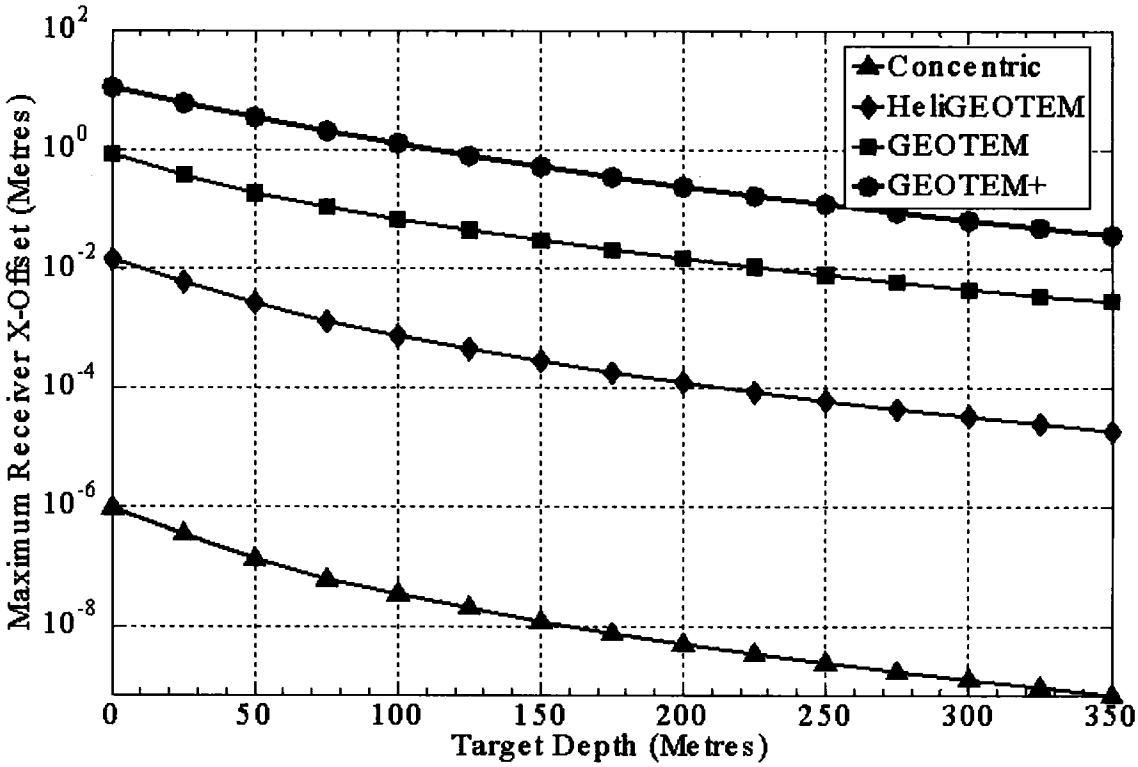


Figure 5.1: Maximum tolerable variations in order to successfully detect and identify a vertical plate with a conductance of 10000 Siemens as a function of target depth, for variations of the receiver location in the $x$-direction for each of the systems analyzed.

followed by the HeliGEOTEM, the GEOTEM and the GEOTEM+, respectively. It is apparent that for variation along the *x*-direction, the closer the receiver is to the transmitter, the more sensitive the configuration is to variation in the geometry.

Figure 5.2 illustrates the impact of variation of offset in the *y*-direction for each system for various target depths. As with the *x*-direction, the most sensitive system is the Generic Concentric system, followed by the HeliGEOTEM, the GEOTEM, and the GEOTEM+ respectively. It is important to note that variations in the *y*-direction are several orders of magnitude less than for the offset in the *x*-direction. In fact, variation in the *y*-direction has the least effect of the parameters tested.

Figure 5.3 shows the impact of variation of the offset in the *z*-direction for each system for various target depths. As with the *x*-direction and *y*-direction, the most sensitive system is the Generic Concentric system, followed by the HeliGEOTEM, the GEOTEM and the GEOTEM+ respectively. Offset in the *z*-direction has a larger impact than offset in the *y*-direction but less than offset in the *x*-direction for the fixed-wing systems (GEOTEM and GEOTEM+). However, for the helicopter systems (HeliGEOTEM and Generic Concentric) offset in the *z*-direction has a much greater impact than either *x*- or *y*-directions.

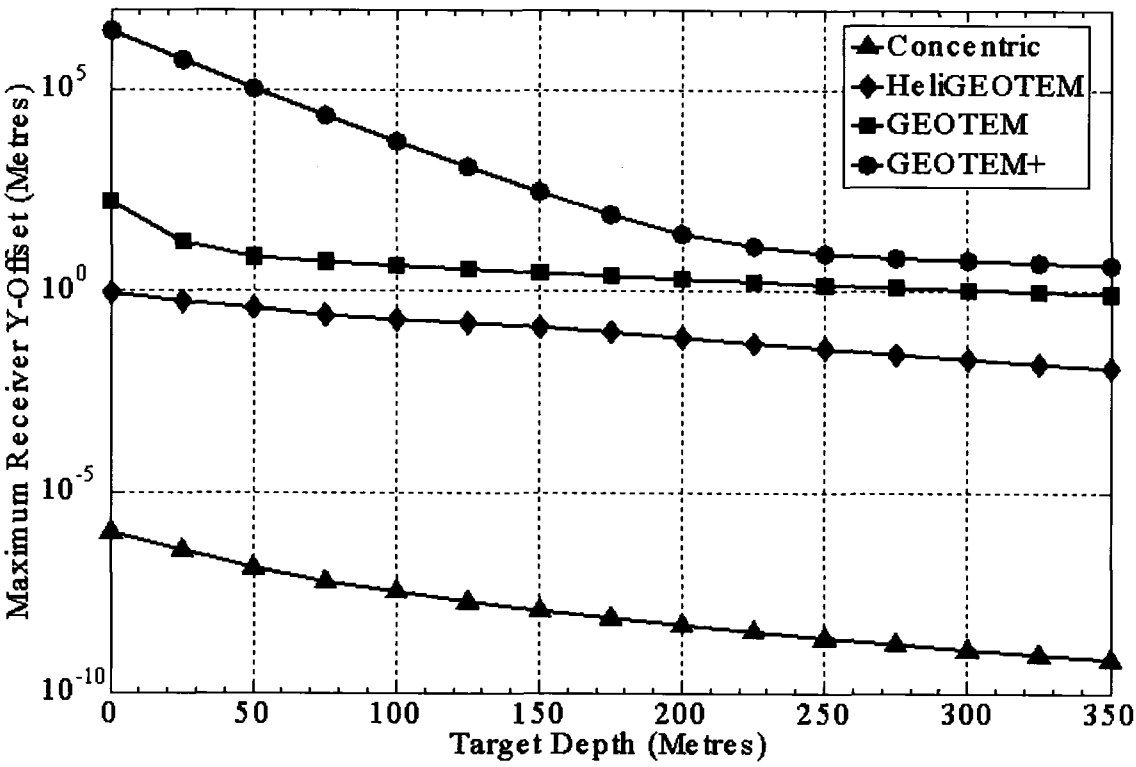


Figure 5.2: Maximum tolerable variations in order to successfully detect and identify a vertical plate with a conductance of 10000 Siemens as a function of target depth, for variations of the receiver location in the *y*-direction for each of the systems analyzed.

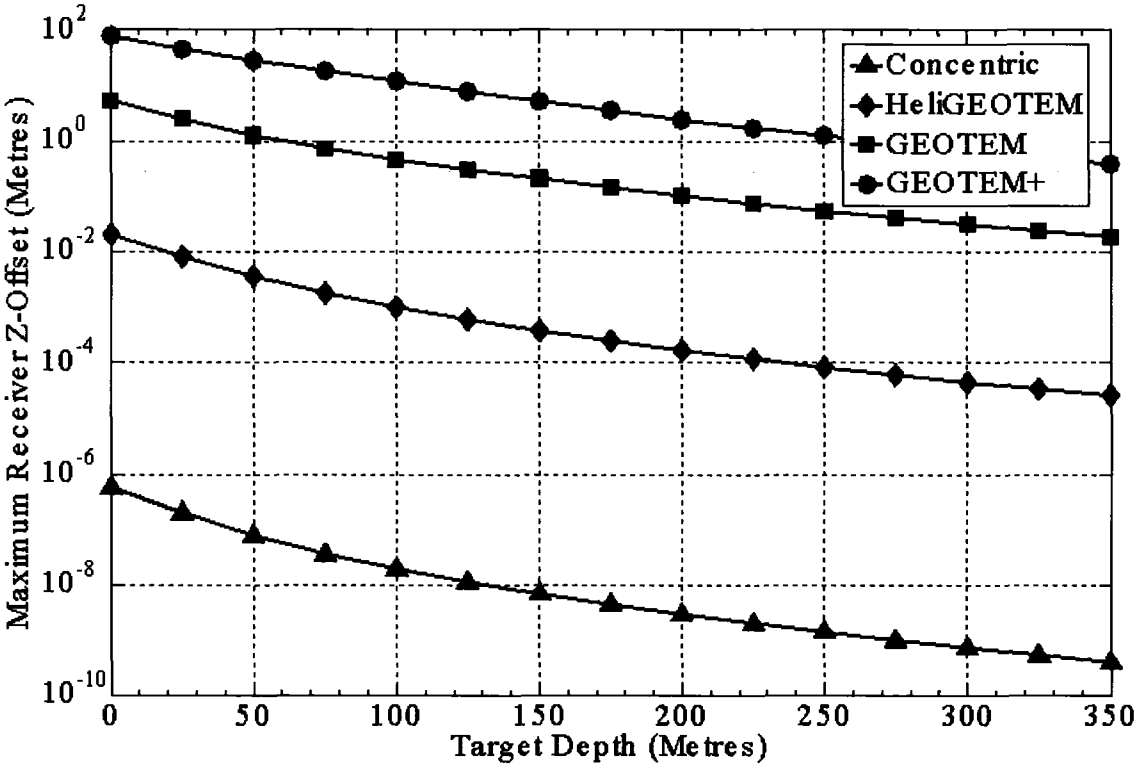


Figure 5.3: Maximum tolerable variations in order to successfully detect and identify a vertical plate with a conductance of 10000 Siemens as a function of target depth, for variations in the *z*-direction for each of the systems analyzed.

### 5.5.2 Variations in Roll, Pitch and Yaw

As with offset in the $x$, $y$, and $z$-directions, roll has the most significant impact on the transmitter receiver geometry for the Generic Concentric system, followed by the HeliGEOTEM, GEOTEM, and then the GEOTEM+ systems as shown in Figure 5.4.

Pitch also has the most significant impact on the transmitter receiver geometry for the Generic Concentric system, followed by the HeliGEOTEM, GEOTEM, and then the GEOTEM+ systems as shown in Figure 5.5. However, it is important to note that pitch also has the greatest impact, of all the variables analyzed, on the primary field that is measured at the receiver for the GEOTEM system, the GEOTEM+ system, and the HeliGEOTEM system as shown in Figures 4.5, 4.14, and 4.23 respectively. For the Generic Concentric system, since the receiver is in the centre, pitch and roll have an equivalent impact.

The yaw has a negligible impact on the primary field measured at the receiver for all the systems. This is expected since, for all systems, the transmitter has a largely vertical axis and a rotation about this axis does not change the distance or orientation between the transmitter and the receiver when the total component is measured at the receiver.

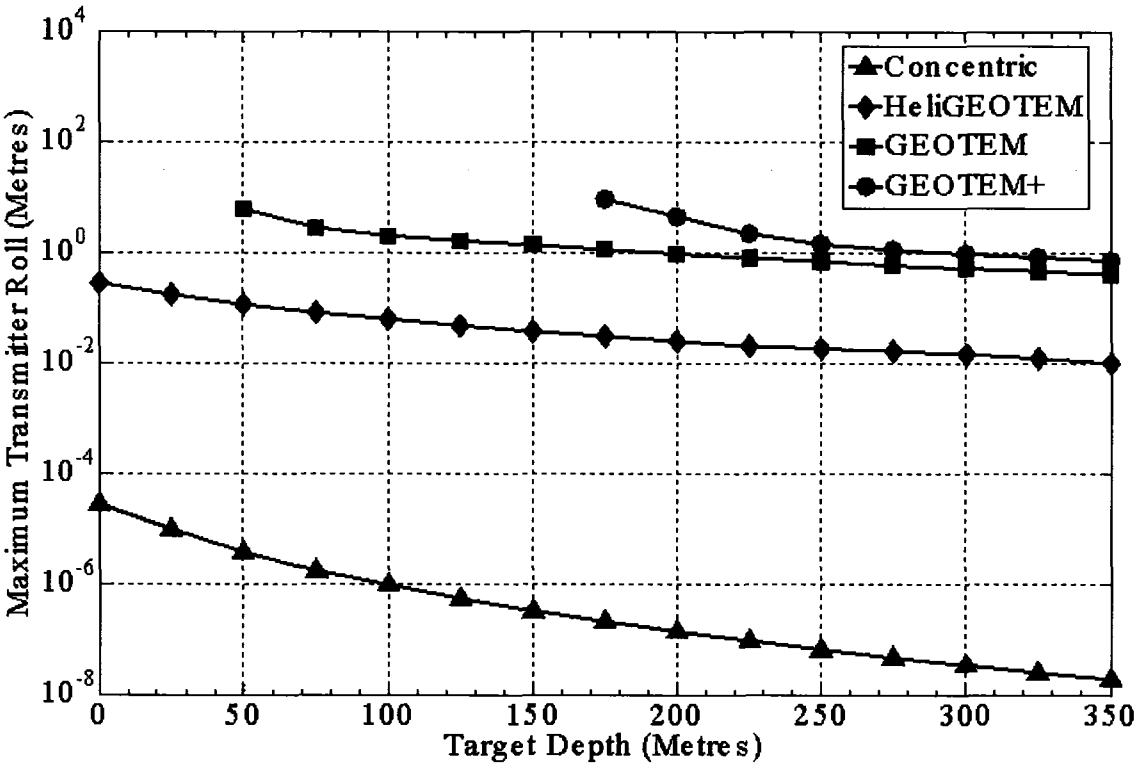


Figure 5.4: Maximum tolerable variations in order to successfully detect and identify a vertical plate with a conductance of 10000 Siemens as a function of target depth, for variations in roll for each of the systems analyzed. Units for roll have been converted to a distance measurement at the edge of the transmitter.

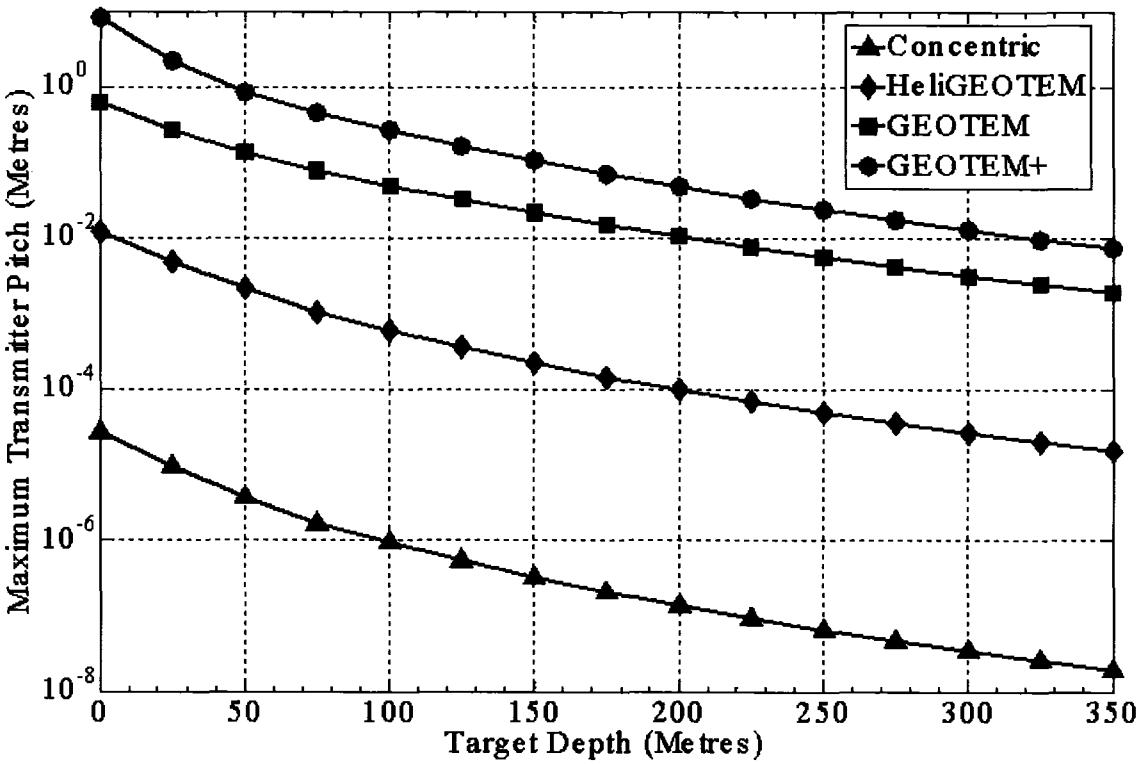


Figure 5.5: Maximum tolerable variations in order to successfully detect and identify a vertical plate with a conductance of 10000 Siemens as a function of target depth, for variations in pitch for each of the systems analyzed. Units for pitch have been converted to a distance measurement at the edge of the transmitter.

### 5.5.3 Variations in Loop Deformation

Figure 5.6 shows how variations in the transmitter loop shape rank for each of the four systems analyzed. For the Generic Concentric system, loop deformation has the greatest impact of all the variables on the primary field measured at the receiver. This is due to the close proximity of the receiver with the transmitter. As the concentric system analyzed in this thesis is generic, the transmitter loop construction has not been specified. For the Geotech VTEM system, the loop is constructed out of a flexible material while for the Aeroquest AeroTEM system, the loop is constructed out of a rigid fiberglass material. The amount of transmitter loop deformation typical of these systems is unknown. It is likely, though, that deformation is more of an issue for the flexible loop of the VTEM system.

After pitch variations, variations in the transmitter loop shape have the most significant impact on the primary field measured for the GEOTEM, GEOTEM+ and the HeliGEOTEM systems. The transmitter loop for the fixed-wing systems is constructed out of a flexible material and therefore has the potential to deform slightly. The HeliGEOTEM transmitter loop is constructed out of rigid tubing and is likely not to deform significantly.

## *5.6 Potential Solutions*

There are two general approaches to correct the primary field for variations in system geometry. The first is to limit the variations themselves; the second is to determine what

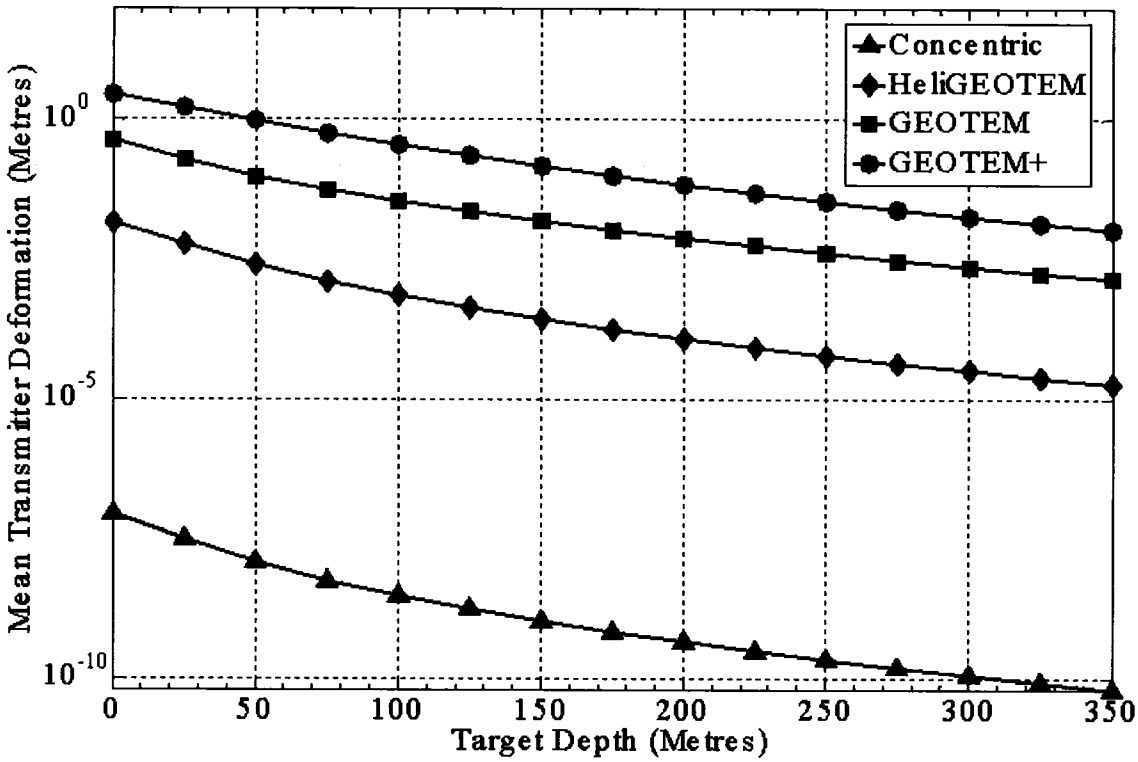


Figure 5.6: Maximum tolerable variations in order to successfully detect and identify a vertical plate with a conductance of 10000 Siemens as a function of target depth, for the mean variation in transmitter shape for each of the systems analyzed.

the variations are and mathematically correct for them in the data. There are limitations with each approach. To ensure that the transmitter and the receiver do not move with respect to one another is very difficult and becomes progressively more as the distance between the transmitter and receiver increases. The systems analyzed are airborne systems and as such they are subject to a variety of stresses and forces, not all of which can be accounted for. The materials from which each system is constructed are limited to various plastics and fiberglass as metallic materials cause interference with the receiver. Steps have already been taken to minimize the geometric variations between the transmitter and the receiver in most of the systems currently available. Whatever geometric variations remain must be first removed by determining what the variation is, and then by making the appropriate corrections to the data.

Determination of the geometric variation between the transmitter and the receiver is limited by technology. As stated earlier, there is no current method to directly measure the distance between an aircraft and a towed receiver. In the case of the GEOTEM system specifically, the market was surveyed to identify promising technologies that could track the receiver and measure its distance relative to the plane during flight. The Appendices presents several systems spanning various technologies such as laser, optical, and satellite, that have been evaluated for the purpose of accurately measuring the variation of the geometry of the transmitter and the receiver. Three systems have been identified as potential solutions (1) a total station positioning system, (2) video photogrammetry and (3) Global Positional Satellites (GPS). Considerations for cost-

effective implementation, operational complexity, and system durability have all been taken into account.

### 5.6.1 Surveying total stations

There are several devices that are potentially capable of locating and tracking an object such as the receiver behind an aircraft. One such system is a total station used in surveying. Modern surveying total stations combine the functionalities of traditional theodolites with the ability of making distance measurements. A theodolite is an instrument for measuring both horizontal and vertical angles, as used in triangulation networks. It consists of a telescope mounted movably within two mutually perpendicular axes, the horizontal and the vertical axis. A theodolite tracking mechanism uses an apparatus that can be mounted directly to the target to allow the Electronic Distance Measurements (EDM) device to locate and track the target.

During this project, preliminary tests were carried out using a Leica TPS-1100A total station. When tested, the total station did not perform well when it was subjected to slight vibrations resembling those on an aircraft. Refer to Appendix A for further information on these tests. Although the TPS1100-A was not selected for further testing, the testing that was completed did help develop a better understanding of the desired characteristics of a future system for the application of tracking a receiver towed behind an aircraft. Although a total station performs well for its intended use, it requires a stable environment for operation. Further development of such a tracking system should include the following specifications:

1. Ability to withstand the vibrations associated with an aircraft.
2. Ability to measure accurately the distance and offset to 7 centimetres or less to detect a target at 100 metres depth in the case for the GEOTEM system.
3. Ability to withstand the electrical interference associated with the aircraft, transmitter and static effects from the air.
4. Offer no interference with the recording of the data or the electromagnetic fields measured.
5. Ability to be integrated with the existing software and hardware easily.
6. Easy to mount on the outside of aircraft fuselage with minimal disruption.
7. Easy to maintain.
8. Easy and quick to calibrate.
9. Reasonably priced.
10. Supported by the manufacturer.

Appendix A presents the testing and evaluation results of this system for the purpose of locating the GEOTEM receiver from the aircraft.

### 5.6.2 Vision Systems

Another option evaluated to measure the location of a towed receiver behind an aircraft, as is the case for the GEOTEM system, was a vision system. Vision systems are based on the principles of photogrammetry. Photogrammetry is a measurement technology in which two or more photographic images, taken from different positions, are used to

determine the three-dimensional coordinates of points on an object. This is accomplished by identifying common points on each image. A line of sight (or ray) can be constructed from the points identified on the object to the camera location. By identifying the intersections and triangulating these rays, the three-dimensional location of the points can be found.

As part of this project, preliminary discussions were held with Neptec of Ottawa, Canada. Neptec uses photogrammetry in their Space Vision System (SVS). The SVS is currently used to ensure accuracy in assembling the different modules of the International Space Station. Several problems would have to be overcome before the SVS could be used to address the problem of the transmitter-receiver geometry in airborne EM geophysical systems. At present, the SVS is not capable of calculating a location quickly enough to measure the location accurately. This means either the calculations would have to be simplified, or generated at a faster rate. Another problem is that the range of motion of the receiver with respect to the transmitter in the GEOTEM system extends beyond the field of view of the SVS system. Although a wide angle lens is an option, there are additional errors associated with this type of lens. Additional information on the SVS is presented in Appendix B.

### 5.6.3 Global Positioning Satellite (GPS) systems

The Global Positioning System (GPS) is the only fully-functional satellite navigation system operating at present. It consists of a constellation of more than two dozen satellites that broadcasts precise timing signals by radio to electronic GPS receivers. This allows the receiver to accurately determine the location (longitude, latitude, and altitude) in real time, day or night, in any weather, virtually anywhere on Earth.

GPS technology continues to advance with the Wide-Area Augmentation System (WAAS), available since August 2000, which increases the accuracy of GPS signals to within 2 metres. GPS accuracy can be improved further, to about 1 centimetre over short distances, using techniques such as Differential GPS (DGPS). DGPS requires at least one extra receiver.

There is a possibility of introducing DGPS to help solve the problem of transmitter-receiver geometry in airborne EM systems. However, there are several factors that must be considered. The DGPS antenna would have to be mounted on the receiver itself. Not only would the weight distribution be changed significantly, but also it may involve a redesign of the whole EM receiver casing. Furthermore, as the DGPS receiver it is an electronic device, it could introduce interference with such close proximity to the receiver coils.

Data transfer between the GPS antenna and the aircraft where data is recorded is problematic. The analogue signal from the receiver would have to be converted to digital, or boosted before being sent the long distance to the aircraft. This adds electronic components to the receiver that may provide a source of interference to the measured data at the receiver and manipulating the signal from the GPS antenna heightens the risk of error to the positional data. The distance the signal has to be sent to aircraft for recording may also provide a means to introduce interference and therefore may be an additional source of error.

Monitoring the transmitter loop deformation of the GEOTEM (or GEOTEM+) with GPS is a substancial obstacle. The transmitter loop would have to be monitored at several different locations with a high degree of accuracy. The transmitter loop carries a considerable amout of electrical current that would more than likely have an adverse impact on the GPS antennae's ability to properly determine the postion with the required accuracy.

A GPS system would have to overcome several hurdles in order to be appropriate to determine the transmitter and receiver geometry variations for an airborne EM system. In the case of the GEOTEM system, the following considerations must be considered:

1. Ability to withstand the vibrations associated with the receiver and the transmitter loop.
2. Ability to measure accurately offset to 7 centimetres or less to detect a target at 100 metres depth in the case for the GEOTEM system.
3. Ability to withstand the electrical interference associated with the aircraft, transmitter and static effects from the air
4. Offer no interference with the recording of the data or the electromagnetic fields measured.

   Ability to be integrated with the existing software and hardware easily
5. Offer easy installation with little impact on aerodynamics or weight distribution.
6. Easy to maintain.
7. Easy and quick or no calibration.
8. Reasonably priced.
9. Supported by the manufacturer.

## 6. Conclusions

Time-domain electromagnetic systems are a useful tool to locate conductive targets in the Earth's subsurface. The ability to detect and distinguish targets of high conductance from those of lesser conductance is dependent on the system's ability to measure the secondary in-phase component during the transmitter on-time. Currently, this is difficult because the secondary in-phase component is indistinguishable from the primary field. If a method could be developed to accurately determine transmitter-receiver geometric variations, the primary field could be estimated and correctly removed from the total response. The secondary in-phase response could then be measured more accurately. The secondary in-phase response is of particular interest because it contains signal from targets of high conductance in the subsurface.

Transmitter and receiver geometry, transmitter attitude, and loop deformation all have a significant effect on the measured primary field at the receiver, for each system. Although the accuracy required to detect a particular target varies as the depth to the target changes, the relative importance of each of the variables remains the same. To successfully detect a conductive target it is not necessary for each of the variables to be measured to the same degree of accuracy since each variable has a different level of impact.

This research project has demonstrated that, as the transmitter and the receiver become further separated, the impact from variations in geometry is reduced. The primary magnetic field from the transmitter diminishes with distance (inverse cube power law).

Therefore, the further the receiver is from the transmitter the less effect a constant change in offset will have on the data collected by the receiver. However, increasing distance between the transmitter and the receiver reduces the stability of the system and therefore increases deviations from the nominal position.

The significance of transmitter attitude is greatly dependant upon the system configuration. The magnitude and direction of the primary magnetic field is not only dependent on the distance, but also the angle from the centre of the transmitter loop to the receiver. A transmitter mounted on a fixed-wing aircraft, has the same attitude as the aircraft itself. Most aircraft have the capability to measure attitude already. Helicopter systems have a transmitter separate from the aircraft and would require a separate apparatus to measure the transmitter attitude.

At present, there is no practical way of estimating the transmitter loop deformation, which makes it difficult to determine what is considered normal motion. It is also difficult to conceive a method by which to constrain the transmitter loop so that its movement is minimized.

Taking into account the above results, the GEOTEM+ system seems to be a feasible and cost-effective way to improve the existing GEOTEM system. Provided that transmitter loop deviations are small (e.g. <35.8 cm for a target of 100 metres) or can be accounted for, the GEOTEM+ system addresses the problem of geometric variations in airborne EM systems by extending transmitter-receiver separation. Although this strategy will not

solve the problem completely, it reduces the problem to within manageable limits. However, further testing is required to determine the viability of this option.

The HeliGEOTEM system is a good alternative, as it offers much more rigidity than the fixed-wing systems (i.e. GEOTEM and GEOTEM+). This rigidity keeps the transmitter and receiver geometric variations to a minimum. However, since the distance between the transmitter and receiver are much closer than either fixed-wing system, the geometric variations have a greater impact. Further testing is necessary to determine if the system is rigid enough to ensure that any geometric variations are within manageable limits.

Using the Generic Concentric system to measure the on-time in-phase component would require complete rigidity or extremely accurate measurement of relative movement between the transmitter and the receiver, both of which are unattainable at this time. It is interesting to note that, at present, no commercial operator of a concentric EM survey system records on-time in-phase data during field surveys. The problem of removing the secondary response from the primary field is too severe to overcome.

None of the technologies evaluated met the criteria for an effective tracking of the GEOTEM receiver. The accuracy requirements are either too high and/or limitations on physical stability are exceeded for the Total Station and Vision systems. The GPS system does not meet the accuracy requirements and there are also interference considerations that would be very difficult to overcome.

The inability to accurately account for the geometric variations and hence measure the time-domain in-phase response does not always diminish the ability of airborne EM methods to detect highly conductive targets. Highly conductive targets commonly have more weakly conductive parts that are quite detectable using this technology. However, the technology may not be capable of distinguishing a target of moderate conductance (e.g. a sulphide deposit) from a target with very high conductance (e.g. a nickel-rich sulphide deposit).

Although this thesis concentrated on the magnitude of the primary field vector, typical systems currently available have a multiple component receiver so that the three components of the primary field can be recorded independently. Breaking down the analyses for each of the components would add another level of complexity beyond that considered in this thesis.

## 7. References

BALCH, S.J., 2000. Geophysics in mineral exploration: fundamentals and case studies: Ni-Cu sulphide deposits with examples from Voisey's Bay. Geological Association of Canada/Mineral Association of Canada short course, Sudbury ON., May 2000.

BEAMISH, D. and MATTSSON, A., 2003. Time-lapse airborne EM surveys across a municipal landfill, J. Environmental Engineering Geophysics, 8, p. 157-165.

CHRISTIANSEN, A.V. and CHRISTENSEN, N.B, 2003. A quantitative appraisal of airborne and ground-based transient electromagnetic (TEM) measurements in Denmark Geophysics 68, p. 523-534.

DEBLOIS, P. 2004. Leica Geosystems, Montreal, Personal communication.

DOBRIN, M.B. and SAVIT, C.H. 1988. Introduction to Geophysical Prospecting 4th ed. McGraw-Hill Book Co., New York.

ENGLISH, C., 2004. Neptec, Personal communication.

FITTERMAN, D.V. and STEWART, M.T., 1986. Transient electromagnetic sounding for groundwater, Geophysics 51, p. 995-1005.

FITTERMAN, D.V. and Yin, C., 2004. Effect of bird maneuver on frequency-domain helicopter EM response: Geophysics, 69, p. 1203-1215.

FOUNTAIN, D., 1998. Airborne electromagnetic systems – 50 years of development. Exploration Geophysics, 29, p. 1-11.

FRISCHKNECHT, F.C., LABSON, V.F., SPIES, B.R. AND ANDERSON, W.L., 1991. Profiling methods using small sources, in Nabighan, M.N., Ed., Electromagnetic methods in applied geophysics, 02: society of Exploration Geophysics, p. 105-270.

FRISCHKNECHT F.C., 1988. Electromagnetic physical scale modeling, *in* Nabighian, M. N., Ed., Electromagnetic methods in applied geophysics, 01: Society of Exploration Geophysicists, 365-442.

GRANT, F.S., and WEST, G.F., 1965. Interpretation Theory in Applied Geophysics. McGraw-Hill Book Co., New York.

HAMMACK, R.W. and MABIE, J.S., 2002. Airborne EM and magnetic surveys find fault(s) with Sulphur Bank Mercury Mine Superfund site: The Leading Edge, 21, no. 11, p. 1092-1095.

HEFFORD, S.W., SMITH, R.S., and SAMSON, C. 2006. Quantifying the effect that changes in the transmitter-receiver geometry have on the capabilities of an airborne

electromagnetic survey system to detect good conductors. Exploration Mining Geology, vol. 15:1 or 2 (In Press).

HEFFORD, S.W., SMITH, R.S., and SAMSON, C. 2005. Quantifying the effect that changes in the transmitter-receiver geometry have on the capabilities of an airborne electromagnetic survey system with a towed receiver to detect good conductors. Presented at Ontario Prospector's Association Annual Symposium, Toronto, ON, Dec.13-14.

HEFFORD, S.W., C. SAMSON, and SMITH, R.S. 2004. Tracking the Transmitting-Receiving Offset in Fixed-Wing Transient Electromagnetic Systems: Methodology and Application. 6th GEOIDE Annual Conference, Gatineau, May 30th –June 2nd.

HEFFORD, S.W., C. SAMSON, and SMITH, R.S. 2005. The Effects of Transmitter–Receiver Geometry on the Target Detection Capabilities of an Airborne Electromagnetic Survey System. 7th GEOIDE Annual Conference, Quebec City, May 29th –31st.

HOHMANN, G.W., 1988. Numerical modeling for electromagnetic methods of geophysics, *in* Nabighian, M. N., Ed., Electromagnetic methods in applied geophysics, 01: Society of Exploration Geophysicists, Geophysical, 313-364.

KITMAN, JAMIE LINCOLN, 2000. The Secret History of Lead: Special Report, March 20th, The Nation.

LAWYER, L.C., BATES, C.C. and RICE, R.B., 2001. Geophysics in the affairs of mankind, Geophysics in the affairs of mankind: Society of Exploration Geophysicists, Geophysical Reference Series Vol. 10.

LEICA, 2002. TPS1100 Professional Series - User Manual, Switzerland.

MAGNUS, B. 2004. Fugro Airborne Surveys Ottawa, Personal communication.

MORRISON, D. "Some old Books" December 2005. Preview, Issue No. 119.

PAINE, J.G., DUTTON, A.R., MAYORGA, J.S. and SAUNDERS, G.P., 1997. Identifying oil-field salinity sources with airborne and ground-based geophysics: A West Texas example: The Leading Edge, 16, no. 11, p. 1603-1607.

PALACKY, G.J., 1988. Resistivity characteristics of geologic targets, *in* Nabighian, M. N., Ed., Electromagnetic methods in applied geophysics, 01: Society of Exploration Geophysicists, 53-130.

PALACKY, G.J. and WEST, G.F., 1991. Airborne electromagnetic methods, in Nabighian, M.N., Ed., Electromagnetic methods in applied geophysics, 02: Society of Exploration Geophysicists, p. 811-879.

PLONUS, M.A., Applied Electromagnetics. 1978. McGraw-Hill, New York p. 441-450

SAMSON, C., SMITH, R.S., and HEFFORD, S.W. 2004. Tracking the transmitting-receiving offset in fixed-wing transient electromagnetic (EM) systems: methodology and application. 6th Annual Scientific Conference of the GEOIDE Network, Gatineau, QC, 30 May-1 June.

SHANG, J., MORRIS, R., and HOWARTH, P., 2001. Using airborne magnetic and electromagnetic data to monitor mine tailings in Copper Cliff, northern Ontario, CIM bulletin, Nov/Dec 2001, vol. 94, no. 1056, p. 73-80

SMITH, R.S., and ANNAN, A.P., 1997. Advances in Airborne Time-Domain EM Technology in Gubins, A.G., ed., Proceedings of Exploration '97: Fourth Decennial International Conference on Mineral Exploration, p. 497-504.

SMITH, R.S., and ANNAN, A.P., 1998. The use of B-field measurements in an airborne time-domain system: Part 1. Benefits of B-field versus dB/dt data. Exploration Geophysics, 29, p. 24-29.

SMITH, R.S., and ANNAN, A.P., 2000. Using an induction coil sensor to measure the B-Field response in the bandwidth of the transient electromagnetic method. Geophysics, 65, no. 5, p. 1489–1494.

SMITH, R.S., 2001a. On removing the primary field from fixed-wing time-domain airborne electromagnetic data: some consequences for quantitative modeling, estimating bird position and detecting perfect conductors. Geophysical Prospecting, 49, p. 405-41.

SMITH, R.S., 2001b. Tracking the transmitting-receiving offset in fixed-wing transient EM systems: methodology and applications. Exploration Geophysics, 32, p.14-19.

SMITH, R.S., FOUNTAIN, D., and ALLARD, M., 2003. The MEGATEM fixed-wing transient EM system applied to mineral exploration: a discovery case history. First Break, July, p 73-77.

SMITH, R.S., O'CONNELL, M.D. and POULSEN, L.H., 2004. Using airborne electromagnetic surveys to map the hydrogeology of an area near Nyborg, Denmark. Near Surface Geophysics, 2, p 123-130.

SPIES, B.R. AND FRISCHKNECHT, F.C., 1991. Electromagnetic sounding, *in* Nabighian, M. N., Ed., Electromagnetic methods in applied geophysics, 2: Society of Exploration Geophysicists., p. 285-425.

SWIFT, C.M., Jr., 1988. Fundamentals of the electromagnetic method, *in* Nabighian, M. N., Ed., Electromagnetic methods in applied geophysics, 01: Society of Exploration Geophysicists, 5-12.

TELFORD, W.M., GELDART, L.P. and SHERIFF, R.E., 1990. Applied Geophysics. Cambridge University Press, New York 2nd edition.

VRBANCICH, J., SMITH, R., 2005. Limitations of two approximate methods for determining the AEM bird position in a conductive environment. Society of Exploration Geophysicists, 36, no. 4.

WOLFGRAM, P.A. and GOLDEN, H.C., 2002. Examples of Nickel Sulphide Detection with Airborne EM, 64th Meeting: European Association of Geoscientists and Engineers, D037.

YIN, C. and FRASER, D.C., 2004. Attitude corrections of helicopter EM data using a superposed dipole model: Geophysics, 69, p. 431-439.

ZANDEE, A.P., BEST, M.E. and BREMNER, T.G.T., 1985. Sweepem, a new airborne electromagnetic system, 55th Annual International Meeting: Society of Exploration Geophysicists, Session: MIN1.7.

# Appendices

## *A. Total Station Positioning System*

### A.1 Background

An optical instrument consisting of a small mounted telescope rotatable in horizontal and vertical planes, used to measure angles in surveying. Angle measurements are usually done electronically. Modern systems are usually equipped with integrated electro-optical distance measuring devices and tracking mechanisms. A theodolite tracking mechanism uses an apparatus that can be mounted directly to the target to allow the Electronic Distance Measurement (EDM) device to locate and track the target. The tracking and distance measurement are completed with the use of a laser system. Theodolite Total Stations require frequent calibration and they are extremely sensitive to movement and temperature variations. Normally, a theodolite is mounted on a tripod by means of a forced centring plate or tribach, containing three thumbscrews for easy setup. Usually, before use, a theodolite must be centred (i.e. placed precisely and vertically over the point to be measured), and leveled (i.e. its vertical axis aligned with local gravity). The former is done using a plumb, the latter using a spirit level (or bubble level). Fast and accurate procedures for doing both have been developed and can be somewhat automated.

Early in this research project, preliminary testing of a total station positioning system was undertaken to see if it could be a viable way of tracking the GEOTEM receiver. The Leica TPS1100-A was selected for preliminary testing. This section will present the system, and the results of the preliminary tests.

## A.2 System Description

The system selected for preliminary testing was a Total Station Positioning System TPS1100-A manufactured by Leica Geosystems[7] AG from Heerbrugg, Switzerland. The TPS1100-A (Figure A.1) is a highly sophisticated instrument meant to help automate land surveying. It has the capability of recognizing and tracking targets and measuring distances and angles to a high degree of accuracy (Figures A.1 and A.2). It is usually mounted on a tripod and can be controlled from a remote location so that a single user can operate it. It has several degrees of automation ranging from completely manual to almost entirely automatic operation. It has an optical telescope, visible laser beam sight, and an infrared laser for automatic measurements. The specifications for the system are outlined in Table A.1. The accuracies of the TPS1100-A are outlined in Table A.2.

The TPS1100-A is almost always used with a cooperative target, or with a cooperative target attached to the target of interest. Cooperative targets are easier to detect at long distances because they have a high reflection coefficient and are designed to reflect back the laser beam strongly irrespective of the targets orientation. For this analysis, the cooperative target selected was the 360 degrees Standard Survey Prism (Leica model no. GZR121) (Figure A.2). This target is comprised of a series of glass prism targets and is available in a variety of sizes. Its maximum range is 1300 metres, which is far more than necessary for this project. The prism used was about 0.20 metres tall not including the mounting bracket.

---

[7] www.leica.com

Figure A.1: Leica Total Station TPS1100-A. The device weighs ~4.8 kilograms and is ~40 centimetres tall and 25 centimetres wide. The TPS1100-A components are: 1-Optical Sight, 2-Horizontal Drive Screw, 3-Battery Compartment, 4-Vertical Drive Screw, 5-Alphanemeric Keypad and Display, 6-Eyepiece, 7-Mounting Bracket, 8-RS232C Serial Interface, 9-Power Search Sensor, 10-Exit Port for infrared & Visible Laser Beams.

Figure A.2: Leica Standard 360° Survey Prism

| | Function | | |
|---|---|---|---|
| Description | PS | ATR | EDM |
| Beam divergence | 0.4 x 700 mrad | 26.2 mrad | 1.8 mrad |
| Pulse duration | 80 ns | 9.8 ms | 800 ps |
| Maximum radiant power | 1.1 mW | 0.76 mW | 0.33 mW |
| Measurement uncertainty | ± 5% | ± 5% | ± 5% |

Table A.1: Specifications for the Power Search Function (PS), Automatic Target Recognition Function (ATR), and Electronic Distance Measurement Function (EDM) at a range of 1000 metres.

| EDM Measuring Program | Accuracy | Time per measurement |
|---|---|---|
| Standard Measurement | 2 mm + 2 ppm | 1.0 sec |
| Fast Measurement | 5 mm + 2 ppm | 0.5 sec |
| Normal Tracking | 5 mm + 2 ppm | 0.3 sec |
| Rapid Tracking | 10 mm + 2 ppm | < 0.15 sec |
| Averaging | 2 mm + 2 ppm | ---- |

Table A.2: Measurement accuracies for the TPS1100-A Electronic Distance Measurement Function (EDM) function at a distance of 1000 metres. Note: Beam interruptions, severe heat shimmer and moving objects within the beam path can result in deviations of the specified accuracy.

The TPS1100-A is a versatile instrument with multiple functionalities. There are three primary functions of interest for this analysis:

1. The Power Search (PS) function is used to locate a cooperative target.
2. Once a target has been found using the Power Search function it can be identified and tracked with the Automatic Target Recognition (ATR) function.
3. The Electronic Distance Measurement (EDM) function is used while the object is being tracked by the ATR function. It determines the distance of the cooperative target. The angle to the target is also measured.

The Power Search (PS) function is available when a visual reference to the target is initially unavailable or has been lost. This function allows the instrument to automatically search and recognize a target. This function would be necessary for our application since the instrument requires a direct line of sight to the target and would have to be mounted outside an aircraft fuselage. The PS sensor consists of a transmitter and a receiver installed in the lower part of the telescope. An invisible, vertical laser swath of about 36 degrees in height and 0.0225 degrees horizontally is transmitted while the instrument rotates around its standing axis. Once the swath encounters an object, the reflected signal is evaluated to determine if it is coming from the target. If the reflected signal patterns correspond to known characteristics, the horizontal position of the target is determined and the rotation is terminated. Now, a second PS with a much smaller vertical line swath is launched. This process locates the target centre precisely so its position can be tracked.

The ATR sensor emits an invisible laser beam. The beam is reflected by the cooperative target and collected by an internal high-resolution Charged Coupled Device (CCD) camera. CCD cameras are electronic image sensor devices that are capable of transforming a light pattern into an electric charge pattern (an electronic image. The intensity of the reflected signal and the CCD element illuminated are estimated with respect to the camera centre. The offset components from this reference are computed in both the vertical and horizontal planes. These offsets are then used to control the motors of the telescope axes. The motors react immediately to maintain the position the instrument's crosshairs onto the target. To minimize measurement time, the crosshairs are only positioned within a small tolerance of the actual target centre. The remaining offsets are then mathematically applied to determine the horizontal and vertical angles.

The infrared (IR) electronic distance mode (EDM) sensor emits an invisible laser beam to specular cooperative targets such as a prism or reflector tape. Based upon light detection and ranging (LIDAR) technology, the reflected light is detected by a sensitive photo receiver and converted into an electrical signal. After the signal has been digitized (at a sampling frequency of 100 MegaHertz) and stacked, the distance is determined by comparing the phase of the original and reflected pulses.

### A.3 Preparation & Setup

Before any testing could be started, the system had to be modified from its default sample rate of 2 Hertz to a sample rate of 4 Hertz to accurately track the path of the target, and harmonize with the sampling rate of other data acquired by the GEOTEM receiver. The

interface with the computer had to be established and the information converted into a useful format for testing and analysis purposes. The software interface was completed by Bruce Magnes of Fugro Airborne Surveys (Magnus, 2004).

Pre-testing setup included compiling a C based program to run in the MSDOS operating system. The program ran under interrupts through the RS232C serial interface connected to a laptop. The received data was timed tagged using the DOS system timer that has an accuracy of 55 milliseconds (18.2 ticks/s). After the data was time tagged, it was written to the hard drive in ASCII format. Figure A.3 shows the computer and the TPS100-A setup.

The software specialist from Leica recommended the command sequence to use in acquiring the distance and angular offset measurements. Before initiating any measurements, the operator needs to insure that the target is in the field of view. This can be achieved by sending a search command "AUT_PS_SearchNext". This initiates a PS during which the system will locate the target prism. Once located, a fine adjustment is made using the command "AUT_FineAdjust". This locks the target in the field of view and measurements can now be made using the "TMC_QuickDist" command. This is the command that queried for a distance measurement and time tagged the reply as it was written to the disk. This command is set up in a loop so that distance tracking is performed until the program is stopped. During the tests, the total station was not in a stable environment so it was necessary to deactivate the double axis compensator system. This was done by setting the "TMC_SetInclineSwitch" set to "off".

Figure A.3: Total Station, Prism, laptop setup.

## A.4 Basic Testing

### A.4.1 Objective

The objective of the preliminary tests with the total station was to determine if this instrument could be used for the purpose of tracking the GEOTEM receiver in flight and what further tests would be required. For the TPS1100-A to be a suitable instrument for this application, it would have to make measurements at a minimum of 4 Hertz. The measurements would have to be at regular time intervals. The instrument would have to withstand vibrations and motions analogous to this associated with an aircraft during flight.

### A.4.2 Testing Procedure

The functionalities tested were finding a cooperative target, and tracking a cooperative target. Initially, basic tests were completed inside a laboratory to determine if the system was working after being shipped. Tests were also conducted to ensure that the program on the laptop was controlling the system and logging the data. These were short distance tests in the order of 1 to 10 metres. This testing was followed by tests outside in a parking lot where the instrument could be tested at representative distances of ~125 metres.

All tests were to determine the instrument's ability to measure distance under a variety of circumstances. Although tracking abilities were the main test objective, coarse accuracy tests were also completed. Once it was determined that the system could make

reasonable measurements, it could pass to the next stage of testing to estimate how accurately the instrument could measure offsets.

A Cartesian coordinate system was used for the purpose of basic testing as illustrated in Figure A.4. The $x$-direction is positive towards the target. The positive $z$-direction is vertically upward. The $y$-direction is orthogonal to the $x$-$z$ plane. It is positive to the right as viewed from the instrument to the target.

## A.5 Testing Results

### A.5.1 Short Distance Laboratory Testing

The testing began with the Total Station, interfaced with a computer, mounted on a table, and the prism across the room at a distance of about 10 metres. The system was able to locate the target with the PS function and track it. However, it was immediately apparent that the system could not track the target at short distances if the target was moved quickly and then continued to move slowly. The total station power search function could only find the target if the target was immobile. It became obvious that it was necessary to test this system at more representative distances.

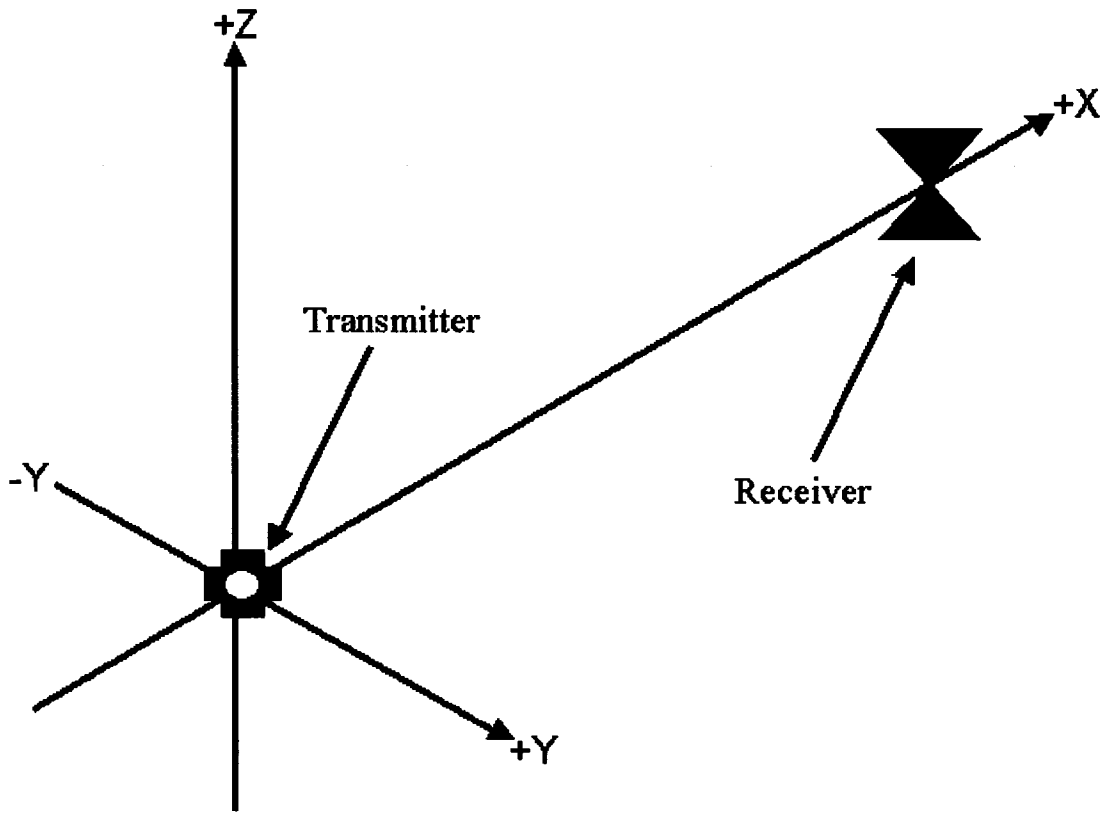


Figure A.4: Coordinate system for the Total Station testing.

### A.5.2 Long Distance Field Testing

Once outside, the system had little difficulty finding the prism. The horizontal $x$-component distance ranged from about 100 metres to 200 metres. The horizontal $y$-component, which was limited to the width of the parking lot, was about 5 metres. The vertical $z$-component was limited by the height of the person holding the prism. Its overall range was 1-2 metres.

Testing the tracking function was completed with someone moving the prism in all three directions at various distances from the instrument. The prism was moved slowly and quickly. Without vibrations the system tracked and recorded the movements of the desired object well. There were a few instances of losing track of the prism. If the prism was lost, the system found it again within a few seconds, even though the object was still moving. Figure A.5 is an example of the 3-dimensional tracking capabilities of the device.

There were several other objects (e.g. cars) in the general area of the testing that did interrupt the measurements at times. On several occasions, the instrument began to track a stationary car rather than the prism. Although the possibility of this happening when the instrument is mounted on the aircraft is quite slim, there are other objects that the tracking system could mistake as the target (e.g. the magnetic receiver). Figure A.6 shows an example of when the system locks on to a stationary object rather than tracking the desired object.

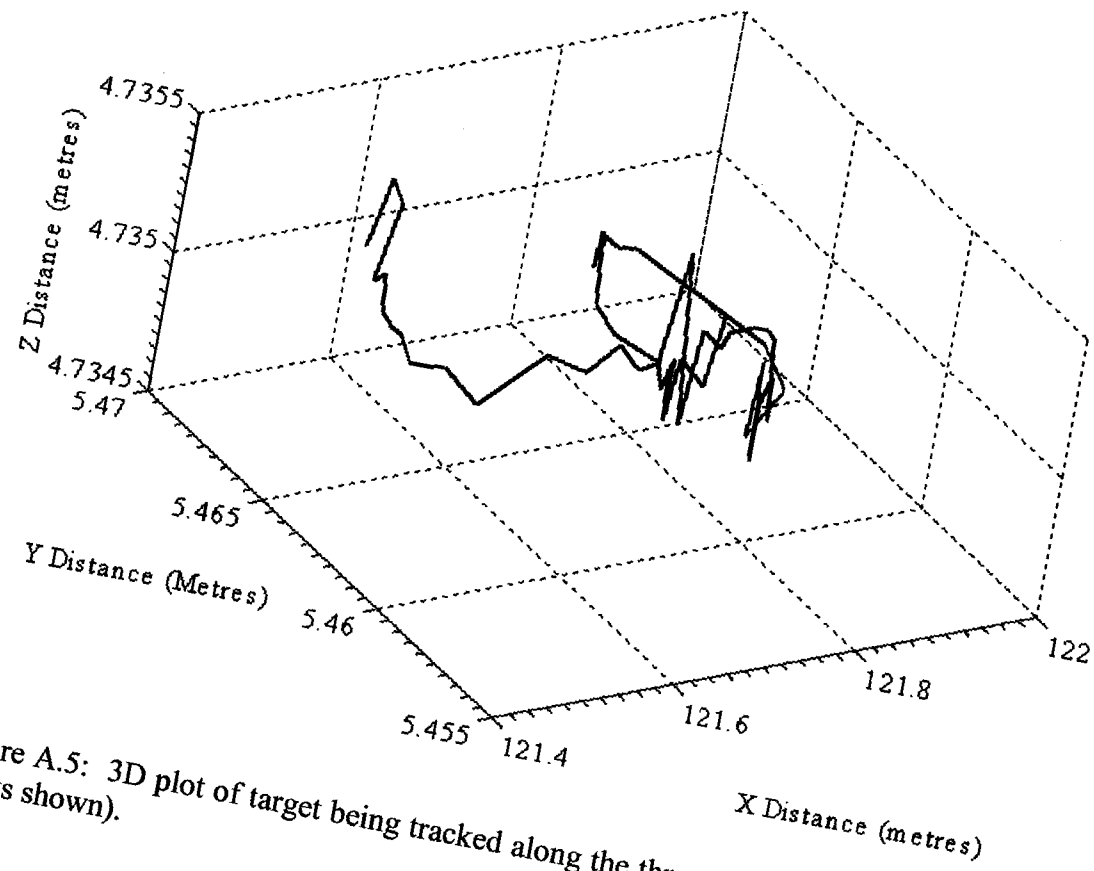


Figure A.5: 3D plot of target being tracked along the three $x$-, $y$-, and $z$-axes (50 data points shown).

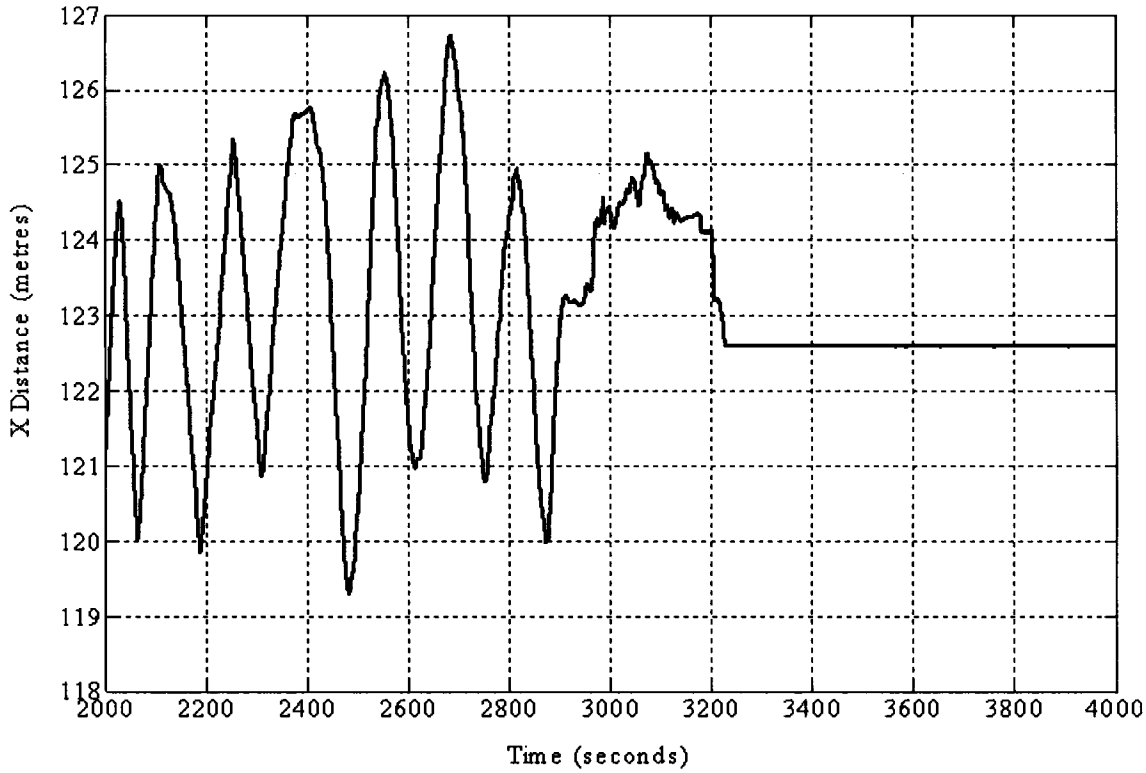


Figure A.6: Distance in the x-direction as a function of time. Between 200 and 3200 seconds, the TPS1100-A tracked the target well for variations of ±4 metres. From 3200 seconds, the TPS1100-A locked on a stationary object near the testing environment instead of the target.

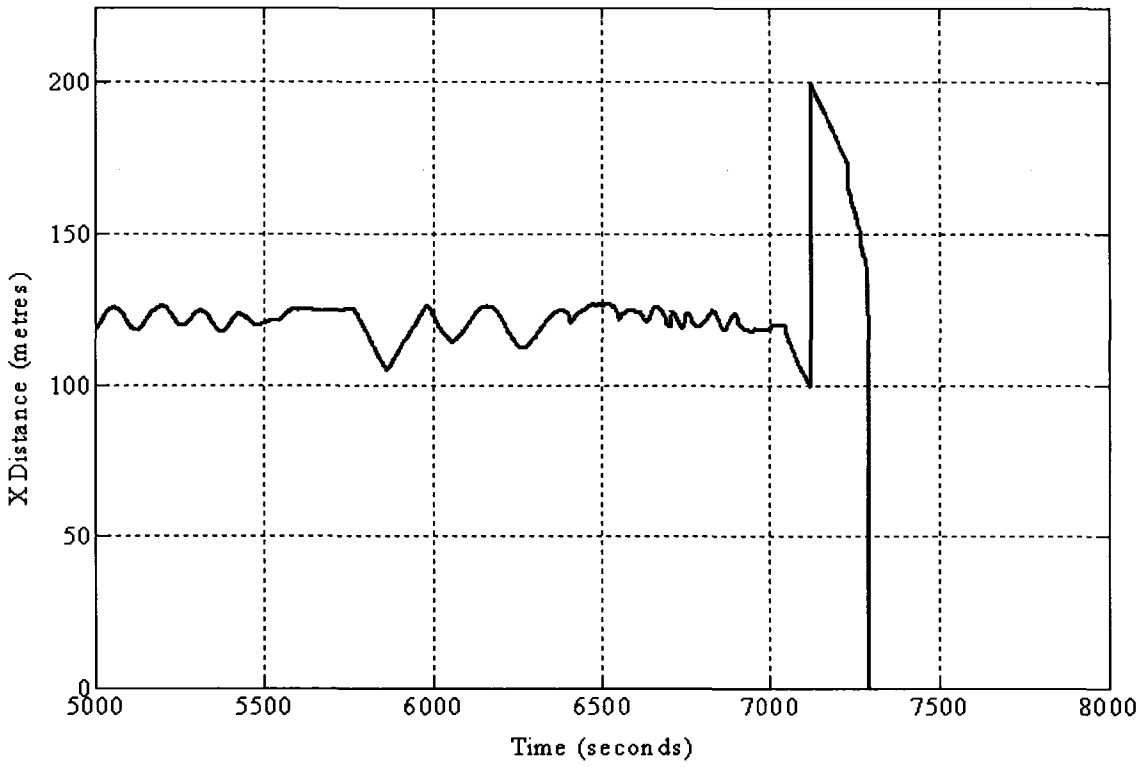


Figure A.7: Distance in the $x$-direction as a function of time. Between 5000 seconds and 7125 seconds, the system tracked the target well. The TPS1100-A was subjected to vibrations at 7125 seconds and the system failed to track any further.

Any testing that involved the TPS1100-A being moved or vibrated distorted the measurements in one form or another. With a higher frequency vibration, the system would essentially shutdown (Figure A.7). If the system is disabled in this fashion, it has to be disconnected from the power supply and then reconnected in order to resume.

### A.6 Conclusions and Recommendations

A system like the TPS1100-A has several advantages for the application of tracking a receiver sensor towed behind the GEOTEM aircraft. Since it is an "off the shelf" system, development, testing, calibration etc., is completed by the manufacturer. System support is also in the responsibility of the manufacturer (DeBlois, 2004).

Some advantages of the TPS1100-A include the interface with the computer, remote access via remote panel, and minimal power consumption. As noted in the specifications for this system (Table A.2), it surpasses the accuracy necessary for the purposes this application, which were estimated at 7 centimetres along the $x$-direction for the GEOTEM system (Section 4.1).

The action sequence of the TPS1100-A are outlined in Figure A.8. The TPS1100-A has not been designed for flight operations. The most problematic challenge would be the mounting of the system on the outside of the aircraft. Since the system is delicate and not really meant for such a strenuous environment, it would be both costly and difficult to properly mount this on the outside of the fuselage of the aircraft. Moreover, the

TPS1100-A behaves very poorly when subjected to vibrations. A very sophisticated mount would have to be designed to isolate the instrument from vibrations during flight. Finally, there are several circumstances that could lead to a decrease in the accuracy of the system including humidity, strong sunlight, heat shimmer, haze, and any type of precipitation where most are present during normal flying conditions.

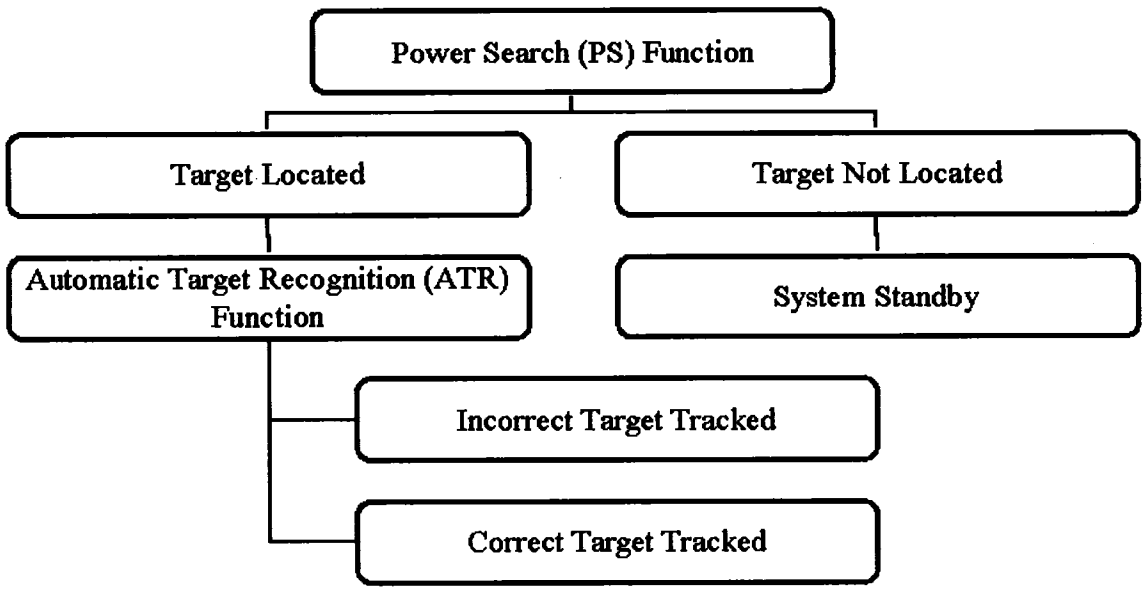


Figure A.8: The action sequence of the TPS1100-A.

## A.7 References

DEBLOIS, P. 2004. Leica Geosystems, Montreal, Personal communication.

ENGLISH, C., 2004, Neptec, Personal communication.

Leica Geosystems, 2002, TPS1100 Professional Series - User Manual, 2.2, Switzerland.

## *B. Video photogrammetry*

### B.1 Background

Photogrammetry is the art, science, and technology of obtaining reliable information about physical objects and the environment through the processes of recording, measuring, and interpreting photographic images and patterns of electromagnetic radiant energy and other phenomena. It uses physical and mathematical principles, to analyze an image of a three dimensional scene on multiple two dimensional photographs, to reconstruct a reliable and accurate model of the original three-dimensional scene. Although photographs are still used, modern techniques often employ the use of computers and digital imagery rather than photographs. Photogrammetry is often used to obtain the coordinates of an object, to make topographical and thematical maps, and rectified photographs. Rectified photographs (or orthophotos) are aerial photographs that rendered such that it is equivalent to a map of the same scale. These act as a photographic map that can be used to measure true distances, as an accurate representation of the earth's surface.

A photographic image is a "central perspective" because every light ray that reaches the recording surface passed through the camera lens, which is mathematically considered as a single point. This point is called the "perspective centre". The ray bundle must be reconstructed in order to take measurements of objects from photographs. This is why the internal geometry of the camera has to be known. This includes parameters like the

focal length, the position of the principal point and the lens distortion. Figures B.1 and B.2 help illustrate how the size of an image is a function of focal length, and how the size and or distance can be calculated once the focal length is known.

**B.2 System Description**

A photogrammetry system, the Space Vision System (SVS), was considered for the application of tracking the receiver sensor towed behind the GEOTEM aircraft. The SVS has been developed by Neptec[8] of Ottawa, Canada. The system is currently in use by NASA as an optical locating and tracking system designed to assemble the various modules of the international space station.

The SVS uses a photogrammetric method analogous to a pinhole camera to track and locate cooperative targets. All the targets are strategically placed on the object to be located. Each target is at a known distance from the other targets. When two or more targets are recoded to a two dimensional image, the distance can be calculated as a function of the image offset of the targets, the actual known offset of the targets, and the focal length.

Rather than one camera, the SVS consists of a series of cameras and targets in known positions on the object of interest. The cameras are high-resolution digital video cameras with a fixed focal length. They have been calibrated very carefully using a specially

[8] www.neptec.com

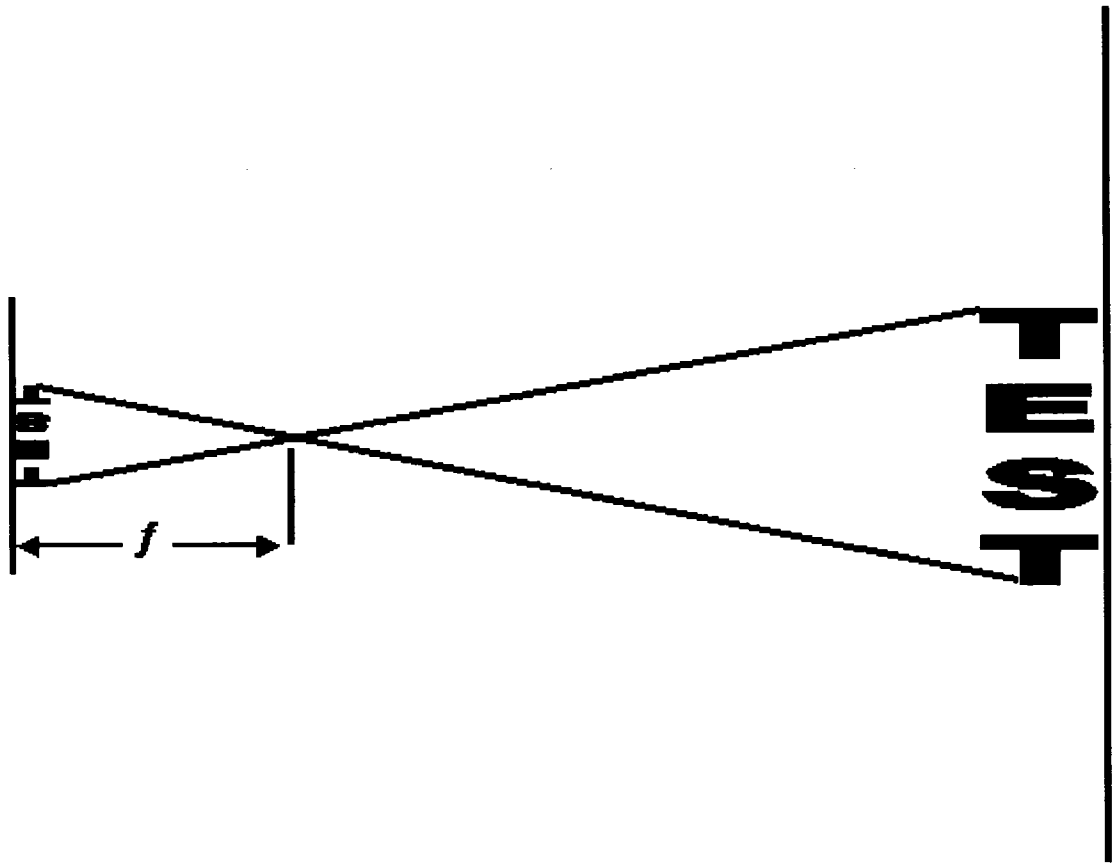


Figure B.1: The pinhole camera inverts the image. The size of the image TEXT is a function of the focal length.

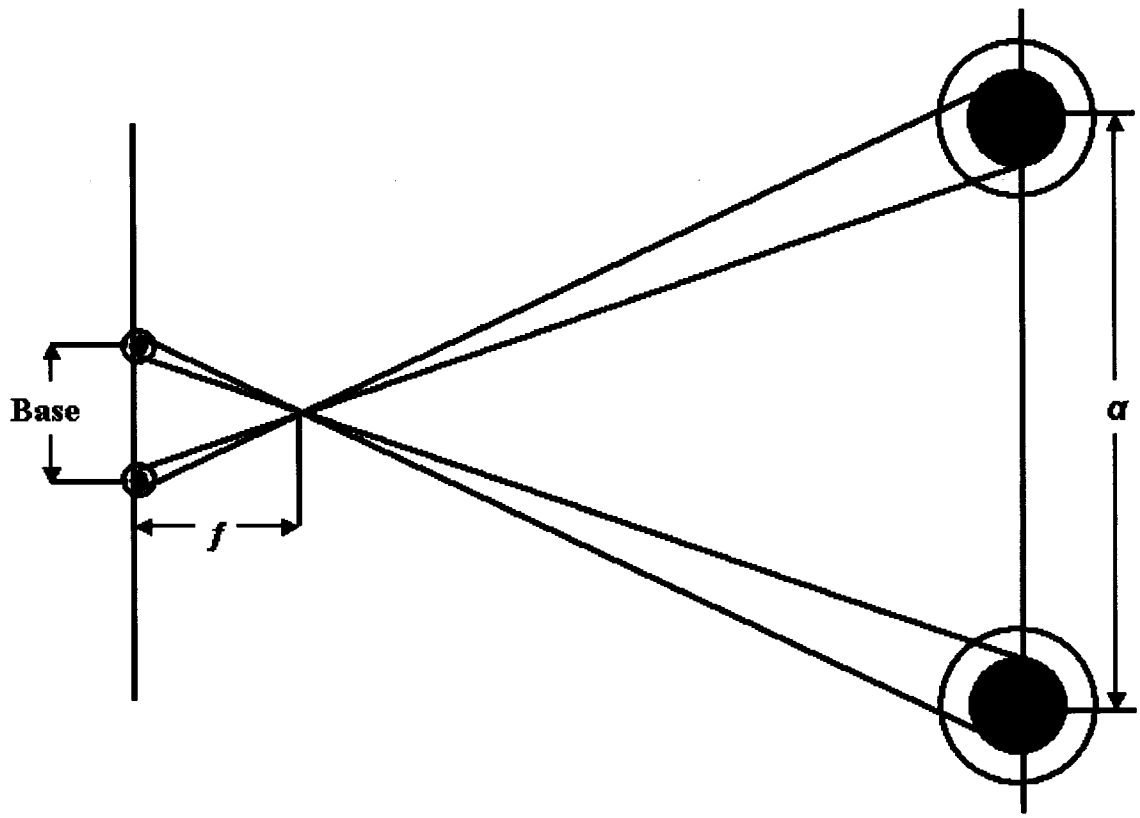


Figure B.2: Target separation. The distance $\alpha$ can be calculated once the base distance and the focal length $f$ is known.

designed camera calibration procedure. Figure B.3 shows the device used to calibrate the camera array. By using a fixed focal length, the cameras are more robust and have less error than a camera that has zoom capabilities. However, by using a fixed focal length, the cameras have a limited field of view and the objects must be within expected ranges to be accurately located. These problems can be overcome with carefully designed camera and target arrays, and a series of iterative error minimizing calculations.

There must be at least two targets to measure distance and at least three targets to measure all six degrees of freedom ($x$, $y$, $z$, roll, pitch, yaw). The problem is much more complicated than this as the measurements depend of several other factors such as:

1. The size of the targets on the image;
2. Size of the target array;
3. Number of targets;
4. 3D Depth of the targets;
5. Geometry of the array.

Generally, increasing the targets and the target array will increase precision. A target array that is concentrated on only one part of the object or very small targets will have a negative impact on the precision of the calculations.

The SVS records 30 frames per second and calculates one pose estimation per frame. Using a "sliding window" technique reduces the pose estimation error (Figure B.4).

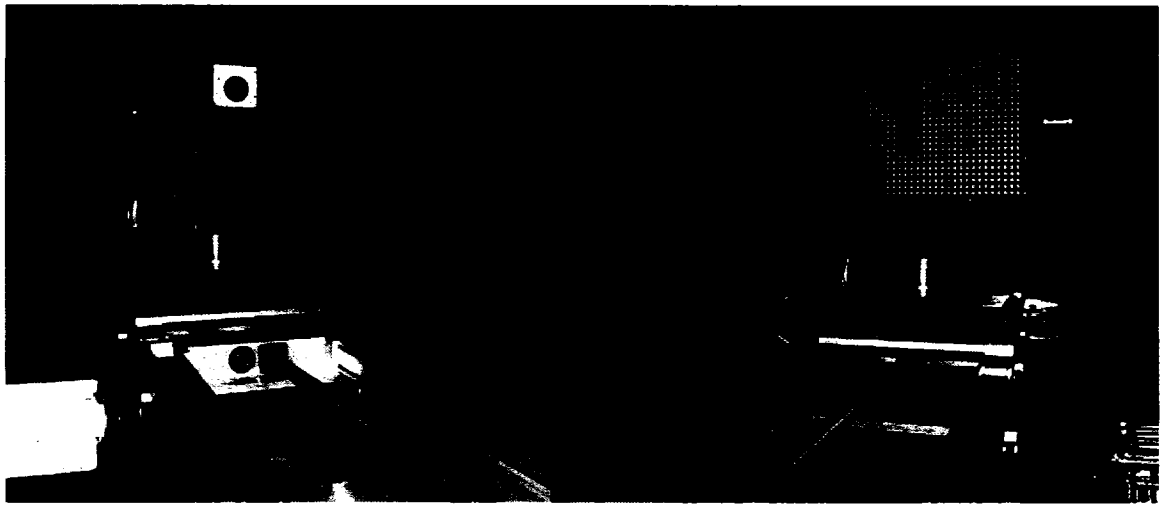

Figure B.3: Neptec camera array and calibration system

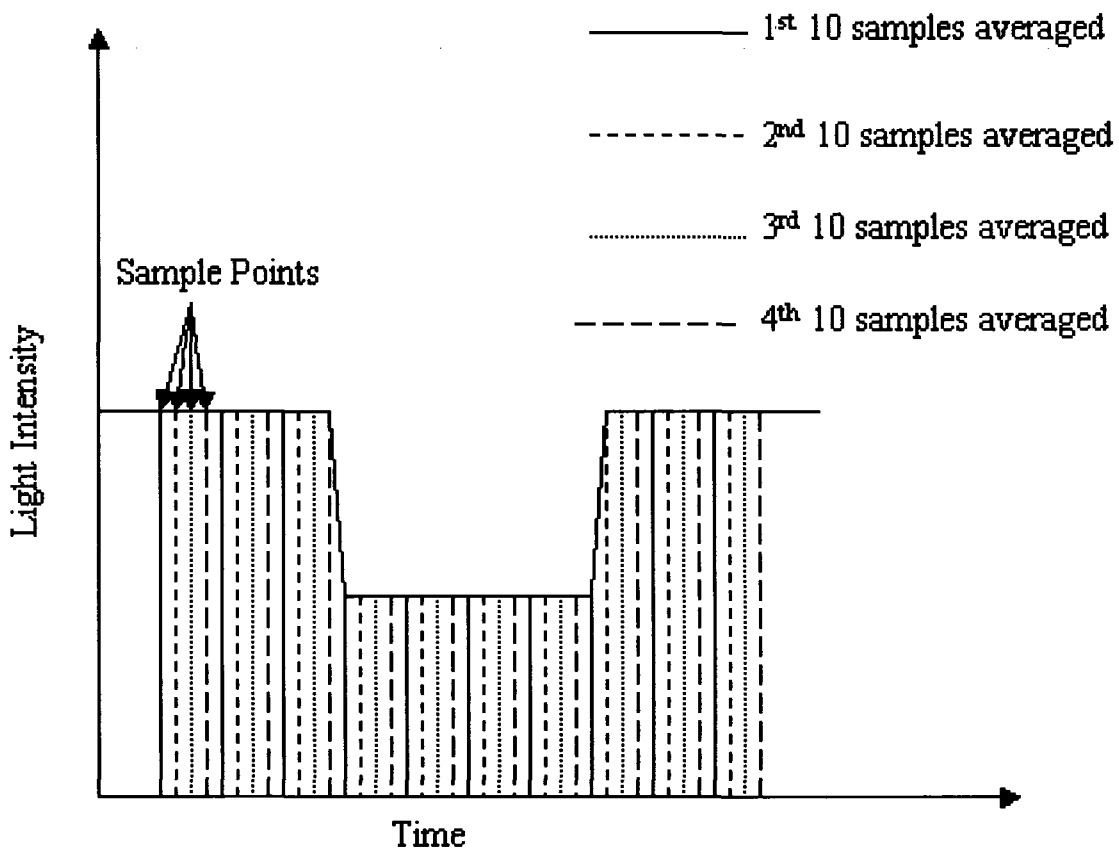


Figure B.4: SVS error reduction.

This involves averaging the response ten frames at a time, then moving one frame and averaging the next 10. By using this process, the error is reduced and the target is located more precisely. If the pose estimations were averaged along the same points each time without a sliding window, the precision would not improve. This technique attempts to average out the bias.

### B.3 Conclusions and Recommendations

For the application of locating the EM receiver behind the aircraft there are several factors that severely limit the SVS technology from performing well. Perhaps most prominent are:

1. Camera Location;
2. Target placement on the receiver;
3. Small target size with respect to the camera's field of view;
4. Relatively high speed of receiver's movements.

Two cameras would have to be on the outside of the fuselage with a large enough separation to accurately locate the targets. Taking into account the distance that the receiver is from the plane the cameras would have to be place at a larger separation than the plane can support. From wingtip to wingtip, the plane flexes to the point that these locations would have too much error in the distance calculations to be useful. A similar problem exists for the front to rear of the aircraft. Also, the front of the aircraft is tipped upwards 4 degrees during straight and level flying. To work properly, the cameras would

require an environment that is structurally secure and without vibration or appreciable displacements. Designing special mounts for the cameras on the outside of an aircraft is also an expensive engineering project.

Perhaps a more obvious problem with this system is the lack of space to place the targets on the EM receiver. The receiver is enclosed in an aerodynamic case that is designed to be streamlined and steady as it flies though the air. The receiver enclosure is egg-shaped and there is no room for the targets of the required size to fit on the front of the pod. Targets on the sides of the receiver would not be in the field of view of the cameras regardless of where the cameras are mounted on the aircraft.

The relatively small size targets would mean that the cameras would have to have a small field of view (short fixed focal length). The range of receiver motion is such that the receiver would frequently move outside the field of view of the cameras.

The SVS has been optimized to work in a very slow moving environment (~0.25 metres per second). Since the receiver is moving at a relatively high speed, the SVS may not be capable of delivering the same precision as for space operations.

For the reasons discussed above, the SVS system was determined to be unsuitable for the application of locating and tracking the receiver for the GEOTEM system. Therefore, no

further evaluation of this system was completed so no further time was spent quantifying all the other ways it would be unsuitable.

## B.4 References

WOLF, P.R., 1983, Elements of Photogrammetry, with Air Photo Interpretation and Remote Sensing. McGraw-Hill, Inc.

AVERY, T.E. and BERLIN, G.L., 1985, Fundamentals of Remote Sensing and Air photo Interpretation. Macmillan Publishing, Company, New York.

ENGLISH, C., 2004, Neptec, Personal communication.